NTIS # PB95-100376

SSC-374

EFFECT OF HIGH STRENGTH STEELS ON STRENGTH CONSIDERATIONS OF DESIGN AND CONSTRUCTION DETAILS OF SHIPS

SHIP STRUCTURE COMMITTEE

1994

Member Agencies:

American Bureau of Shipping
nce Research Establishment Atlantic
Maritime Administration
Military Sealift Command
Naval Sea Systems Command
Transport Canada
United States Coast Guard

Ship Structure Committee

An Interagency Advisory Committee

Address Correspondence to:

Executive Director
Ship Structure Committee
U.S. Coast Guard (G-MI/SSC)
2100 Second Street, S.W.
Washington, D.C. 20593-0001
Ph:(202) 267-0003
Fax:(202) 267-4677

3 October, 1994

SSC-374
SR-1339

EFFECT OF HIGH STRENGTH STEELS ON STRENGTH CONSIDERATIONS OF DESIGN AND CONSTRUCTION DETAILS OF SHIPS

In the past decade we have seen the premature cracking of ship and offshore structures built of high strength steels. In some cases high strength steels had been substituted for mild steels in the construction phase without fully analyzing the long term ramifications. This project has examined this problem and applied a review technique to assess the fatigue strength of structural details using high strength steels. Recommendations for improvements to the example details are given and comparative analyses are made.

J. C. Card

J. C. CARD
Rear Admiral, U.S. Coast Guard
Chairman, Ship Structure Committee

Technical Report Documentation Page

1. Report No. SSC- 374	2. Government Accession No. PB95100376	3. Recipient's Catalog No.
4. Title and Subtitle EFFECT OF HIGH STRENGTH STEELS ON STRENGTH CONSIDERATIONS OF DESIGN AND CONSTRUCTION DETAILS OF SHIPS		5. Report Date March 1994
		6. Performing Organization Code
7. Author(s) R. E. Heyburn, D. L. Riker		8. Performing Organization Report No. SR-1339
9. Performing Organization Name and Address GIBBS & COX, INC. 50 WEST 23RD STREET NEW YORK, N.Y. 10010		10. Work Unit No. (TRAIS)
		11. Contract or Grant No. DTCG23-92-C-E01087
12. Sponsoring Agency Name and Address U.S. COAST GUARD 2100 SECOND STREET S.W. WASHINGTON, D.C. 20593-0001		13. Type of Report and Period Covered FINAL REPORT
		14. Sponsoring Agency Code G-M

15. Supplementary Notes

Project sponsored by the Ship Structure Committee, Washington, D.C.

16. Abstract

Fatigue cracking continues to be a major cause of extensive and costly ship repair work. In the past 10 years, the use of high strength steel (HSS) has come under scrutiny as a significant contributor to fatigue cracking. This investigation calls attention to the problem areas of high strength steel details. Also, a general methodology for assessing the fatigue strength of structural details is presented using existing technology. Examples using this methodology are presented for existing problematic high strength steel details.

17. Key Words Fatigue, Ship Structural Details, Design, Reliability, Loading History, Random Loading, Fatigue Data, High Strength Steel	18. Distribution Statement Document is available to the U.S. public through the National Technical Information Service, Springfield, VA 22161

19. Security Classif. (of this report)	20. Security Classif. (of this page)	21. No. of Pages	22. Price
Unclassified	Unclassified	184	\$12.50 Micro- \$27.00 Paper

Form DOT F 1700.7 (8-72) Reproduction of completed page authorized

METRIC CONVERSION FACTORS

Approximate Conversions to Metric Measures

Symbol	When You Know	Multiply by	To Find	Symbol
		LENGTH		
in	inches	*2.5	centimeters	cm
ft	feet	30	centimeters	cm
yd	yards	0.9	meters	m
mi	miles	1.6	kilometers	km
		AREA		
in^2	square inches	6.5	square centimeters	cm^2
ft^2	square feet	0.09	square meters	m^2
yd^2	square yards	0.8	square meters	m^2
mi^2	square miles	2.6	square kilometers	km^2
	acres	0.4	hectares	ha
		MASS (weight)		
oz	ounces	28	grams	g
lb	pounds	0.45	kilograms	kg
	short tons (2000 lb)	0.9	tonnes	t
		VOLUME		
tsp	teaspoons	5	milliliters	ml
Tbsp	tablespoons	15	milliliters	ml
fl oz	fluid ounces	30	milliliters	ml
c	cups	0.24	liters	l
pt	pints	0.47	liters	l
qt	quarts	0.95	liters	l
gal	gallons	3.8	liters	l
ft^3	cubic feet	0.03	cubic meters	m^3
yd^3	cubic yards	0.76	cubic meters	m^3
		TEMPERATURE (exact)		
°F	Fahrenheit temperature	5/9 (after subtracting 32)	Celsius temperature	°C

*1 in = 2.54 (exactly). For other exact conversions and more detailed tables, see NBS Misc. Publ. 286, Units of Weights and Measures, Price $2.25, SD Catalog No. C13.10:286.

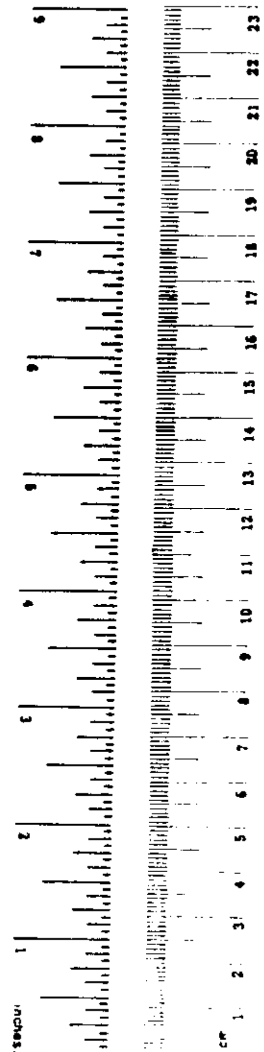

Approximate Conversions from Metric Measures

Symbol	When You Know	Multiply by	To Find	Symbol
		LENGTH		
mm	millimeters	0.04	inches	in
cm	centimeters	0.4	inches	in
m	meters	3.3	feet	ft
m	meters	1.1	yards	yd
km	kilometers	0.6	miles	mi
		AREA		
cm^2	square centimeters	0.16	square inches	in^2
m^2	square meters	1.2	square yards	yd^2
km^2	square kilometers	0.4	square miles	mi^2
ha	hectares (10,000 m^2)	2.5	acres	
		MASS (weight)		
g	grams	0.035	ounces	oz
kg	kilograms	2.2	pounds	lb
t	tonnes (1000 kg)	1.1	short tons	
		VOLUME		
ml	milliliters	0.03	fluid ounces	fl oz
l	liters	2.1	pints	pt
l	liters	1.06	quarts	qt
l	liters	0.26	gallons	gal
m^3	cubic meters	35	cubic feet	ft^3
m^3	cubic meters	1.3	cubic yards	yd^3
		TEMPERATURE (exact)		
°C	Celsius temperature	9/5 (then add 32)	Fahrenheit temperature	°F

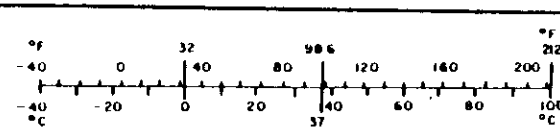

TABLE OF CONTENTS

TABLE OF CONTENTS (Cont'd)

LIST OF FIGURES

LIST OF FIGURES (Cont'd)

LIST OF FIGURES (Cont'd)

LIST OF FIGURES (Cont'd)

LIST OF FIGURES (Cont'd)

LIST OF TABLES

LIST OF TABLES (Cont'd)

1.0 INTRODUCTION

1.1 BACKGROUND

Fatigue cracking of ships has been responsible for much costly repair work. In recent years, high strength steel (HSS) has been substituted for mild steel (MS) in the design and construction of ships. Many of these high strength steel ships have experienced an acceleration of fatigue cracking, especially the Class III or nuisance cracking of internal structural members. The Trans-Alaska Pipeline Service (TAPS) Tankers have received much attention in the area of fatigue cracking. Therefore, they are a prime source of data on cracking of HSS ships.

Classification societies have allowed for reduced high strength steel scantlings based upon the increased strength capacity, with the stipulation that calculations be performed to insure that buckling failure modes do not occur. This, in conjunction with the direct substitution of high strength steel in standard mild steel details, may be aggravating initially poor structural details. Inherent stress concentrations in mild steel detail configurations, which did not previously exhibit cracking because of the thicker material and lower states of stress, are now cracking due to the reduced high strength steel scantlings and higher stress states. Corrosion of the thinner high strength steel elements may also be playing a significant role in the acceleration of fatigue cracking.

1.2 OBJECTIVE AND SCOPE OF INVESTIGATION

The objectives of this task were to:

a. Analyze in-service failures in construction details using high strength steel.

b. Call attention to the problem areas.

c. Recommend design and construction details to reduce problem areas.

The study achieved these objectives by reviewing documentation for in-service structural damage to high strength steel ships. From this review, representative details were chosen for fatigue analysis. Finally, improved configurations, which extend the fatigue life, were developed for those details chosen for analysis.

To accomplish the above objectives, the study has included the following:

a. A literature survey covering:

   (1) Ship structural details.

   (2) Ship fatigue damage.

   (3) Fatigue analysis methods.

b. An industry survey. Many owners and operators were contacted to obtain current cracking information on high strength steel ships from which to choose representative details for fatigue analysis.

c. Determination of fatigue analysis methodology using existing documentation and "design" loads.

d. Fatigue analysis of representative details using the methodology outlined in step c.

e. Proposed improved configurations for the representative details analyzed.

The results of the study are presented in the following sections and appendices.

2.0 APPROACH

2.1 BACKGROUND OF IN-SERVICE PROBLEMS

Local buckling and cracking failures of ship structural details have been a concern for many years. In 1978-80, the Ship Structure Committee published the Structural Detail Failure Survey, contained in References (a) and (b). The survey classified ship structural details into 12 families:

a. Beam Brackets (Family 1)

b. Tripping Brackets (Family 2)

c. Non-tight Collars (Family 3)

d. Tight Collars (Family 4)

e. Gunwale Connections (Family 5)

f. Knife Edge Crossing (Family 6)

g. Miscellaneous Cutouts (Family 7)

h. Clearance Cutouts (Family 8)

i. Structural Deck Cuts (Family 9)

j. Stanchion Ends (Family 10)

k. Stiffener Ends (Family 11)

l. Panel Stiffeners (Family 12)

The families were then further subdivided into specific types (i.e., corner, continuous, end, etc.) and detail numbers (i.e., 1,2, etc.). A total of 607,584 details were observed, with 6,856 observed failures. The failures were summarized by family and were attributed to either one or a combination of the following causes:

a. Design

b. Fabrication

c. Welding

d. Maintenance

e. Operations

This study concentrates on presenting an analysis philosophy which will help to eliminate fatigue problems by proper design of the details in the design phase.

The Tanker Structure Co-operative Forum has published the "Guidance Manual for the Inspection and Condition Assessment of Tanker Structures", Reference (c). Appendix IV of this manual catalogues structural detail failures and their recommended repairs. Most of the failures documented were reported on Very Large Crude Carrier (VLCC) type ships.

In 1990-91, the U.S. Coast Guard published a failure study on the Trans-Alaska Pipeline Service (TAPS) Tankers, References (d) and (e). This study identified a disproportionate number of structural failures occurring in TAPS Tankers. As a result of this study, it became necessary to prepare Critical Area Inspection Plans (CAIPs), which document structural failures, corrective action and scheduled inspection of the critical areas on TAPS Tankers. These CAIPs are a valuable source of structural failure information for tankers. A summary of typical failures documented in these plans are shown in Figure 2-1. It should be noted that ABS performed an independent study of the TAPS vessels, Reference (f). However, this study did not reach a conclusion regarding the use of high strength steel and its effects on the frequency of fatigue cracking.

Owners and operators were also contacted during this study to attempt to broaden the data base of current available failure information. The response, however, did not provide significant additional data.

2.2 DETAIL SELECTION

Several months of surveying the U.S. shipbuilding industry for existing high strength steel ship structural details, which have experienced fatigue problems, has provided disappointing results. The only significant source of documented fatigue problems in high strength steel ships, uncovered to date, has been the Trans-Alaskan Pipeline Service (TAPS) Tankers. However, this has provided only a limited selection in terms of ship type, ship size and operational location.

Each TAPS tanker has a Critical Area Inspection Plan (CAIP) which documents past cracking problems, their corrective fixes and the required frequency of inspection. The inspection plans listed in Table 2-1, as well as TAPS inspection reports published by the U.S. Coast Guard and ABS, were reviewed for existing problems and resolutions. The shell longitudinal to web frame connections (Family 1 of Reference (a)) have proven to be a significant cause for concern. Cracking has also been experienced in the tripping brackets (Family 2), non-tight collars (Family 3), tight collars (Family 4), stiffener endings (Family 11) and various cut-outs (Families 7,8 and 9).

Two details were chosen to demonstrate the fatigue assessment methodology. The first detail is a sniped innerbottom longitudinal girder stiffener ending from a naval combatant. The typical configuration of this detail is shown in Figure 2-2. Ship outline and characteristics of the naval combatant are shown in Figure 2-3. The midship section for the naval combatant is shown in Figure 2-4. The innerbottom girder configuration is shown in Figure 2-5. This detail represents a typical sniped stiffener end detail, family 11.A.1 of Reference (a), which is subjected to cyclic loading during the life of the ship.

The second detail is a shell longitudinal to web frame connection from a tanker. The typical configuration of this detail is shown in Figure 2-6. Ship outline, characteristics and basic compartmentation of the tanker are shown in Figure 2-7. The midship section for the tanker is shown in Figure 2-8. This shell longitudinal detail represents a typical problem area associated with longitudinal strength structure. Although reviewed several times previously, this detail provides a classic example to demonstrate the fatigue methodology.

These details were chosen because they:

a. Are fabricated from high strength steel.

b. Fit into the family of details as categorized in References (a) and (b).

c. Represent typical in-service problems.

d. Represent two different ship configurations.

e. Represent two different structural elements and loading configurations.

2.3 FATIGUE ANALYSIS APPROACH

The fatigue design method used in this study is taken from the Ship Structure Committee Report No. SSC-318, Reference (g). This procedure was chosen because it is general enough to encompass a wide range of specific ship details as well as a wide range of ship types. The design procedure takes into account the three most significant factors affecting the fatigue behavior of ship details.

a. The mean fatigue resistance of the local detail.

b. A "Reliability Factor" (factor of safety) that is a function of the slope of the S-N curve, the level of reliability and a coefficient of variation.

c. A "Random Load Factor" which is a function of the expected loading history of the ship and the slope of the particular detail's S-N curve.

The maximum allowable fatigue stress range, at the point in question, is the maximum peak-to-trough stress range expected once under the most severe sea state during the entire life of the ship. For this design method, the maximum allowable fatigue stress range, S_D, is defined as follows:

$$S_D = S_N \ x \ \xi \ x \ R_F$$

where: S_N = Mean Fatigue Stress Range (for the Local Detail)

ξ = Random Load Factor

R_F = Reliability Factor

The design method proceeds as follows:

a. The expected loading history for the ship detail must be established. This data is normally presented in the form of a Weibull probability density function and can be obtained from ship testing or analytical results. The shape factor for the selected Weibull probability density function must be calculated. An example of the development of a Weibull probability density function is shown in Appendix C.

b. The ship details to be analyzed are identified and broken down in terms of local fatigue details.

c. For each detail, the fatigue strength and slope of the S-N curve is obtained.

d. The random load factor (ξ) is determined based on the shape parameter (k) of the Weibull probability density function and the slope (m) of the S-N curve for the particular detail. A reprint of the table of random load factors is provided for convenience in Table 2-2.

e. The appropriate reliability factor (R_F) is obtained for the detail being considered. A reprint of the table of reliability factors is provided for convenience in Table 2-3.

f. The maximum allowable stress range is then compared to the one time maximum stress range expected during the lifetime of the ship.

2.4 S-N DATA

The S-N data used in this study is obtained from fatigue testing of actual welded details. The stress range for each detail is based upon the critical or "Hot Spot" stress in the detail. The S-N data for the details considered in this study are shown in Figures 2-9 through 2-13. This set of S-N data was chosen because it was consistent with the methodology employed. It should be noted, however, that difficulties arise in the use of "Hot Spot" S-N curves since there is no widely accepted collection embraced by the shipbuilding industry. To provide an acceptable collection of S-N curves for use in the design of structural details, the S-N data must be obtained from tests which are performed in a uniform and consistent manner. Other fatigue data exists and can be incorporated into the methodology.

Since the S-N data used in Reference (g) are based upon testing of actual welded details, the residual stresses from welding are inherently accounted for in the development of the allowable stress ranges. Should S-N data that does not account for residual stresses be used, an estimate of the effect of the residual stresses may be necessary. Fabrication procedures, such as post-weld heat treatment, can be used to reduce residual stresses from welding.

2.5 DEVELOPMENT OF MAXIMUM ALLOWABLE FATIGUE STRESS RANGE

The maximum allowable fatigue stress range, S_D, at the point in question is the maximum peak-to-trough stress range expected once under the most severe sea state during the life of the ship. It is defined as follows:

$$S_D = S_N x \ \xi \ x \ R_F$$

where: S_N = Mean Fatigue Stress Range (for the Local Detail)

ξ = Random Load Factor

R_F = Reliability Factor (Safety Factor)

2.5.1 Service Life

Naval Combatant - Naval design philosophy for this ship is a 30 year service life at 100,000,000 cycles.

Tanker - For the tanker design, a 20 year life at 100,000,000 cycles is assumed.

2.5.2 Mean Fatigue Stress Range, S_N

Naval Combatant - The critical "Hot Spot" in the naval combatant detail is equivalent to detail 30 of Reference (g). The S-N curve for detail 30 is shown in Figure 2-13. The Mean Fatigue Stress Range for 100,000,000 cycles is shown on this figure.

Tanker - The critical "Hot Spots" in the tanker detail are equivalent to details 18 and 19 of Reference (g). The S-N curves for details 18 and 19 are shown in Figures 2-10 and 2-11, respectively. The Mean Fatigue Stress Range for 100,000,000 cycles is shown on these figures.

2.5.3 Random Load Factor, ξ

Naval Combatant - Current Naval philosophy is to assume that ships respond to ocean waves in the narrow low frequency band. The distribution of peaks in a narrow low frequency band follows a Rayleigh Probability Distribution. This corresponds to a Weibull Shape Parameter, k, equal to 2.0. This distribution does not take into account the high frequency whipping, slamming and vibratory forces which also make up the long term loading history of the vessel. These high frequency loads may tend to shift the Weibull distribution to the left or lower the shape Parameter, k (see Figure 2-14). This study will assume a Weibull Shape Parameter, k, of 1.7 for the naval combatant.

Tanker - The Weibull Shape Parameter, k, for large tankers ranges from 0.7 to 1.0. This study will assume a Weibull Shape Parameter, k, equal to 1.0 for the tanker detail.

2.5.4 Reliability Factor, R_F

The Reliability Factor, R_F, will correspond to the 90 percent reliability level (L(n)). This level of reliability will provide factors of safety between 1.36 and 1.7 depending on the detail. These factors of safety are consistent with factors of safety used in naval specifications for structural design. A Reliability Factor corresponding to the 90% reliability level (L(n)) should be used in the design of new details. For the evaluation of the existing details, a factor of safety of 1.0 should be used (i.e., $R_F=1.0$).

2.6 LOADING DEFINITION

Only loads which are cyclic in nature and applied numerous times will be considered in this study. Ship launching, collision and grounding loads will not be considered. The four major categories of cyclic loads (with estimates of load reversals in a typical ship's lifetime) as outlined in Reference (g) are:

		Est. Load Reversals (Cycles)
a.	Low Frequency, wave-induced	1E7 - 1E8
b.	High Frequency	1E6
c.	Still Water	340
d.	Thermal	7000

The thermal and still water loadings are very low frequency and their effect is only to shift the mean stress. These stresses have very little effect on the lifetime load of the ship. Reference (g) indicates that the fatigue stress range may vary by as much as 25 percent depending on the type of stress reversal and thus the value of the mean stress. A greater fatigue stress range is realized during periods of complete stress reversal (i.e., mean stresses close to zero). The mean midship bending stress experienced by a ship varies with time and is a function of the ship's loading and ballasting configuration. It is assumed that any increases or decreases in the fatigue stress range due to thermal and still water loading will average out over the life of the ship. Therefore, they will not be considered in this method. The fatigue stress range documented in Reference (g) will be used without modification for mean stress variations.

The high frequency dynamic stresses caused by slamming and subsequent whipping of the hull are transient in nature. These high frequency stresses oscillate about the low frequency wave induced stresses causing variation in the maximum stress levels. These high frequency loadings are important in terms of the manner in which they add to the wave-induced stresses to establish the maximum stress ranges.

Predicting the occurrence and maximum values of slamming and whipping stresses is complex. Slamming and whipping do not occur during all operating profiles as do the low frequency wave induced stresses. The period in which the slamming events occur vary. The maximum stresses are a function of the phasing between the high frequency and low frequency stress cycles. Since the magnitude of slamming and whipping stresses are a function of heading and speed, which are controlled by the shipmaster, these stresses may be considered independent of sea condition.

As such, for the design procedure, the high frequency stresses are conservatively added to the low frequency stresses and incorporated into the long term stress distribution. If calculating "actual" loads, estimates of whipping moments can be made using procedures outlined in References (h) and (i).

The low frequency wave-induced loads are the most significant contributor to fatigue life considerations of ship structural details and are the focus of this method. While numerous factors affect wave induced stresses, the most significant factor is sea condition.

Thus, the long term loading histories used will be based upon sea state probabilities. The probability density function takes the form of a Weibull distribution.

The loading components significantly impacted by the low-frequency waves are:

a. Primary stresses resulting from hull girder bending.

b. External hydrodynamic pressures.

c. Internal tank loads.

Three levels of structural response need to be considered when addressing the application of load to the ship structure. The first is the primary response of the ship to the wave loads. Normal and shear stresses due to the global bending of the ship are considered. The next response is the secondary response due to local bending of girders, web frames or longitudinal stiffeners. The last is the tertiary response of plating between the stiffening elements.

The responses of a ship to an oblique sea are very complex. They are a function of many parameters including basic ship form, structural configuration, wave length, wave velocity, ship heading, etc. To further complicate the issue, the maximum vertical bending moment, lateral bending moment, torsional moment and shear loads occur at different combinations of heading and wavelength and are usually out of phase with the incident wave. This is in sharp contrast to the basic longitudinal strength philosophy of supporting the ship on a trochoidal wave of length L and a wave height based upon statistical data.

In recent years, the classification societies, to varying degrees, have allowed the strength design of ships to be based on a first principles approach using computer programs to determine the ship response and loadings. However, this seems to be the exception rather than the rule. As a result, this type of response data is rarely available. If it is, the shipowner is generally reluctant to provide it because of the proprietary nature of the information.

Three loading strategies are considered in the study, they are:

a. Unit loads

b. "Design" loads

c. "Actual" loads

The fine mesh finite element model of each detail being reviewed is first analyzed for unit forces, moments, pressures or stress variations which represent possible applied loadings. The results from these unit load cases are then multiplied by either the "design" or "actual" loads and combined in a rational manner to obtain an estimate of the one time maximum stress variation. Using this approach, the same detail can be assessed for numerous loading conditions without re-running the finite element analysis of the detail. Also, several details may first be rated and modified based upon the stress results of the unit loads, using the stress concentrations as a criteria. Then fatigue lives can be evaluated for the most promising detail configurations based upon the "design" or "actual" load combinations.

This approach assumes a static linear elastic analysis. The numerical accuracy of available finite element programs is such that the results of a 1 pound (4.448 N) unit load analysis, when multiplied by 1000, are essentially the same as those obtained by applying a 1000 pound (4448 N) load directly. The use of unit loads is a widely accepted practice in structural analysis. In Bruhn's demonstration of the shear lag problem, Reference (j), he develops beam stiffness matrices based on unit loads. Bruhn also uses unit loads when comparing finite element solutions to test results. When evaluating existing details, should the stress levels be such that they are no longer linear elastic, or they exceed the buckling limits, it may be required to perform more elaborate elastoplastic or buckling analyses to evaluate the stress levels accurately.

"Design" loads can be based upon either classification society design loads or longitudinal strength calculations. The longitudinal strength calculations evaluate the strength of the ship by supporting it on a trochoidal wave with a wavelength, L, equal to the length between perpendiculars and a wave height based upon statistical data (Example: For naval combatants, the wave height = $1.1 \sqrt{L}$). Two positions of the wave are considered, the first with the wave crest positioned at midship (Hogging) and the other with the trough positioned at midship (Sagging). Estimates of the hydrostatic pressure are made by using the wave profile assumed in the longitudinal strength calculations. Estimates of the accelerations due to the motion in a seaway are made using formulas based upon the ship pitch period and pitch angle assuming head sea conditions consistent with the design wave used.

It should be noted that, although these loads only estimate the true loading experienced by the ship, they should be sufficient to aid the designer in choosing details which will perform satisfactorily under fatigue loading during the early stages of design. However, estimates of fatigue lives based on these loads are only estimates. At this point in time, these "design" loads are more likely to be available to the designer for use in the fatigue assessment.

Programs now exist which will analytically develop "actual" loads experienced in a seaway using first principles and strip theory or linear 3-dimensional hydrodynamic techniques. Hull pressure distributions as well as accelerations due to roll, pitch, sway, yaw, surge and heave can be obtained. These loads can then be applied to obtain the response of the ship to these loads (i.e., bending moment). One method for obtaining the response of a ship in a seaway is by the use of Response Amplitude Operators (RAOs). The RAOs characterize the ship's response per unit wave height. The RAO is a function of ship speed and heading. Therefore, at a particular speed and heading the responses of the ship to a series of varying wavelength waves of unit amplitude are obtained. A plot of the peak response (bending moment) per wavelength is made. Once these unit RAOs have been developed, it is then necessary to multiply the unit RAOs by the wave spectra of interest to obtain the actual response of the ship.

Since the scope of this task did not allow for the development of RAOs, an attempt was made to obtain this information from the owners and operators. Generally, the information was not available or it was considered proprietary and, therefore, was unavailable for distribution. As a result, realistic numerical examples using this procedure could not be developed. A procedure for the development of the "actual" loads is, however, presented.

2.6.1 Unit Load Cases

The unit load cases evaluated for the naval combatant detail are as follows:

a. Vertical Hull Primary Stress

b. External Hydrostatic Pressure

c. Internal Girder Moment

d. Internal Girder Shear

The unit load case for primary stress due to vertical hull bending is shown on Figure 2-15. An applied displacement is used to obtain the stress gradient shown at midship, assuming that plane sections remain plane. The assumed boundary conditions are also indicated in the figure. The unit load case for external hydrostatic pressure is shown in Figure 2-16. A uniform 1 psi (6.895E-3 N/mm^2) pressure is applied to the finite element model. The unit load case for internal girder moment is shown in Figure 2-17. The equivalent strain for a 1 in-kip (112.98 m-N) moment is applied to the finite element model. The unit load case for internal girder shear is shown in Figure 2-18. An applied displacement is used to obtain an equivalent stress distribution for a 1 kip (4448 N) shear load.

The unit load cases for the tanker detail are as follows:

a. Vertical Hull Primary Stress

b. External Hydrostatic Pressure/Internal Hydrodynamic Pressure

c. Internal Shear Stress

The unit load case for vertical hull bending is shown on Figure 2-19. An applied displacement is used to obtain a uniform 1 ksi (6.895 N/mm^2) stress gradient at midship. The unit load case for external hydrostatic pressure/internal hydrodynamic pressure is shown in Figure 2-20 . A uniform 1 psi (6.895E-3 N/mm^2) pressure is applied to the finite element model. The unit load case for internal stiffener shear is shown in Figure 2-21. An applied displacement is used to obtain an equivalent stress distribution for a 1 kip (4448 N) shear load.

2.6.2 <u>"Design" Loads</u>

The "design" loads used for assessing the one time maximum stress range for the naval combatant are shown schematically in Figure 2-22. The actual hogging and sagging primary stresses are shown below. The total variation in primary stress through the wave cycle is 12.52 tsi (28.0 ksi, 193.1 N/mm^2). The total variation in hydrostatic head is equal to the wave height [(1.1 $\sqrt{L}$) = 25.3 feet (7.71 m)]. Internal load variations are based on the maximum ship accelerations in a seaway.

Because the naval combatant under consideration has a compensated fuel system, the innerbottom fuel tanks are constantly pressed-up with either fuel, water or a combination of both. As a result, the non-tight longitudinal girder under consideration (Figure 2-5) will not experience a variation in pressure normal to the girder web due to ship motion accelerations.

The total stress variation will be the summation of the maximum stresses in the hogging and sagging conditions. The maximum stress will be a combination of the primary stress and hydrostatic stress in the longitudinal girder.

A summary of the "design" loads used for the naval combatant detail are listed below:

Hogging at Midship

Primary Stress = -8.19 tsi (-18.35 ksi, -126.5 N/mm^2) compression

Hydrostatic Load = 30.65 feet (9.34 m)

(external pressure = 13.62 psi (9.391E-2 N/mm^2))

Sagging at Midship

Primary Stress = 4.33 tsi (9.70 ksi, 66.88 N/mm^2) tension

Hydrostatic Load = 5.35 feet (1.63 m)

(external pressure = 2.38 psi (1.641E-2 N/mm^2))

A finite element model of the innerbottom grillage was used to obtain the grillage moments and shears at the interface with the fine mesh finite element model. They are:

Grillage Forces & Moments

Hogging

Moment	=	3344.0 in-kips (3.778E5 m-N)
Shear	=	7.63 kips (3.394E4 N)

Sagging

Moment	=	584.0 in-kips (6.598E4 m-N)
Shear	=	1.33 kips (5.916E3 N)

The "design" loads used for assessing the one time maximum stress range for the tanker were developed from the following four loading conditions:

Full Load Departure

Maximum Hogging Moment	1,753,958 ft-tons (5.327E6 m-N)
Maximum Hogging Stress	7.7 tons/in^2 (118.9 N/mm^2)
Location of Maximum Moment	470 feet (143.3 m) aft of the forward perpendicular
Maximum Sagging Moment	2,214,832 ft-tons (6.726E6 m-N)
Maximum Sagging Stress	9.72 tons/in^2 (150.1 N/mm^2)
Location of Maximum Moment	390 feet (118.9 m) aft of the forward perpendicular

Full Load Arrival

Maximum Hogging Moment	1,682,617 ft-tons (5.110E6 m-N)
Maximum Hogging Stress	7.38 tons/in^2 (113.98 N/mm^2)
Location of Maximum Moment	470 feet (143.3 m) aft of the forward perpendicular
Maximum Sagging Moment	2,261,191 ft.-tons (6.867E6 m-N)

Maximum Sagging Stress	9.93 tons/in^2 (153.4 N/mm^2)
Location of Maximum Moment	400 feet (121.9 m) aft of the forward perpendicular

Normal Ballast Departure

Maximum Hogging Moment	2,588,871 ft-tons (7.862E6 m-N)
Maximum Hogging Stress	11.37 tons/in^2 (177.9 N/mm^2)
Location of Maximum Moment	400 feet (121.9 m) aft of the forward perpendicular
Maximum Sagging Moment	711,631 ft-tons (2.161E6 m-N)
Maximum Sagging Stress	3.81 tons/in^2 (58.8 N/mm^2)
Location of Maximum Moment	669 feet (203.9 m) aft of the forward perpendicular

Normal Ballast Arrival

Maximum Hogging Moment	2,518,777 ft-tons (7.649E6 m-N)
Maximum Hogging Stress	11.06 tons/in^2 (170.82 N/mm^2)
Location of Maximum Moment	400 feet (121.9 m) aft of the forward perpendicular
Maximum Sagging Moment	716,269 ft-tons (2.175E6 m-N)
Maximum Sagging Stress	3.16 tons/in^2 (48.8 N/mm^2)
Location of Maximum Moment	237 feet (72.2 m) aft of the forward perpendicular

The maximum variation in primary stress through the wave cycle at the longitudinal of interest is 12.39 tsi (27.8 ksi, 191.7 N/mm^2). The total variation in hydrostatic head is equal to the wave height [(1.1 $\sqrt{L}$) = 32.0 feet (9.75 m)].

Internal tank pressure variations are based on the maximum ship accelerations in a seaway. The fundamental equations for ship motion accelerations for the tanker are based upon roll, pitch, yaw, heave and surge accelerations as follows. These equations were taken from Reference (k).

$$A_x = g\sin\ \theta + s + \frac{4\pi^2}{T_p^2}\theta^2 X + \frac{4\pi^2}{T_p^2}\theta Z$$

$$A_y = g\sin\ \phi + s + \frac{4\pi^2}{T_p^2}\theta X + \frac{4\pi^2}{T_r^2}\phi^2 Y + \frac{4\pi^2}{T_r^2}\phi Z$$

$$A_z = g \pm \left(h + \frac{4\pi^2}{T_p^2}\theta X + \frac{4\pi^2}{T_r^2}\phi Y \right)$$

(In the factor A_z, the plus sign relates to a downward force, and the minus sign relates to an upward force.)

Where:	θ	=	Maximum pitch angle (radians) (Note: Values from Table 2-4 are multiplied by 0.01745 to convert degrees to radians).
	ϕ	=	Maximum roll angle (radians) (Note: Values from Table 2-5 are multiplied by 0.01745 to convert degrees to radians).
	$A_{x,y,z}$	=	Loading factor in x(longitudinal), y(transverse), or z(vertical) direction (in m/sec^2 or ft/sec^2).
	T_p	=	Pitch period (seconds) (From Table 2-4).
	T_r	=	Roll period (seconds) (From Table 2-5).
	h	=	Heave acceleration (in m/sec^2 or ft/sec^2) (Note: Values from Table 2-6 are multiplied by 9.807 to convert g's to m/sec^2 or by 32.15 to convert g's to ft/sec^2).

s	=	Surge acceleration (in m/sec^2 or ft/sec^2) (Note: Values from Table 2-6 are multiplied by 9.807 to convert g's to m/sec^2 or by 32.15 to convert g's to ft/sec^2).
X	=	Longitudinal distance from center of gravity (in meters or feet).
Y	=	Transverse distance from center of gravity (in meters or feet).
Z	=	Vertical distance above center of gravity (in meters or feet).
g	=	Acceleration due to gravity (9.807 m/sec^2 or 32.15 ft/sec^2).

The following parameters were used in the development of the tanker motion accelerations:

Beam (B)	173'-0" (52.73 m)
Length between perpendiculars (LBP)	864'-0" (263.35 m)
Draft	57'-3" (17.45 m)
Displacement	75,272 tons (76,481 kg)
GM	38.1' (11.61 m)
Roll Constant (C)	0.4 sec/$\sqrt{\text{ft}}$ (0.72 sec/$\sqrt{\text{m}}$)
Roll Period (Tr)	11.2 seconds
Pitch Period (Tp)	8 seconds
Maximum Roll Angle	31 degrees
Maximum Pitch Angle	5 degrees
Heave Acceleration	0.2 g

Surge Acceleration 0.1 g

The resulting equations for the longitudinal, transverse and vertical accelerations (g's) for the tanker based on pitch motion only are:

A_x* = 0.1872 + 1.46E-4X + 1.67E-3Z g's

A_y* = 0.00084X g's

A_z* = 1.0 +/- (0.2 + 1.67E-3X) g's

* Constants based on units of feet.

The total instantaneous internal tank pressure (static plus dynamic) for any tank position can be calculated using the following:

$$P=P_o+h_t\,\rho\sqrt{\left(\frac{A_x}{g}\right)^2+\left(\frac{A_y}{g}\right)^2+\left(\frac{A_z}{g}\right)^2}$$

Where:

	P	=	the total instantaneous internal tank pressure at a tank boundary point (in psi or N/mm^2). (Note: P does not include the effects of sloshing.)
	P_o	=	is either the vapor pressure, or the value at the relief valve setting (in psi or N/mm^2).
	ρ	=	the density of the fluid (in lb/in^3 or N/mm^3).
	h_t	=	the total pressure head defined by the height of the projected fluid column in the direction of the total instantaneous acceleration vector (in inches or mm).
	A_x, A_y, A_z	=	the loading factor in the x(longitudinal), y(transverse), or z(vertical) direction from page 2-19 at a tank boundary point (in m/sec^2 or ft/sec^2).
	g	=	the acceleration due to gravity (9.807m/sec^2 or 32.15 ft/sec^2).

A summary of the "design" loads used for the tanker detail are listed below:

Full Load Departure

Primary Stress

Hogging -12,275 psi (-84.64 N/mm^2)

Sagging 15,478 psi (106.72 N/mm^2)

External Hydrostatic Pressure

Hogging 29.1 psi (0.20 N/mm^2)

Sagging 14.9 psi (0.103 N/mm^2)

Internal Stiffener Shear

Hogging 59,389 lbs. (2.642E6 N)

Sagging 30,388 lbs. (1.352E6 N)

Internal Ballast Tank Pressure

Bow Up 0 psi (0 N/mm^2)

Bow Down 0 psi (0 N/mm^2)

Full Load Arrival

Primary Stress

Hogging -11,767 psi (-81.13 N/mm^2)

Sagging 15,813 psi (109.04 N/mm^2)

External Hydrostatic Pressure

Hogging 29.1 psi (0.200 N/mm^2)

Sagging 14.9 psi (0.103 N/mm^2)

Internal Stiffener Shear

Hogging 59,389 lbs. (2.642E6 N)

Sagging 30,388 lbs. (1.352E6 N)

Internal Ballast Tank Pressure

Bow up 0 psi (0 N/mm^2)

Bow Down 0 psi (0 N/mm^2)

Normal Ballast Departure

Primary Stress

Hogging -18,104.0 psi (-124.83 N/mm^2)

Sagging 3,741.0 psi (25.79 N/mm^2)

External Hydrostatic Pressure

Hogging 29.1 psi (0.20 N/mm^2)

Sagging 14.9 psi (0.103 N/mm^2)

Internal Stiffener Shear (from external load)

Hogging 59,389.0 lbs. (2.642E6 N)

Sagging 30,388.0 lbs. (1.352E6 N)

Normal Ballast Arrival

Primary Stress

Hogging -17,606.0 psi (-121.39 N/mm^2)

Sagging 3,763.0 psi (25.95 N/mm^2)

External Hydrostatic Pressure

Hogging 29.1 psi (0.20 N/mm^2)

Sagging 14.9 psi (0.103 N/mm^2)

Internal Stiffener Shear (from external load)

Hogging 59,389.0 lbs. (2.642E6 N)

Sagging 30,388.0 lbs. (1.352E6 N)

Internal Ballast Tank Pressure	Internal Ballast Tank Pressure
Bow up 25.9 psi (0.179 N/mm^2)	Bow up 25.9 psi (0.179 N/mm^2)
Bow down 40.95 psi (0.282 N/mm^2)	Bow down 40.95 psi (0.282 N/mm^2)
Internal Stiffener Shear (from internal load)	Internal Stiffener Shear (from internal load)
Ballast 83,578.0 lbs.(3.718E5 N) (bow down)	Ballast 83,578.0 lbs. (3.718E5 N) (bow down)
Ballast 58,809.0 lbs (2.616E5 N) (bow up)	Ballast 58,809.0 lbs. (2.616E5 N) (bow up)

2.6.3 "Actual" Loads

The second ("actual") loading strategy takes a more precise first principles approach to obtain the maximum one time stress range experienced by the ship. The first step would be to describe the wave environment. The severity of sea state depends to a great extent on the geographical location. It is necessary to statistically analyze long-term significant wave data accumulated in the area of interest. Several probability distributions have been proposed which appear to fit the data:

a. log-normal

b. modified log-normal

c. three parameter Weibull distribution

d. combined exponential and power distribution

e. modified exponential

f. generalized gamma distribution

For predicting the responses of a ship in a seaway, spectral analysis in the frequency domain is most commonly undertaken. This approach is advantageous since the system response can be evaluated for all frequencies including those which may produce resonance conditions.

Ideally, it would be best to evaluate the ship response by employing wave spectra representing various conditions in the area where the ship will be operated. This, however, is not usually done. Instead, the analyses are performed by applying available spectral formulations. Some of the basic spectra currently in use, as summarized by Ochi, Reference (l), are listed below. They are based on significant wave height or significant wave height and wave period.

a. Pierson-Moskowitz Spectrum

b. Two Parameter (Bretschnider)

c. Six Parameter Spectra Family

d. JONSWAP Spectrum

The second step would be to obtain or develop transfer functions or response amplitude operators (RAOs) for the ship for unit wave heights. These may be obtained from sea trial data or evaluated analytically using sea keeping programs which employ strip theory or linear 3-dimensional hydrodynamic techniques. Strip theory provides reasonable results for calculating cumulative responses such as motions and hull girder forces, but has been criticized for inaccurate predictions of hull pressures. The linear 3-dimensional hydrodynamic techniques provide more accurate hull pressures.

The total response spectrum can now be obtained by multiplying the wave spectrum by the transfer function or response amplitude operator. Critical load combinations which include vertical bending, lateral bending, torsional bending, vertical shear and lateral shear with proper consideration for heading, speed and phasing relationships can then be developed.

The current issue of the ABS Rules now allows for a tanker to be classified "DLA" if analyzed by the Dynamic Load Approach (DLA). The DLA takes a first principles approach similar to that discussed above. ABS currently has a PC based ship motions program called SHPMO which is compatible with, and specifically tailored for, the DLA method of tanker strength assessment. Other institutions (e.g. The University of Michigan) have ship motions programs capable of developing the motion loads and pressures required to develop the hull stresses. Many of these programs are, however, still developmental.

2.7 FINE MESH FINITE ELEMENT MODELS

Depending upon the complexity of the loading distributions, several modeling strategies may be required. For complex loading combinations found in oblique seas, it will be necessary to model a portion of the hull and apply the global primary loads to the model. Strains obtained from these global models can be applied at the interface of the fine mesh model to obtain the detailed stress distribution in the detail of interest. For simpler "design" loadings the strains due to primary and secondary loadings may be applied directly to the fine mesh models.

In this study the "design" loadings used in the numerical examples were simple enough that most of the loadings could be applied directly to the fine mesh models. The one exception to this approach was for the naval combatant internal girder moments and shears. A beam representation of the innerbottom between subdivision bulkheads in the area of interest was developed to obtain the internal girder moments and shears due to the hydrostatic loads at the interface with the fine mesh model.

An isometric view of the finite element model for the longitudinal girder stiffener ending for the naval combatant is shown in Figure 2-23. The elements used in the model are planar 3 node and 4 node plate elements, beam elements and rod or axial elements. The effective tank top plating and shell plating of the longitudinal girder were modeled using axial elements. Only one girder stiffener is modeled in detail, the other stiffener properties are represented using beam elements. All other structural elements are modeled using 3 node and 4 node plate elements.

A 1/4" x 1/4" (6.35 mm x 6.35 mm) element mesh is used around the toe of the weld at the stiffener snipe. A view of this region is shown in Figure 2-24. The plate elements transition to a 4" x 4" (101.6 mm x 101.6 mm) mesh away from the area of maximum stress concentration. A triangular plate element is used to represent the weld which softens the stress gradient at the stiffener snipe.

An isometric view of the finite element model for the shell longitudinal to web frame connection for the tanker is shown in figure 2-25. The elements used in the model are 6 node and 8 node first order solid elements and rod or axial elements. The solid elements were chosen to effectively model the lap of the flat bar header to the web of the shell longitudinal. The effective bulkhead plating and shell plating are modeled using axial elements.

A 1/4" x 1/4" (6.35 mm x 6.35 mm) element mesh is used around the critical areas of the lapped connection. A view of this region is shown in figure 2-26. The solid elements transition to a 4" x 4" (101.6 mm x 101.6 mm) mesh away from the area of maximum stress concentration. A 6 node element is used to represent the weld which softens the stress gradient at the lap.

2.8 APPROACH FOR COMPARISON OF ANALYTICAL RESULTS

The approach for evaluation of analytical results is based upon the comparison of the "Hot Spot" stress range with that of the allowable stress range for the area of interest. The fine mesh finite element models used in this study contain elements which represent the weld geometry. This was done to soften the sharp stress gradients which occur at the abrupt discontinuities of welded structural details. Methods for "smoothing out" the sharp stress gradients, by using a weighted average of the element centroidal stresses of a number of elements approaching the discontinuity, are posed by ABS in Reference (m). This method assumes a stable or uniform stress field leading up to the discontinuity. This is not always the case, as can be seen in the longitudinal girder stiffener end detail for the naval combatant. The sniped end is only one inch from the subdivision bulkhead which also has its own stress gradient. Although arguably conservative, it was decided to evaluate the stresses in the elements at the base of the weld.

Since the S-N data being used already includes the effect of the weld, the stresses in the weld elements themselves are not included in the calculation for the critical average nodal stresses. Only the finite elements in the parent material under consideration are included. Principal stresses are calculated in the plane of potential crack propagation. These principal stress ranges are then compared to the allowable stress ranges as calculated in Appendix A.

The critical areas for the existing naval combatant detail are shown in Figure 2-27. The critical areas for the existing tanker detail are shown in Figure 2-28. Stress results for these details are presented in Section 3.0.

2.9 ALTERNATIVE DETAILS

In reviewing methods to eliminate the stress concentrations in the naval combatant and tanker details, several approaches were studied. For the naval combatant detail, the following effects were considered:

a. Locally increasing the web thickness in way of the stiffener snipe (Alternate 1)

b. Reducing the size (depth) of the end snipe (Alternate 2)

c. Reducing the standoff distance from the bulkhead (Alternate 3)

d. Welding the stiffener web directly to the bulkhead, and sniping the flange (Alternate 4)

e. Adding a header to the Alternate 4 configuration (Alternate 5)

f. Welding the stiffener full at the bulkhead (Alternate 6)

These modifications are shown schematically in Figure 2-29.

For the tanker detail, the following effects were considered:

a. Elimination of the lapped connection (Alternate 1)

b. Addition of brackets to reduce the end stresses (Alternate 2)

These modifications are shown schematically in Figure 2-30.

2.10 MATERIAL EFFECTS

Fatigue tests have been conducted on plates and weldments of structural steels with yield strengths ranging from 30 ksi (206.85 N/mm^2) to 100 ksi (689.5 N/mm^2). The steels have been grouped into three categories:

Mild Steel(MS) - 36 ksi (248.22 N/mm^2) yield strength

High Strength Steel(HSS) - 50 ksi (344.75 N/mm^2) yield strength

Quenched and Tempered Steels - 100 ksi (689.5 N/mm^2) yield strength

In general, as the number of cycles is increased, the variation from the mean fatigue strength decreases. Also, this variation decreases further when the specimen is a weldment in a corrosive environment. In view of the small differences generally obtained for the fatigue strengths of most welded members and details fabricated from mild steel, high strength steel and quenched and tempered steels, the material factor has been disregarded in this fatigue design approach. One factor, which substantiates this approach, is the data scatter associated with the S-N data for various steels at large cycles.

Most of the fatigue design methods currently in use disregard the material effects of the various steels. Therefore, from a design perspective, there is no difference in the fatigue performance of higher strength steel from that for mild steel. To illustrate this point, and provide a comparison of the stress levels expected in a mild steel (MS) hull versus the stress levels obtained for the high strength steel (HSS) hull investigated, the existing tanker shell longitudinal detail was modified to reflect comparable MS scantlings. This was accomplished by using the strength ratio (Q) provided in the ABS rules. The strength ratio (Q) is a multiplier on the MS strength requirements to provide an equivalent HSS hull. As an example:

$$SM_{HTS} = Q \ x \ \ SM_{MS}$$

For the H36 steels in the tanker example, this strength factor (Q) is 0.72. Taking the inverse, the equivalent MS hull section modulus must be 38% greater than the HSS hull section modulus. The same holds true for the section modulus requirement for the local shell longitudinal.

The shell plating must first be increased as part of the increased hull girder section modulus. In this case, this requirement is more critical than the local shell plating requirements specified in the shell section of the ABS Rules. Since the weather deck, side shell and bottom shell of the HSS hull investigated are all 0.75" (19.05 mm), the equivalent MS hull form was also assumed to have a uniform thickness. Assuming a symmetric section and equal plate thickness, the increase in plate thickness will be in approximately the same proportion as the increase in section modulus. Therefore, the equivalent MS shell plating was estimated to be 1.38 times 0.75" (19.05 mm), or 1.035" (19.05 mm) thick.

The existing section modulus for the shell longitudinal is 176.0 in^3 (2.884E6 mm^3). The equivalent MS section is 1.38 times 176.1 in^3 (2.884E6 mm^3), or 243.0 in^3 (3.982E6 mm^3). Using the revised shell plating thickness of 1.035" (26.3 mm), the web and flange thicknesses were increased to 0.6875" (17.46 mm) and 1.0" (25.4 mm), respectively. The overall depth and flange width were held constant. This configuration provides the required section modulus of 243.0 in^3 (3.982E6 mm^3).

The solid elements of the mathematical model for the tanker shell longitudinal were modified to reflect the revised MS scantlings. The unit load cases were then re-analyzed using the updated model. Since the structural weight increase is uniform throughout the hull, and the increase in structural weight is a small percentage of the total ship loading, it was assumed that the ship's bending moments would not change. The longitudinal stresses for the various loading conditions were, therefore, reduced by 38%. The internal and external hydrostatic loads will remain essentially constant. However, due to the increase in section modulus for the shell longitudinal, the stress levels in the longitudinal for the hydrostatic loadings will be reduced.

2.11 BUCKLING CONSIDERATIONS

The fundamental structural element used in the construction of ships is the plate. Decks, shell plating, girders, longitudinals, stiffeners, brackets, etc. are generally fabricated from plates. Proper consideration for plate buckling is essential in order to develop the global strength of the ship. There is an inter-dependence between the primary and secondary structural elements. In order for a shell longitudinal to develop its full compressive and bending capacities, the local buckling strength of the flanges and web must exceed the applied compressive loads. In order for the shell plating to develop its full compressive capacity, the buckling strength of the supporting shell longitudinals must exceed the applied compressive load.

The critical buckling stress is a function of material yield strength, modulus of elasticity, Poisson's ratio and geometric parameters (aspect ratio and slenderness ratio). Standard buckling curves for the critical buckling stress can be found in many texts and specifications, such as References (n) and (o). The allowable buckling stress curves contain three regions:

a. Yielding

b. Inelastic buckling (Partial yielding)

c. Elastic buckling (Euler hyperbola)

Buckling is usually considered to be a strength consideration in design. However, should the critical buckling stress of a structural element be low enough, it can become a fatigue consideration. If the critical buckling stress of a structural element is within the critical operating profiles, such that it "pants", this additional stress due to the "panting" should be considered in the fatigue evaluation. This would not normally be a consideration for built-up shapes because of the local buckling requirements (compact sections) necessary to develop the full bending stress. Larger girders, deck panels and shell panels, however, if not considered properly, could become problems.

Should the compressive stress during operation exceed the buckling capacity of a particular element, then estimates of the buckled shape can be made considering the post buckling behavior and large deflection theory. This buckled shape may then be imposed on the structural model to develop the stresses resulting from the buckled shape. These additional stresses will contribute to any fatigue damage of the detail.

Unlike typical wave induced loads, the additional stress due to buckling would only be considered in operational modes in which the buckling capacity of the plate in question is exceeded. Since this stress does not exist for all sea states, it will not be additive to all other wave induced stresses. For this reason, any stresses due to buckling must be reduced prior to their addition to other wave induced stresses. This will account for the reduced number of cycles in which stresses due to buckling act in combination with wave induced stresses.

In this fatigue analysis methodology, additional stresses due to buckling will not be considered. Instead, the design of the structural details will insure that buckling of the detail's components will not occur for the anticipated ship loadings.

2.12 CORROSION

Corrosion of ships is a significant and complex concern. The extent of corrosion can range from minor, for frequently maintained naval combatants, to major for cargo holds and ballast tanks of tankers. Corrosion rates will vary depending upon many factors including surface treatment, cargo composition, steel composition, temperature, etc. It will be necessary to take this steel wastage into account when considering fatigue.

The term "net scantlings" has been used to define the design scantlings minus an allowance for corrosion wastage. It is the "net scantlings" which should be used when evaluating global hull stresses and local element stresses in the fatigue assessment. If specific corrosion rates are unavailable, ship classification societies provide wastage allowances which may be used to determine the "net scantlings".

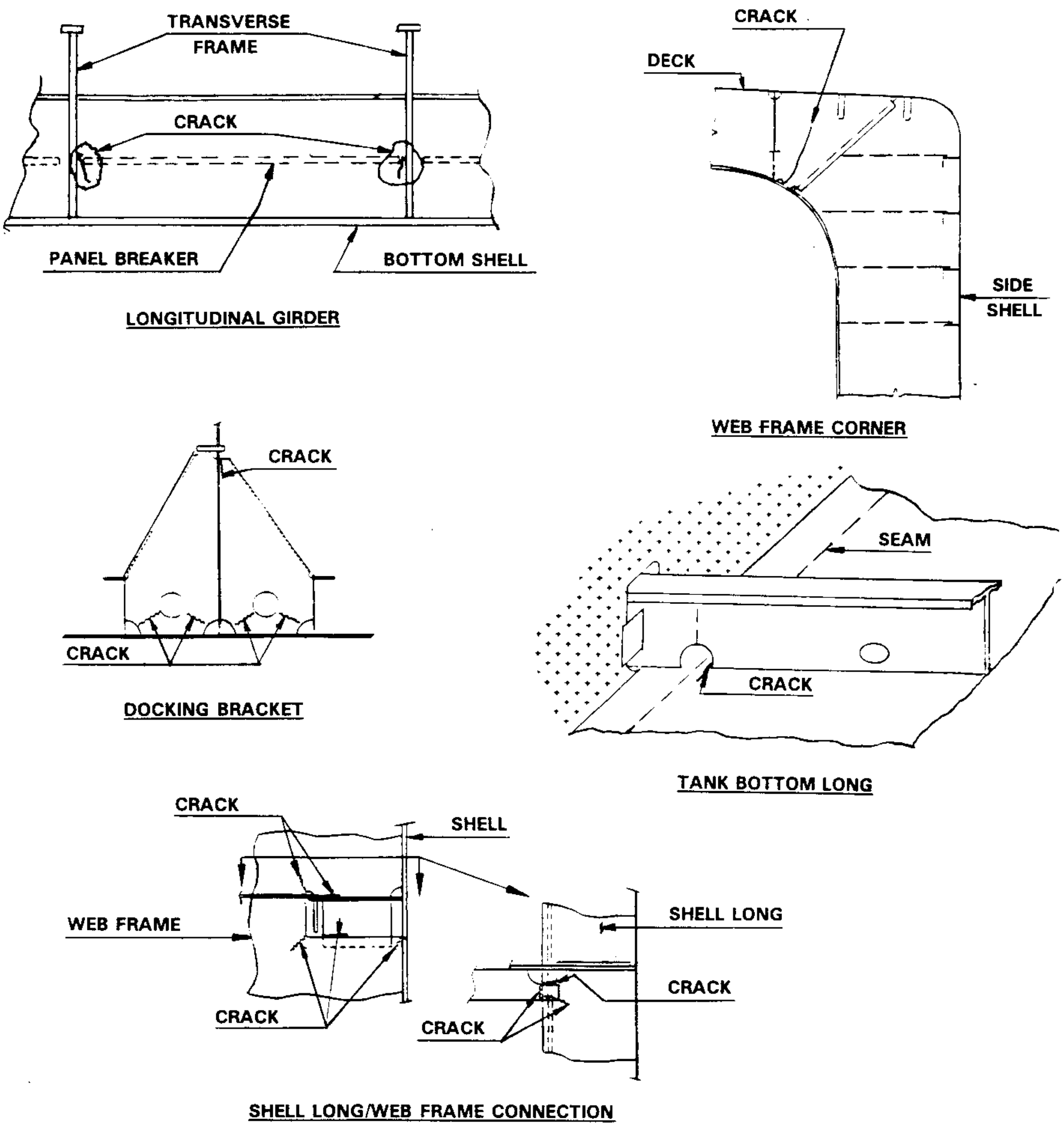

FIGURE 2-1. TYPICAL TAPS TANKER CRACKING PROBLEMS

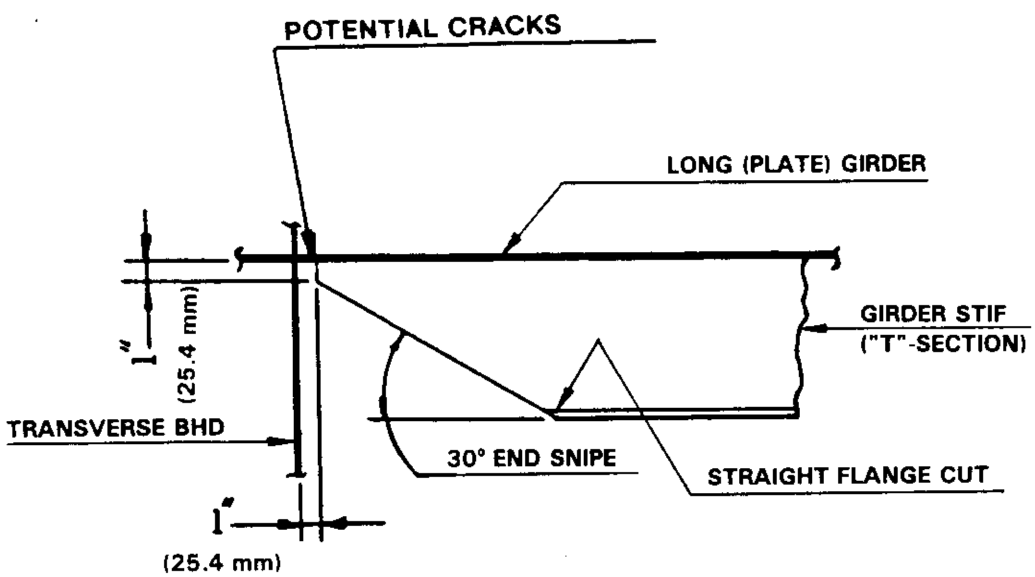

FIGURE 2-2. LONGITUDINAL GIRDER STIFFENER ENDING - NAVAL COMBATANT

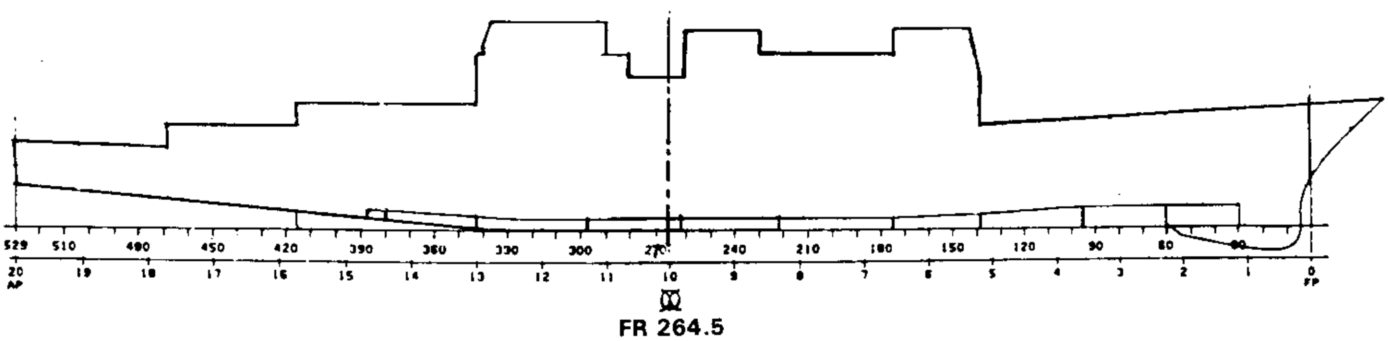

DISPLACEMENT = 8335 LTONS (8.467E6 Kg)

LENGTH BETWEEN PERPENDICULARS = 529 FT. (161.24 m)

FIGURE 2-3. NAVAL COMBATANT OUTLINE AND CHARACTERISTICS

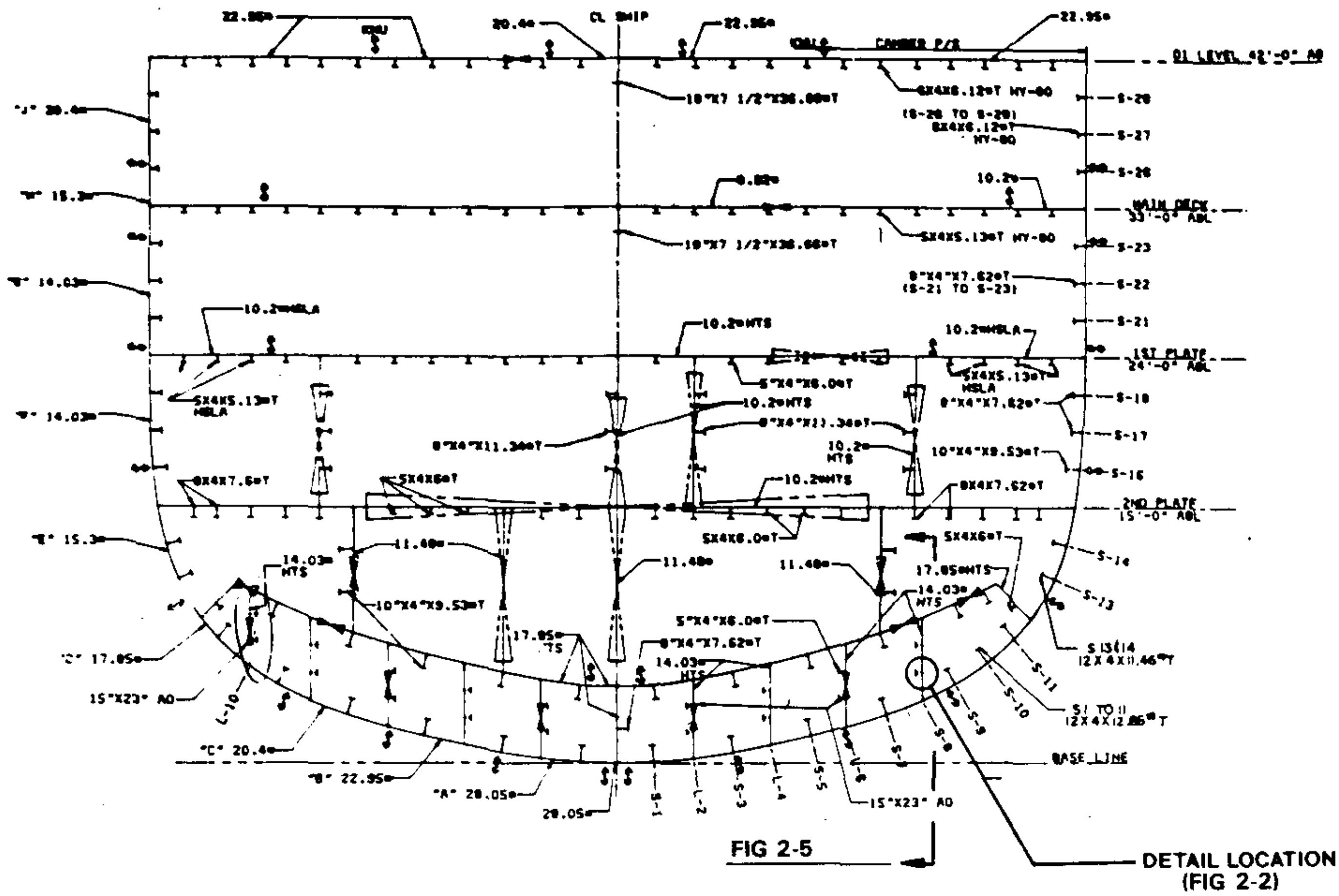

FIGURE 2-4. NAVAL COMBATANT MIDSHIP SECTION

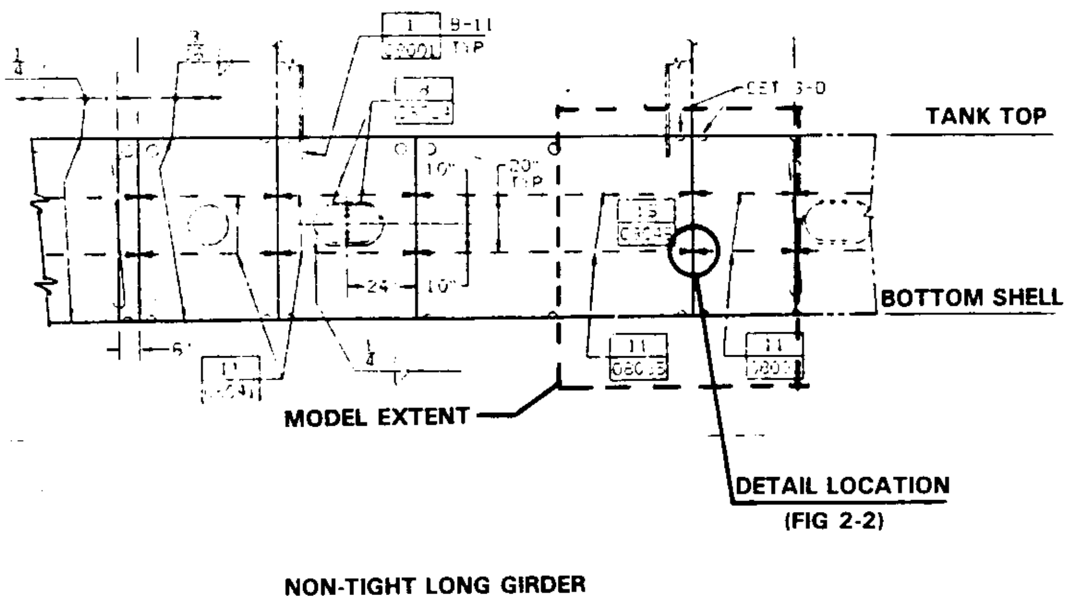

FIGURE 2-5. NAVAL COMBATANT INNERBOTTOM GIRDER CONFIGURATION

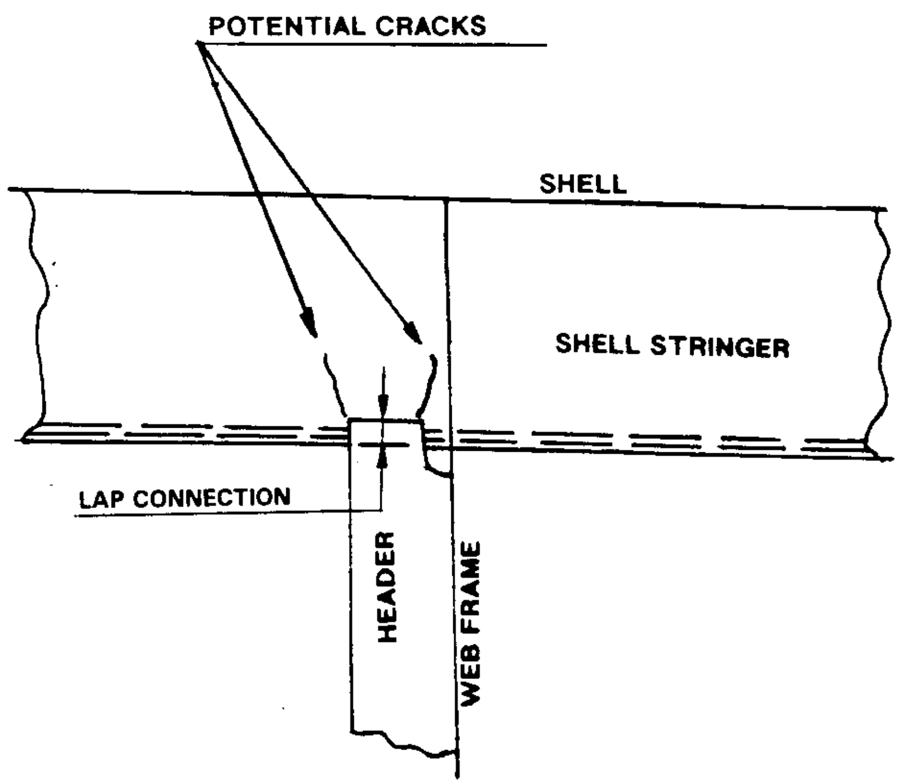

FIGURE 2-6. SHELL LONGITUDINAL TO WEB FRAME CONNECTION - TANKER

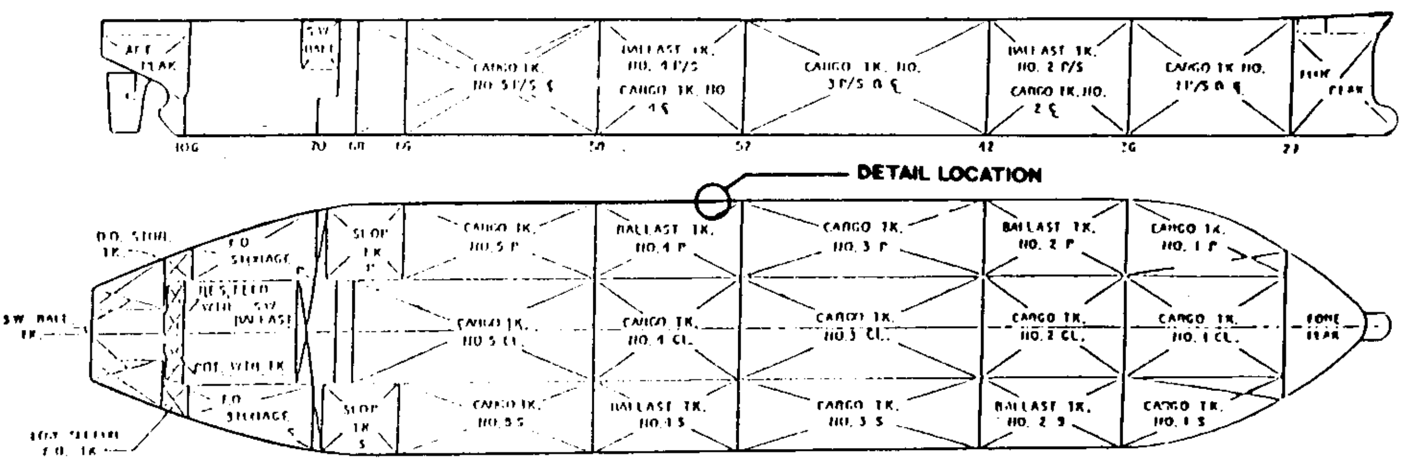

PRINCIPAL PARTICULARS

GROSS REGISTERED TONNAGE - 75,272.14 LTONS (7.647E7 Kg)
LENGTH BETWEEN PERPENDICULARS - 864'-0" (263.35 m)
MOLDED BEAM - 173'-0" (52.73 m)
MOLDED DEPTH TO MAIN DK AT SIDE - 75'-0" (22.86 m)

FIGURE 2-7. TANKER OUTLINE AND CHARACTERISTICS

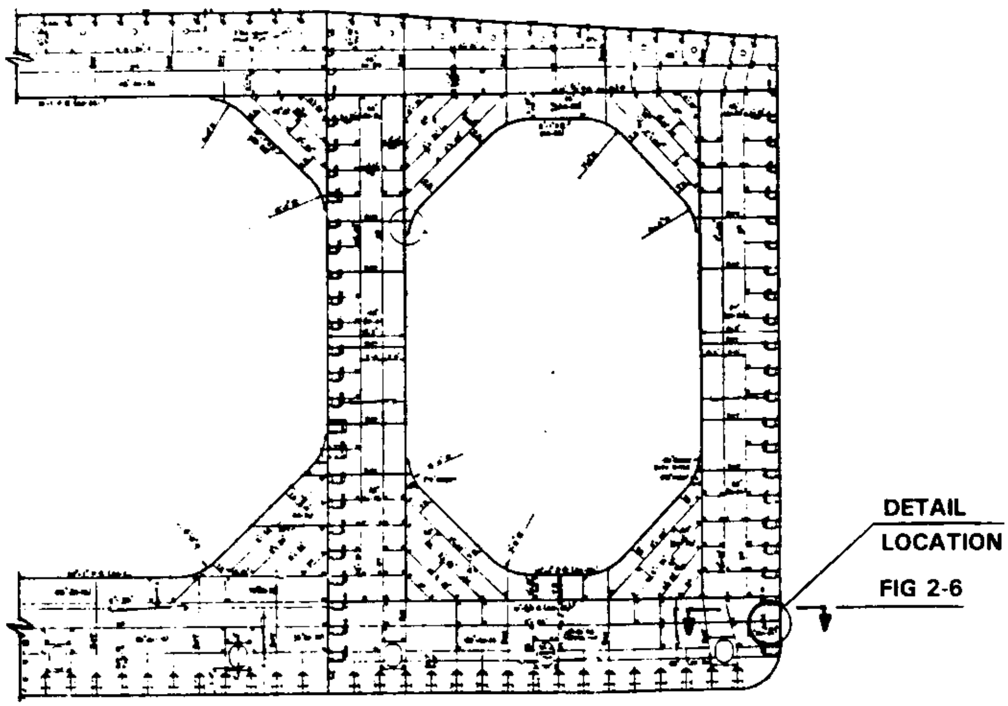

FIGURE 2-8. TANKER MIDSHIP SECTION

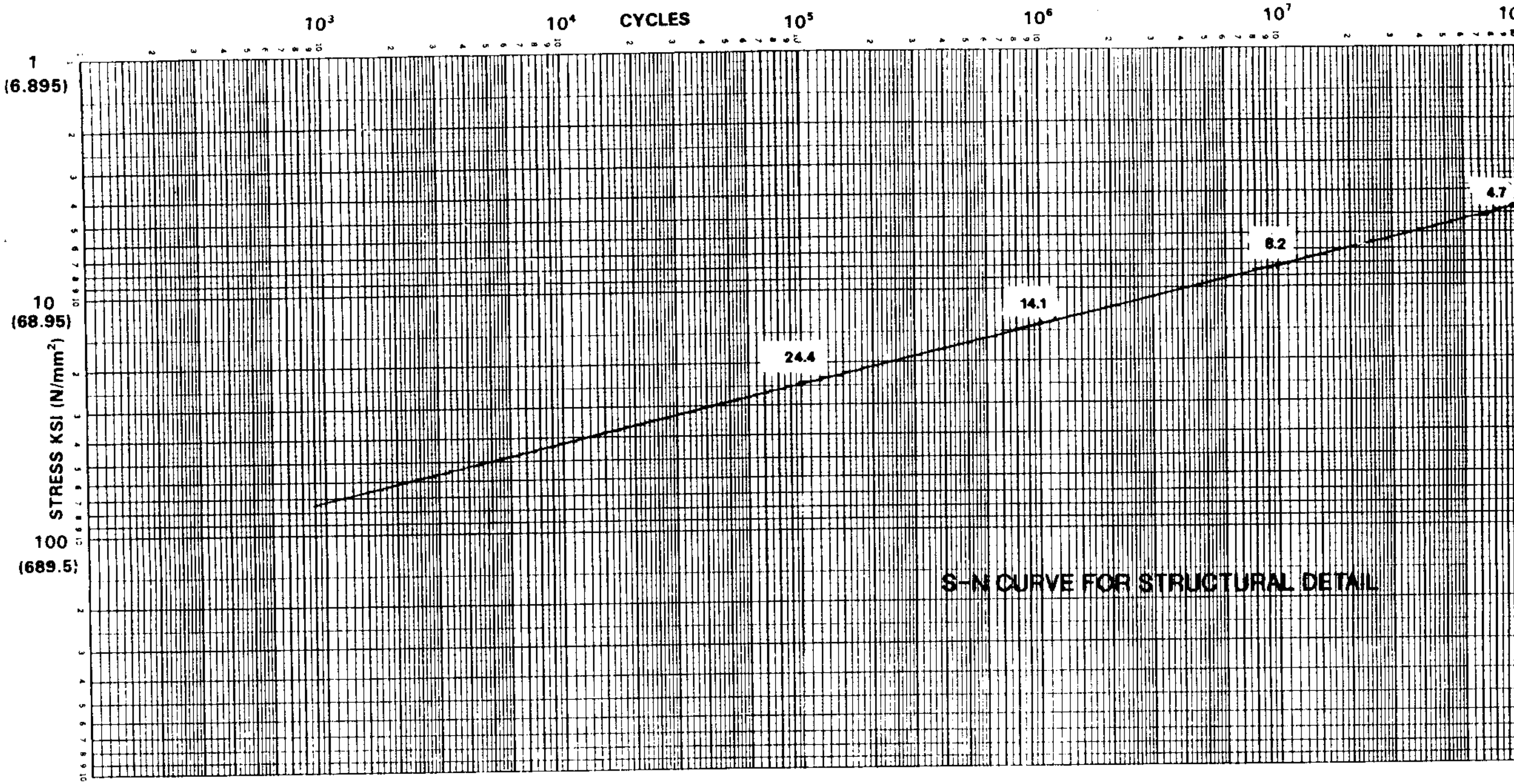

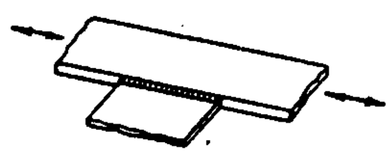

SLOPE $m = 4.200$

RELIABIITY FACTOR (0.90) $R_F = 0.688$

FIGURE 2-9. S-N DATA FOR DETAIL 15

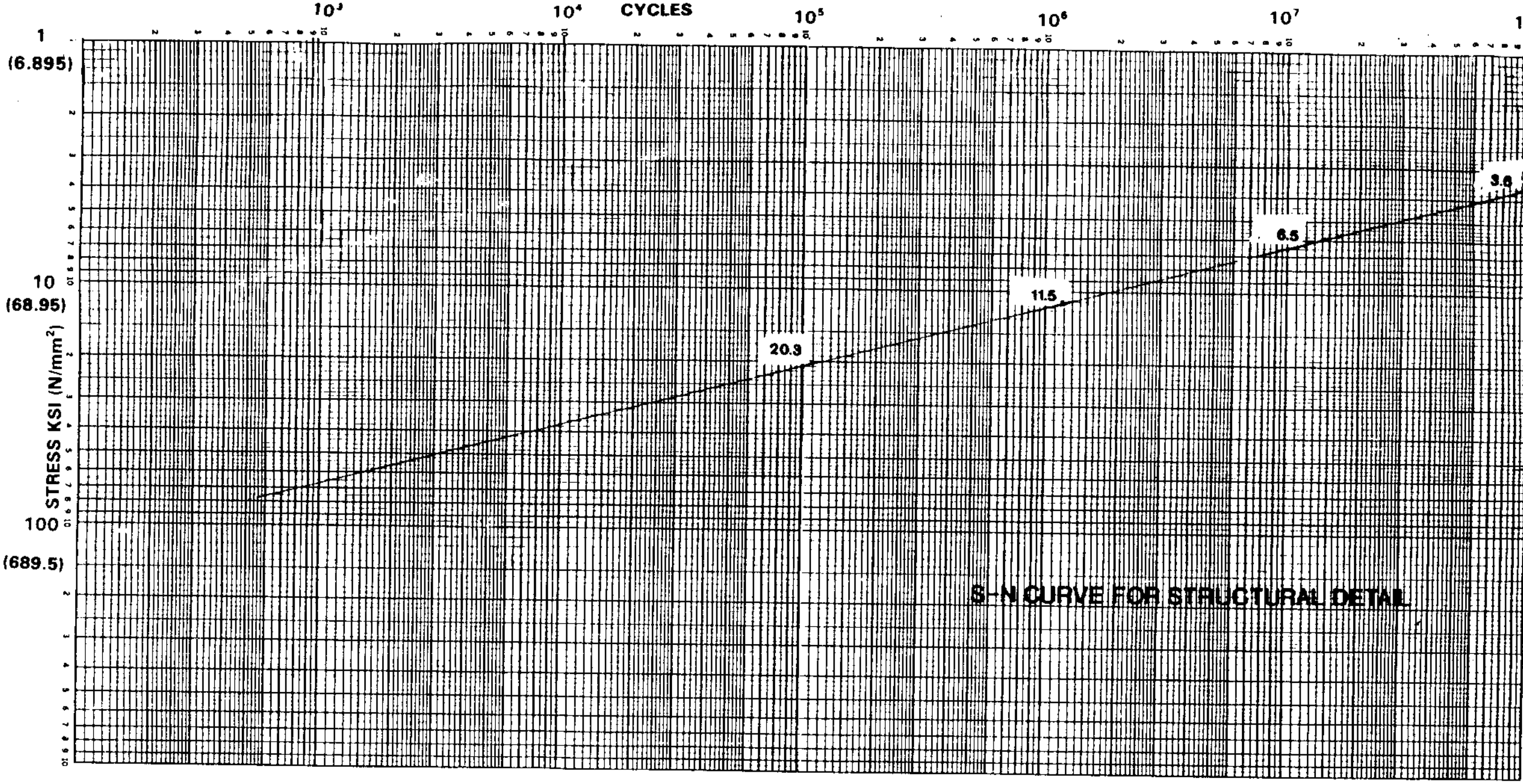

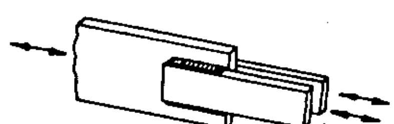

DETAIL 18(S)-18

SLOPE m = 4.027

RELIABIITY FACTOR (0.90) R_F = 0.615

FIGURE 2-10. S-N DATA FOR DETAIL 18

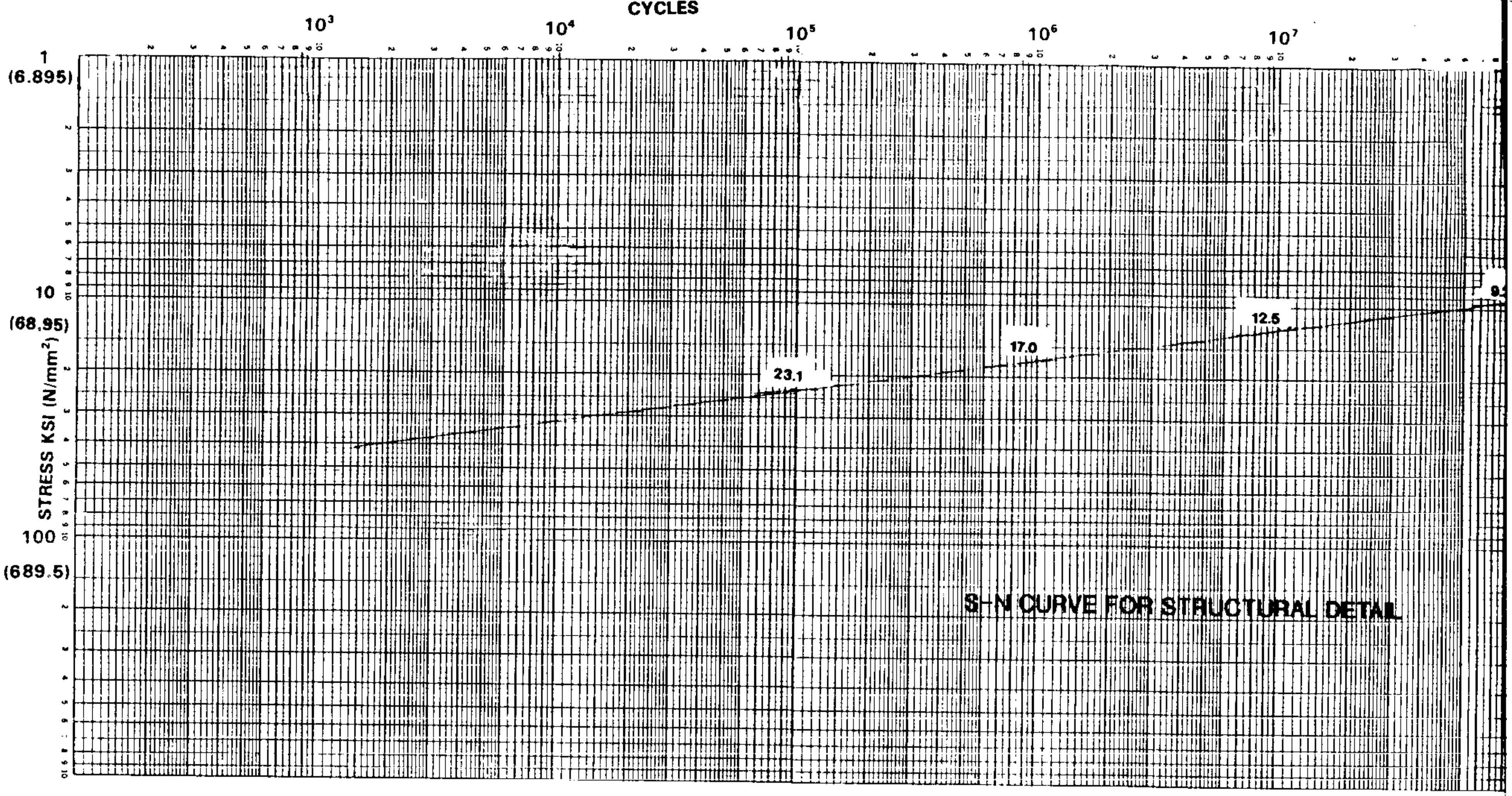

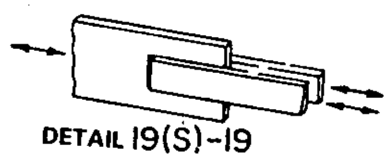

SLOPE m = 7.472

RELIABIITY FACTOR (0.90) R_F = 0.658

FIGURE 2-11. S-N DATA FOR DETAIL 19

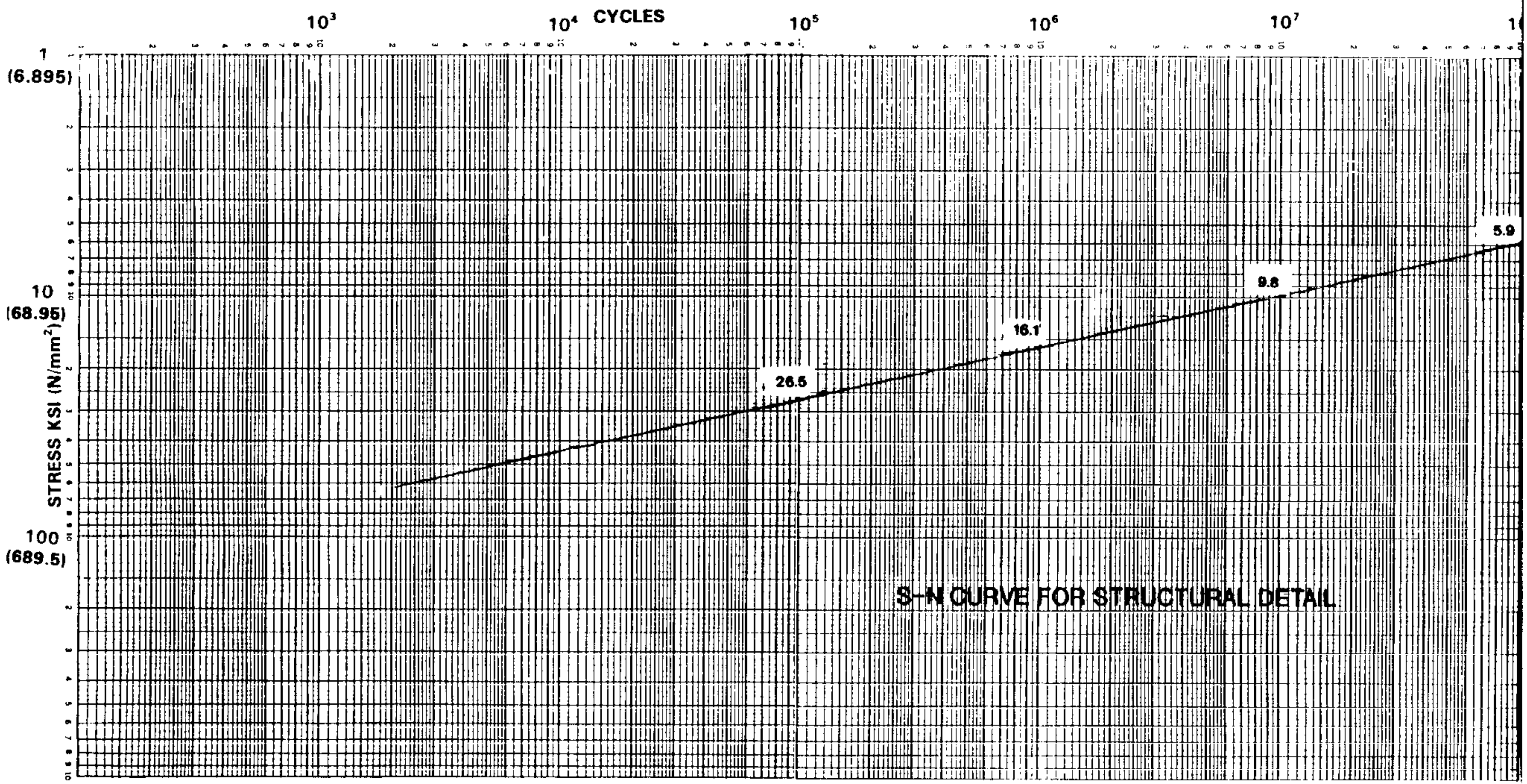

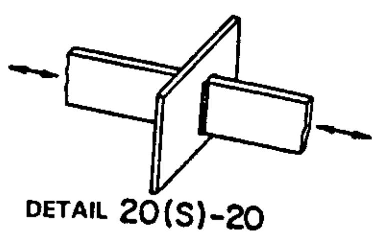

SLOPE m = 4.619

RELIABIITY FACTOR (0.90) R_F = 0.639

FIGURE 2-12. S-N DATA FOR DETAIL 20

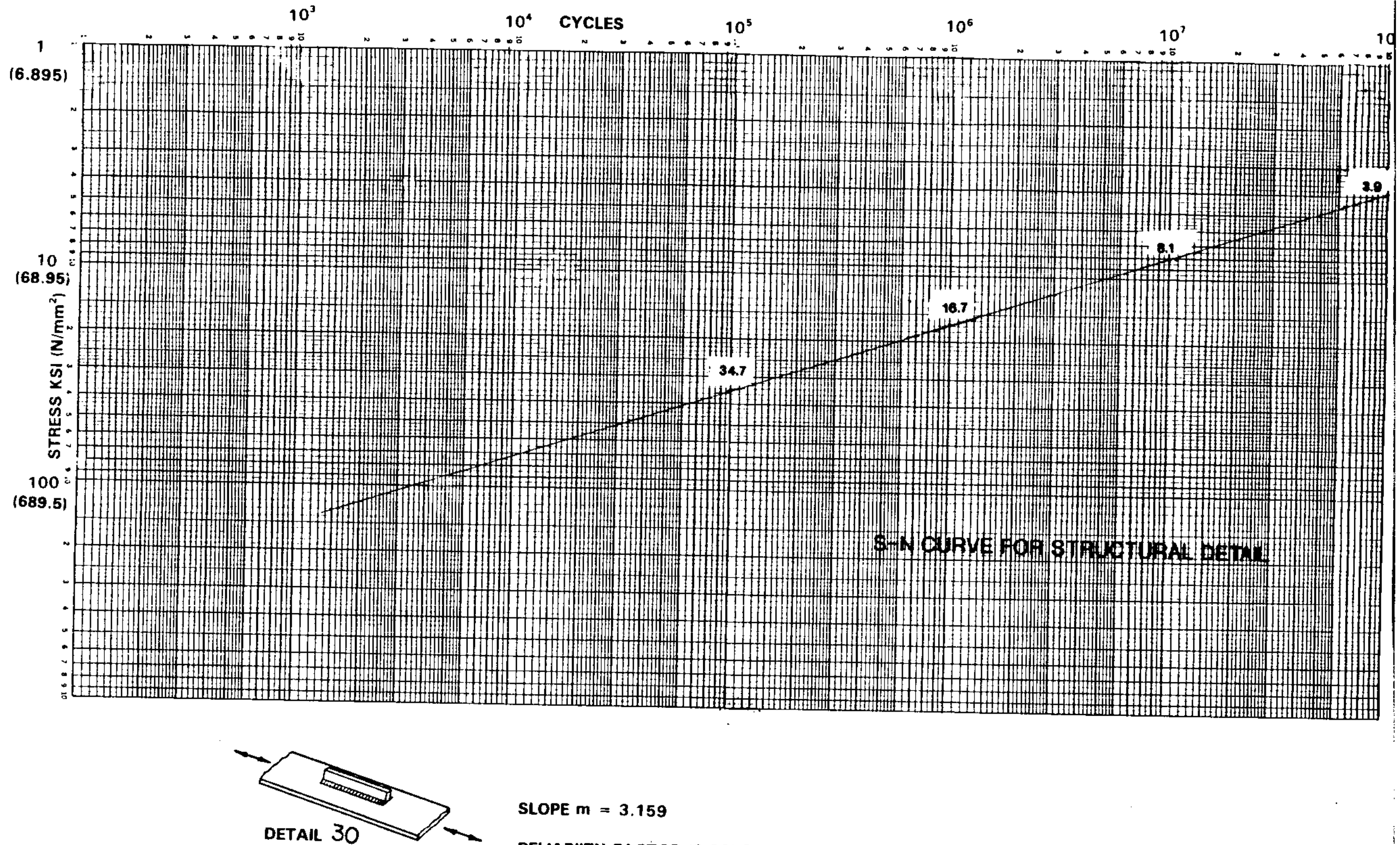

SLOPE m = 3.159

RELIABIITY FACTOR (0.90) R_F = 0.671

FIGURE 2-13. S-N DATA FOR DETAIL 30

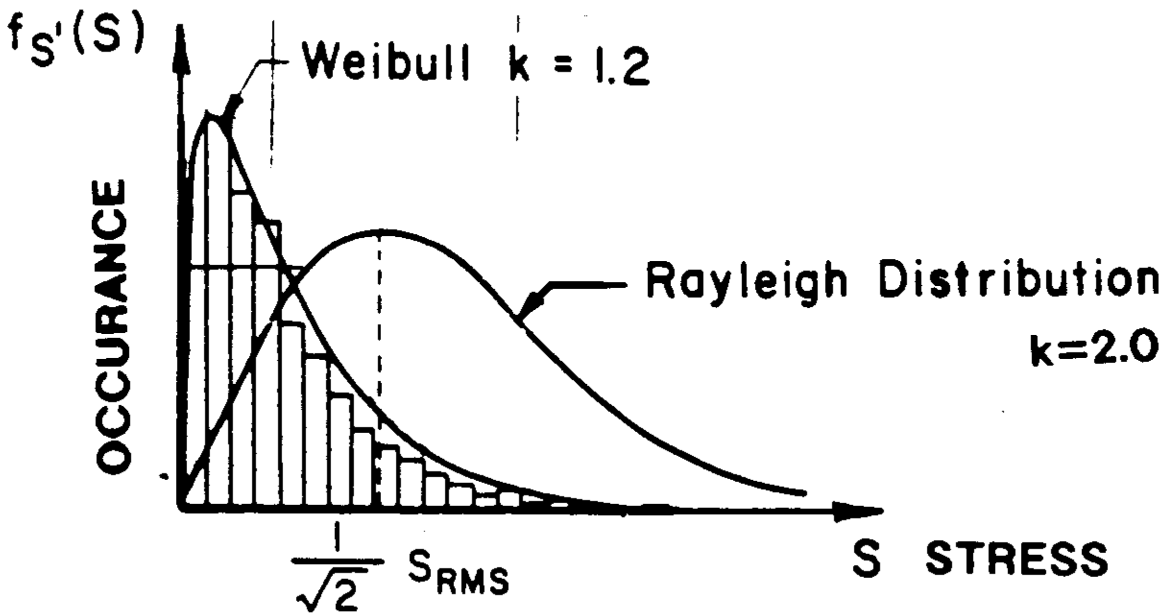

$f_{S'}(S)$
Weibull k = 1.2
OCCURANCE
Rayleigh Distribution
k=2.0
$\frac{1}{\sqrt{2}}$ S_{RMS}
S STRESS

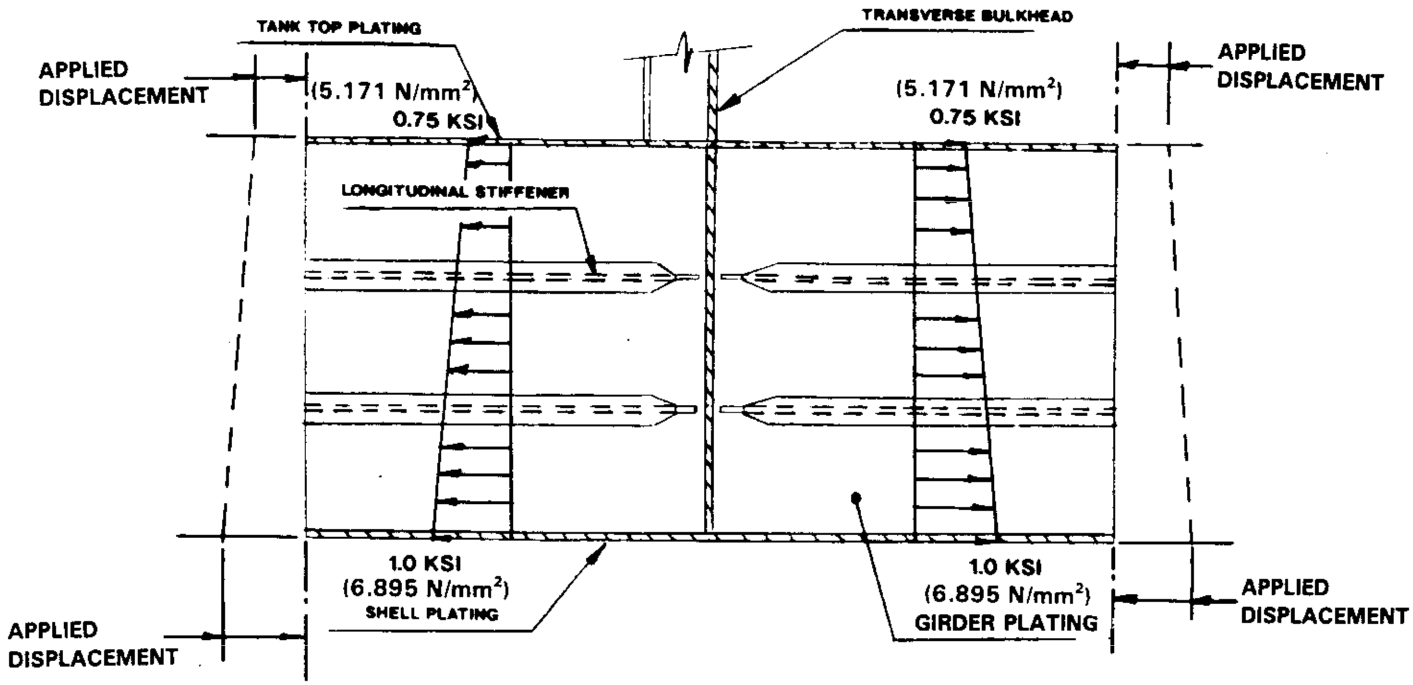

BOUNDARY CONSTRAINTS:

X TRANSLATION (UX)	-	INTERSECTION OF TANK TOP & SHELL WITH TRANSVERSE BULKHEAD
Y TRANSLATION (UY)	-	SHELL PLATING, TRANSVERSE BULKHEAD & TANK TOP PLATING
ROTATION ABOUT X (RX)	-	TRANSVERSE BULKHEAD
ROTATION ABOUT Z (RZ)	-	SHELL PLATING, TANK TOP PLATING, FORWARD & AFT EDGE OF GIRDER PLATING

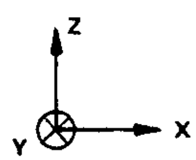

FIGURE 2-15. UNIT LOADS FOR VERTICAL HULL PRIMARY STRESS - NAVAL COMBATANT

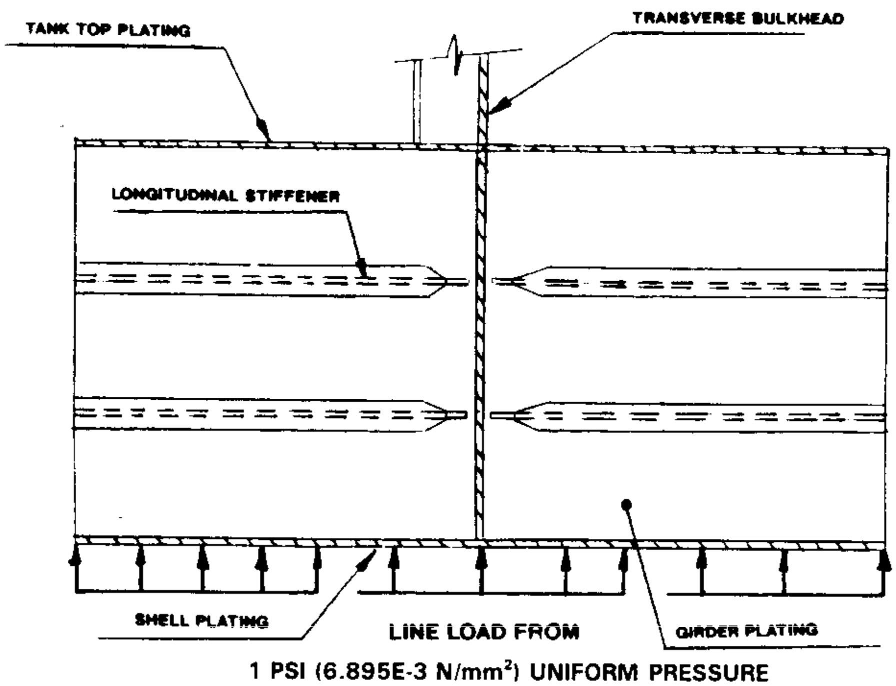

BOUNDARY CONSTRAINTS:

X TRANSLATION (UX)	-	TRANSVERSE BULKHEAD
Y TRANSLATION (UY)	-	SHELL PLATING, TRANSVERSE BULKHEAD & TANK TOP PLATING
Z TRANSLATION (UZ)	-	TRANSVERSE BULKHEAD

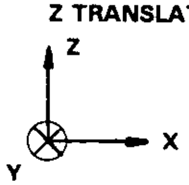

FIGURE 2-16. UNIT LOADS FOR EXTERNAL HYDRODYNAMIC PRESSURE - NAVAL COMBATANT

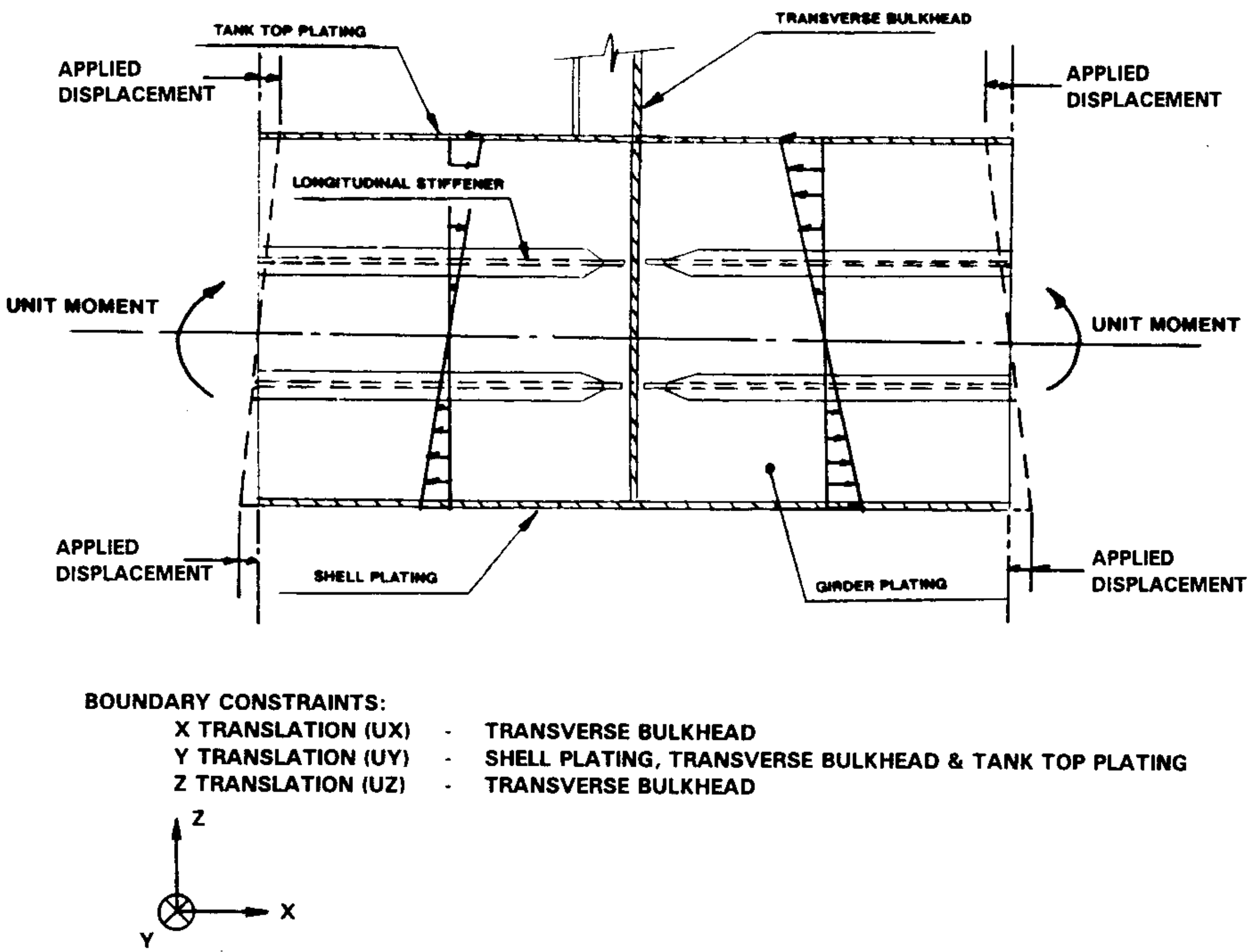

FIGURE 2-17. UNIT LOADS FOR INTERNAL GIRDER MOMENTS - NAVAL COMBATANT

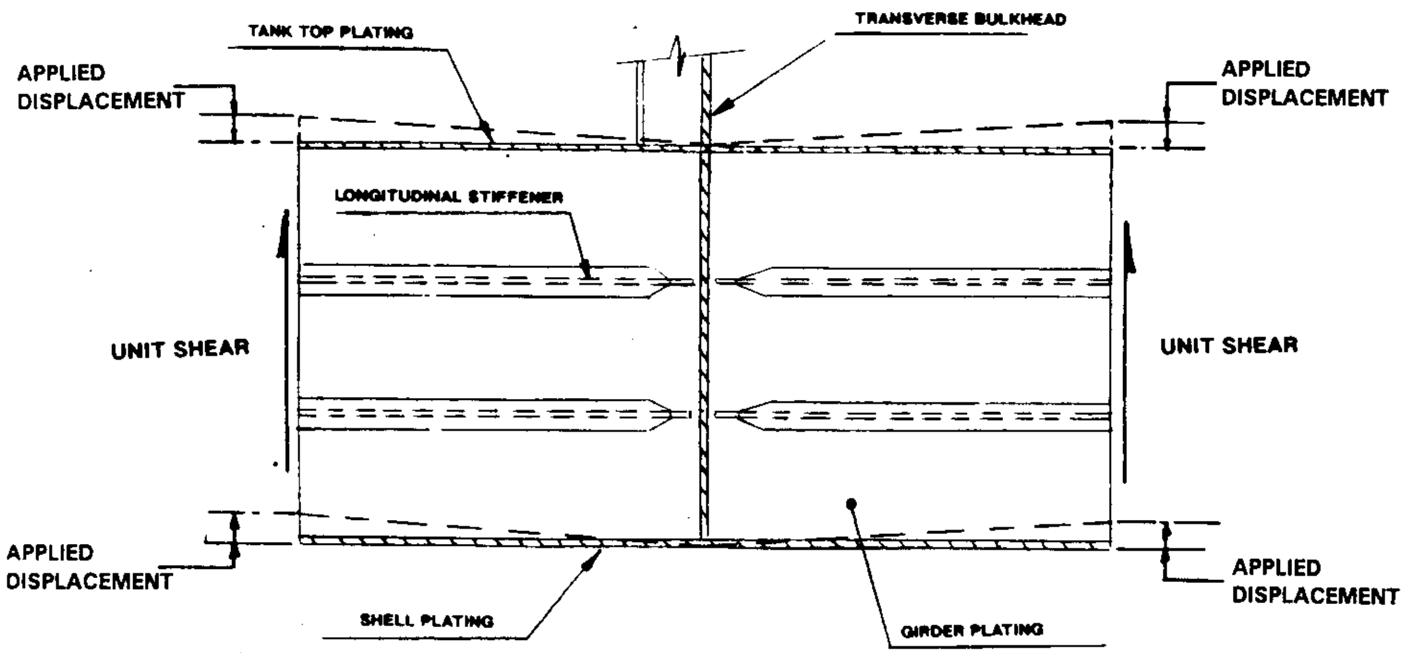

BOUNDARY CONSTRAINTS:

X TRANSLATION (UX)	-	TRANSVERSE BULKHEAD
Y TRANSLATION (UY)	-	SHELL PLATING, TRANSVERSE BULKHEAD & TANK TOP PLATING
Z TRANSLATION (UZ)	-	TRANSVERSE BULKHEAD

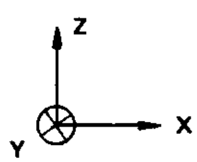

FIGURE 2-18. UNIT LOADS FOR INTERNAL GIRDER SHEAR - NAVAL COMBATANT

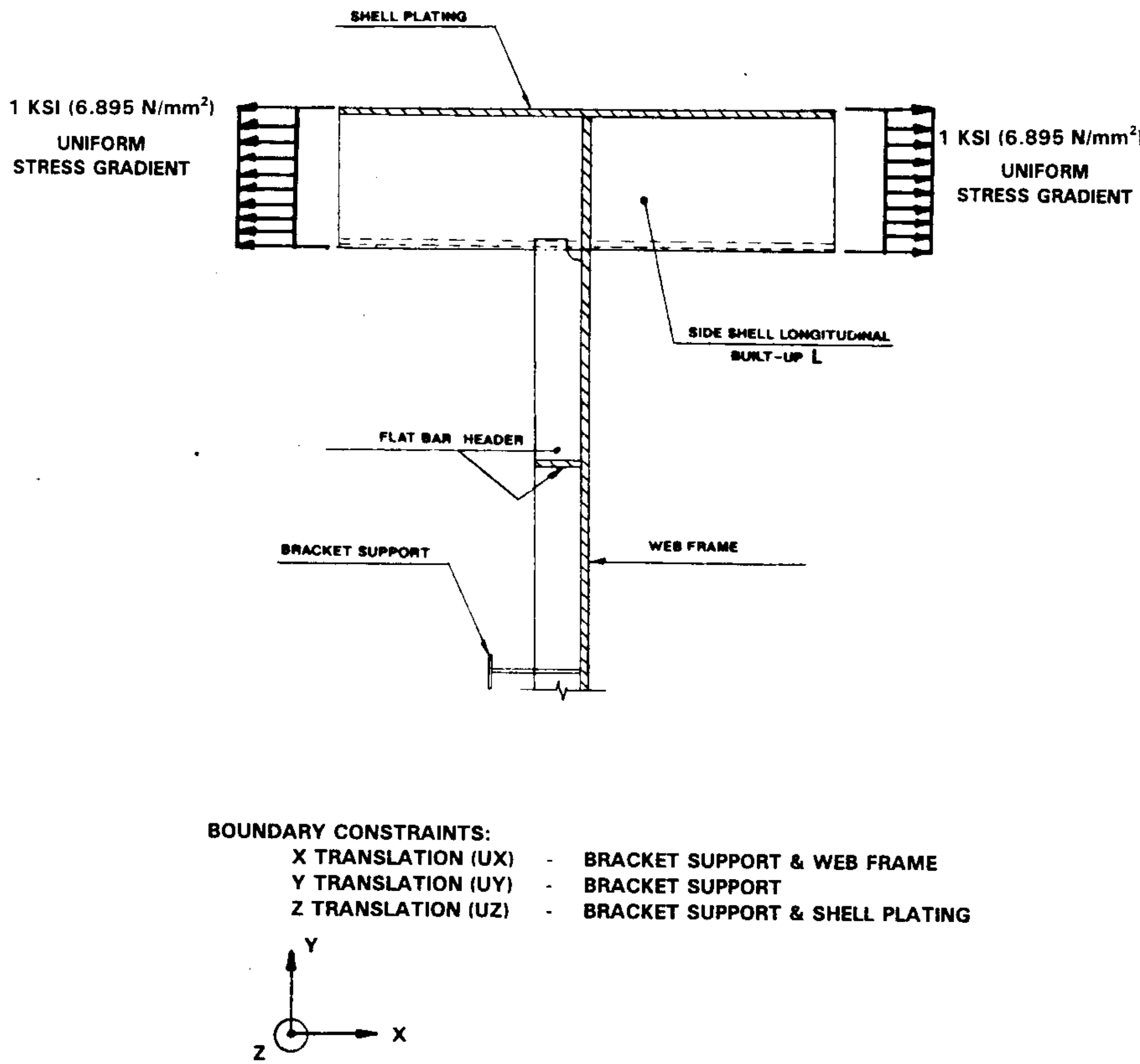

FIGURE 2-19. UNIT LOADS FOR VERTICAL HULL PRIMARY STRESS - TANKER

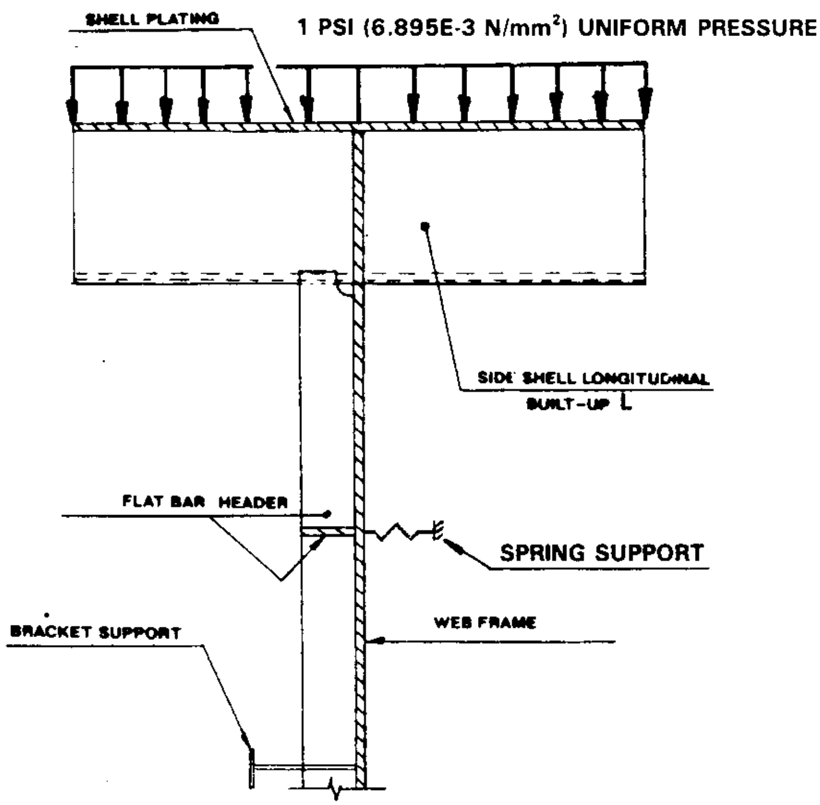

BOUNDARY CONSTRAINTS:

X TRANSLATION (UX)	-	BRACKET SUPPORT & SPRING SUPPORT
Y TRANSLATION (UY)	-	BRACKET SUPPORT & SPRING SUPPORT
Z TRANSLATION (UZ)	-	BRACKET SUPPORT, WEB FRAME & SHELL PLATING

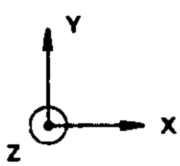

FIGURE 2-20. UNIT LOADS FOR EXTERNAL/INTERNAL HYDRODYNAMIC PRESSURE - TANKER

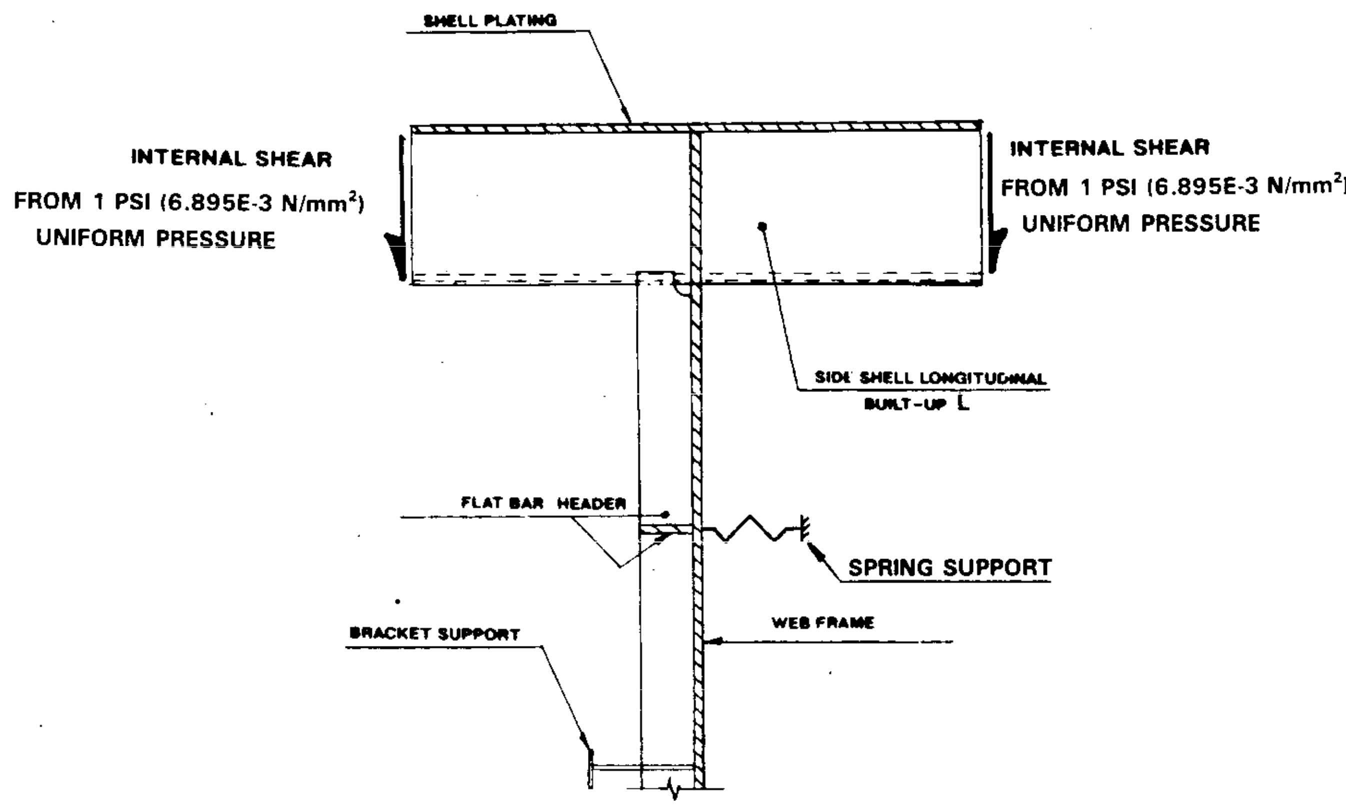

BOUNDARY CONSTRAINTS:

X TRANSLATION (UX)	-	BRACKET SUPPORT & SPRING SUPPORT
Y TRANSLATION (UY)	-	BRACKET SUPPORT & SPRING SUPPORT
Z TRANSLATION (UZ)	-	BRACKET SUPPORT, WEB FRAME & SHELL PLATING

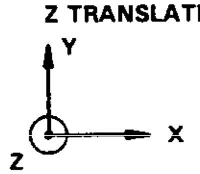

FIGURE 2-21. UNIT LOADS FOR INTERNAL STIFFENER SHEAR - TANKER

HULL GIRDER LOADING

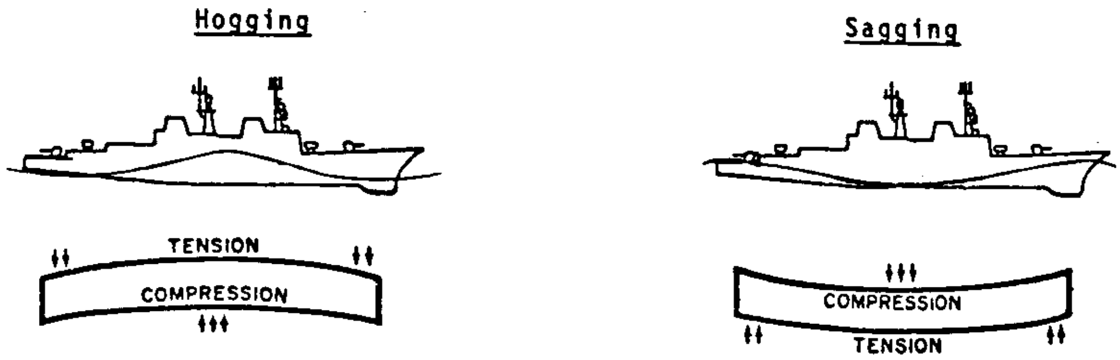

Standard Wave Characteristics:

1. **Wave length:** Ship length (LBP)
2. **Wave height:** $1.1 \times \sqrt{LBP}$

PRIMARY STRESS DISTRIBUTION

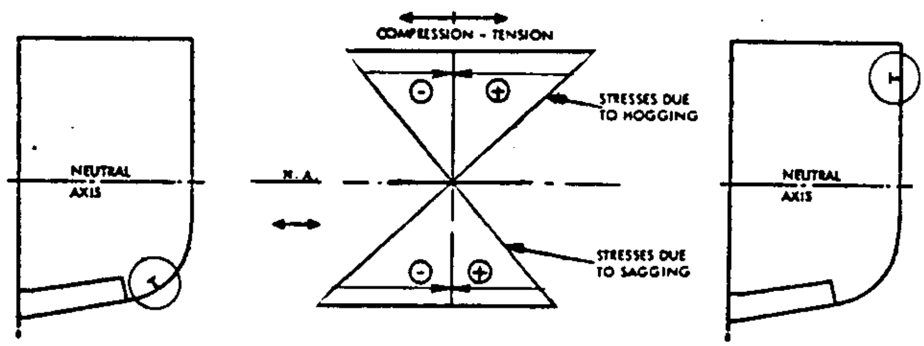

HYDROSTATIC LOADS

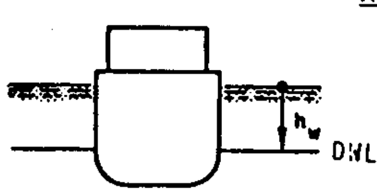

Passing Wave

(Height: 0.55 to $0.675 \sqrt{\text{length of ship}}$)

FIGURE 2-22. SHIP DESIGN LOADS

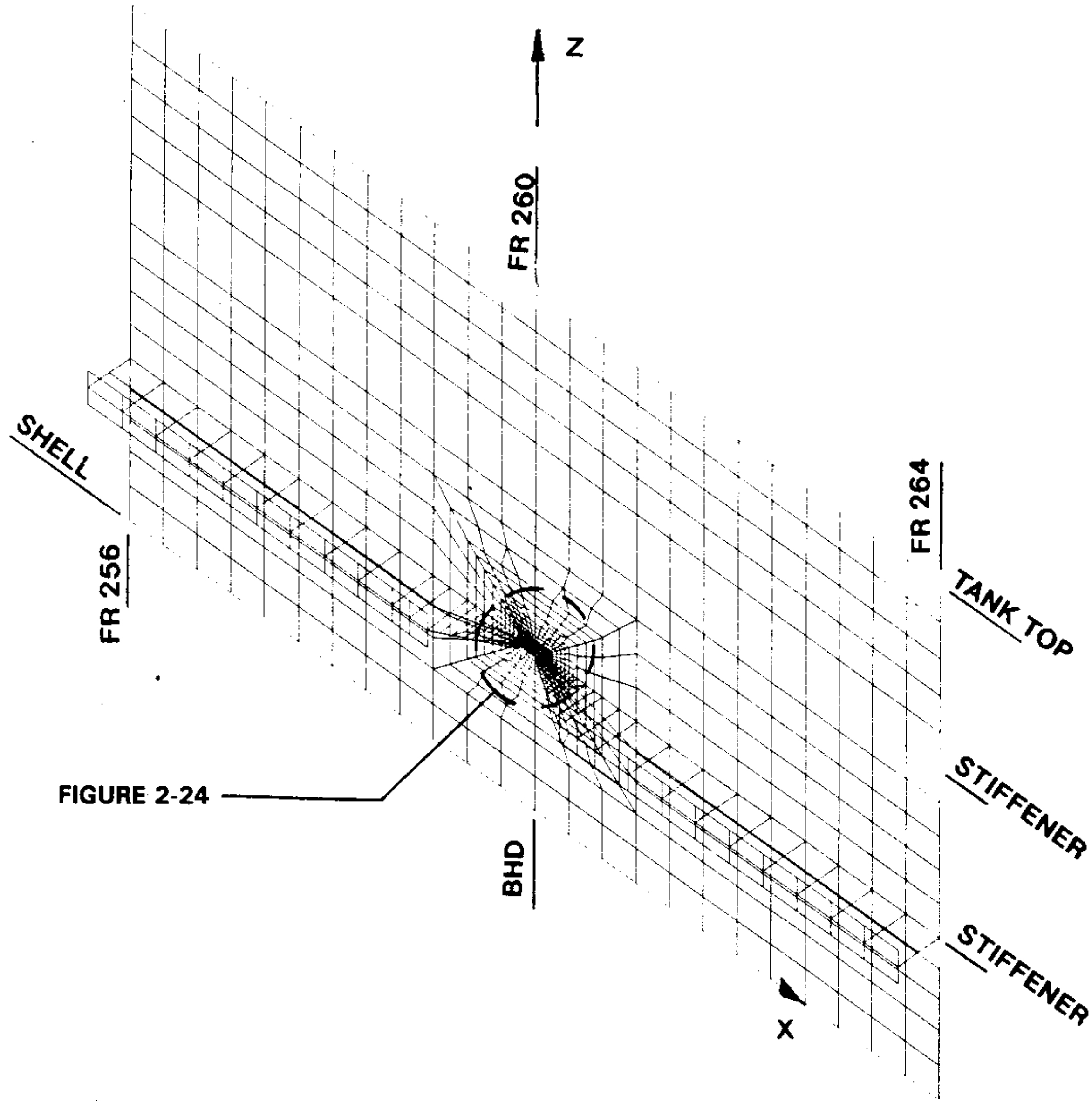

FIGURE 2-23. ISOMETRIC OF NAVAL COMBATANT FINE MESH MODEL

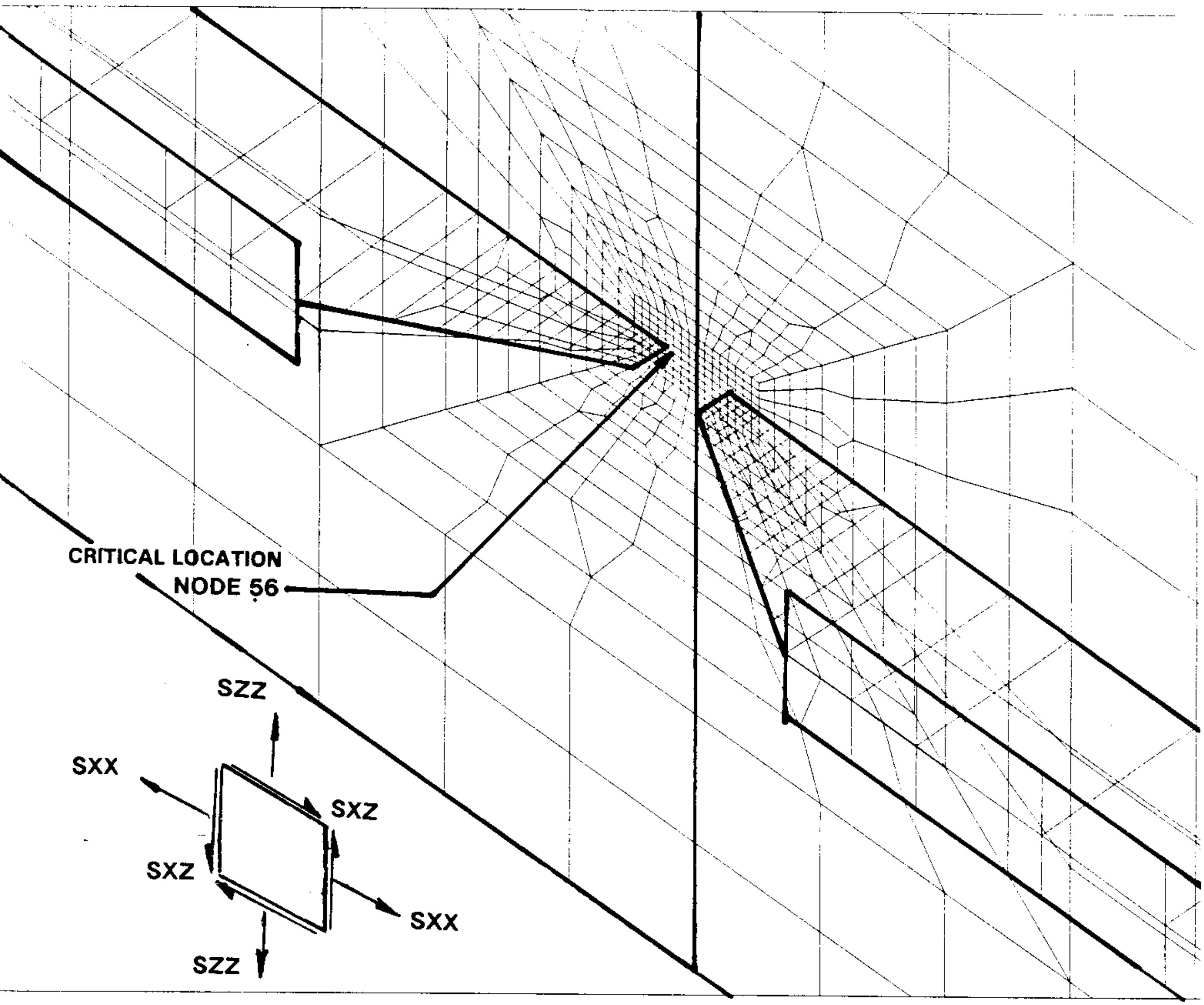

FIGURE 2-24. MESHING CONFIGURATION AT CRITICAL AREA - NAVAL COMBATANT

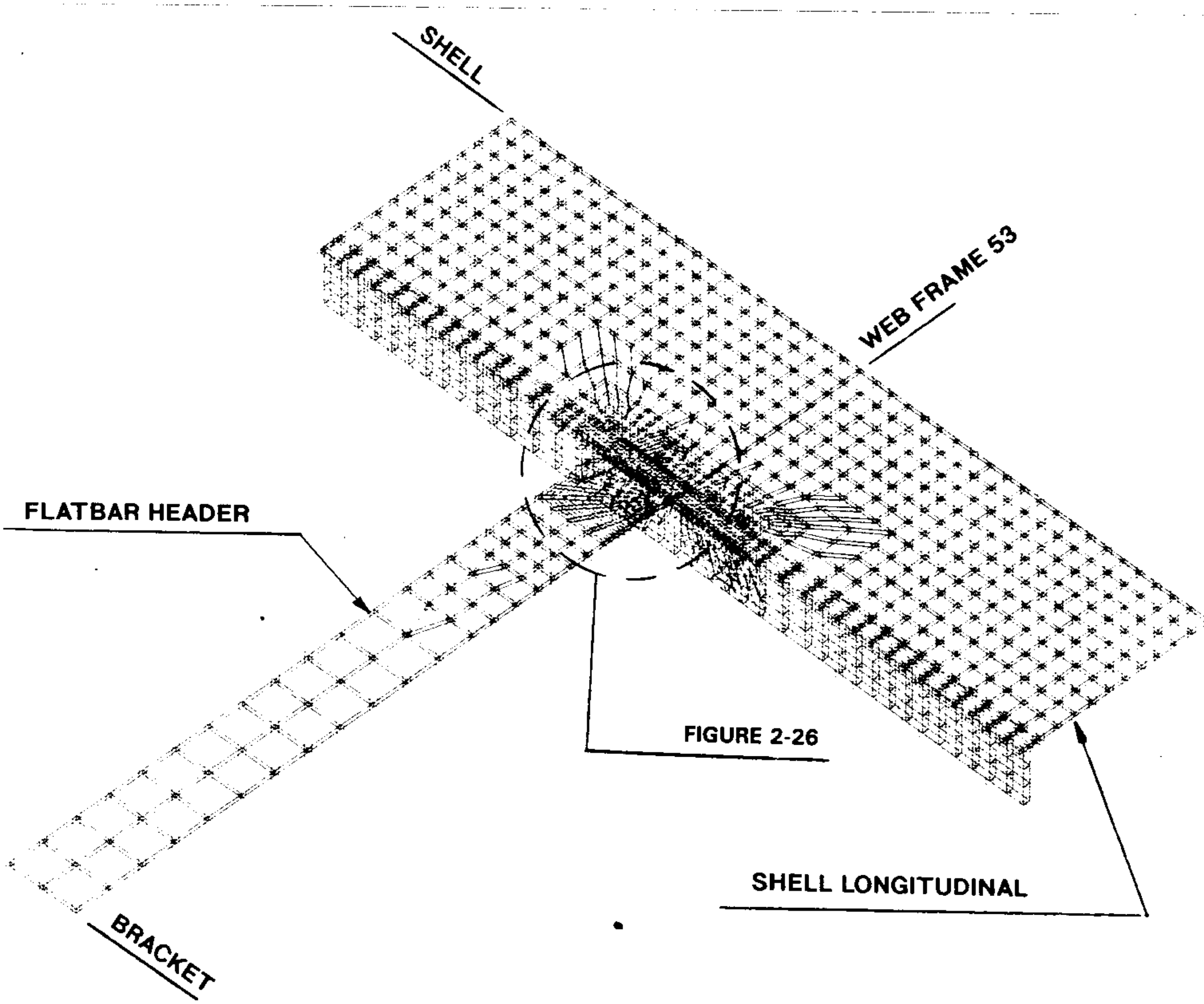

FIGURE 2-25. ISOMETRIC OF TANKER FINE MESH MODEL

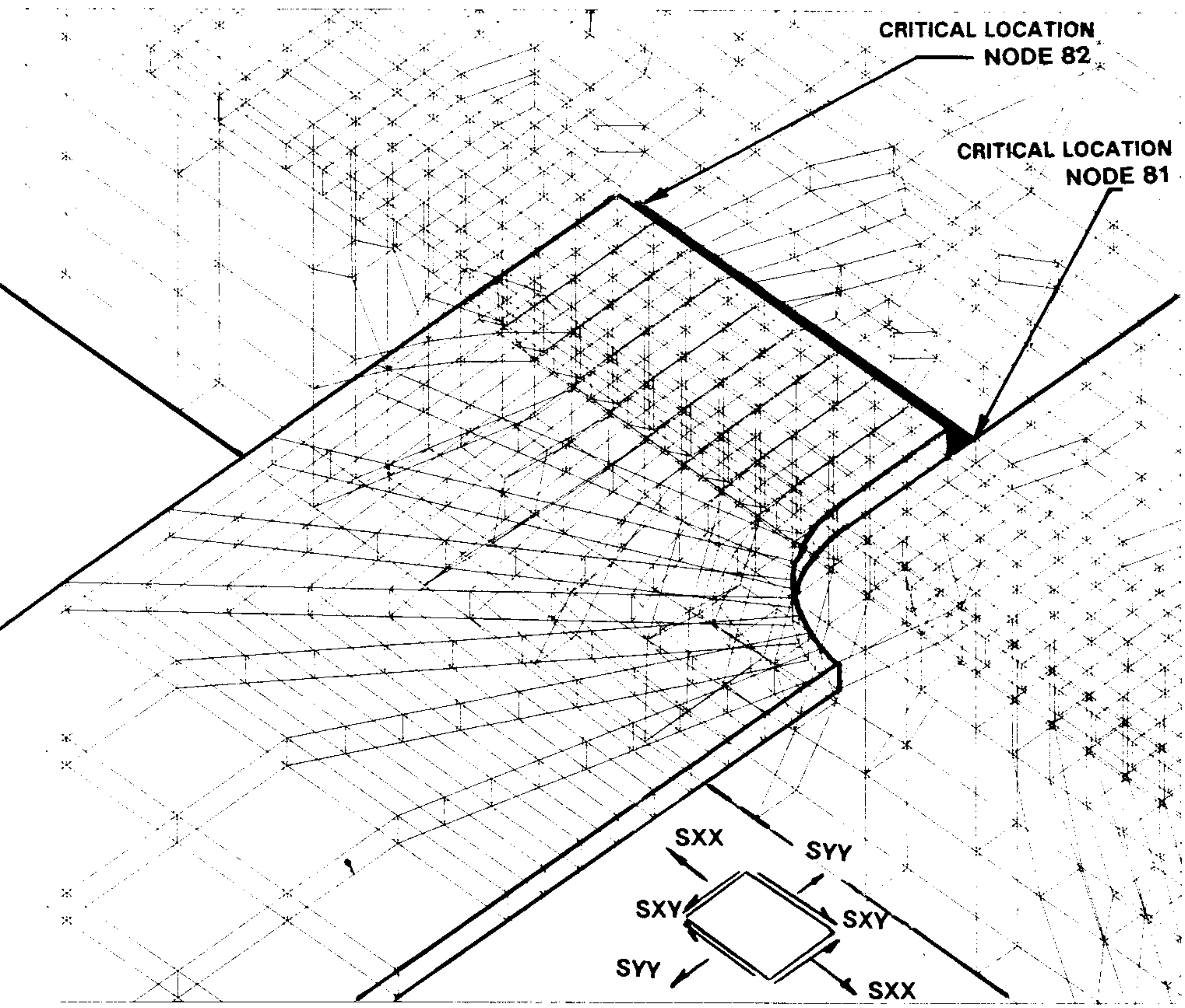

FIGURE 2-26. MESHING CONFIGURATION AT CRITICAL AREA - TANKER

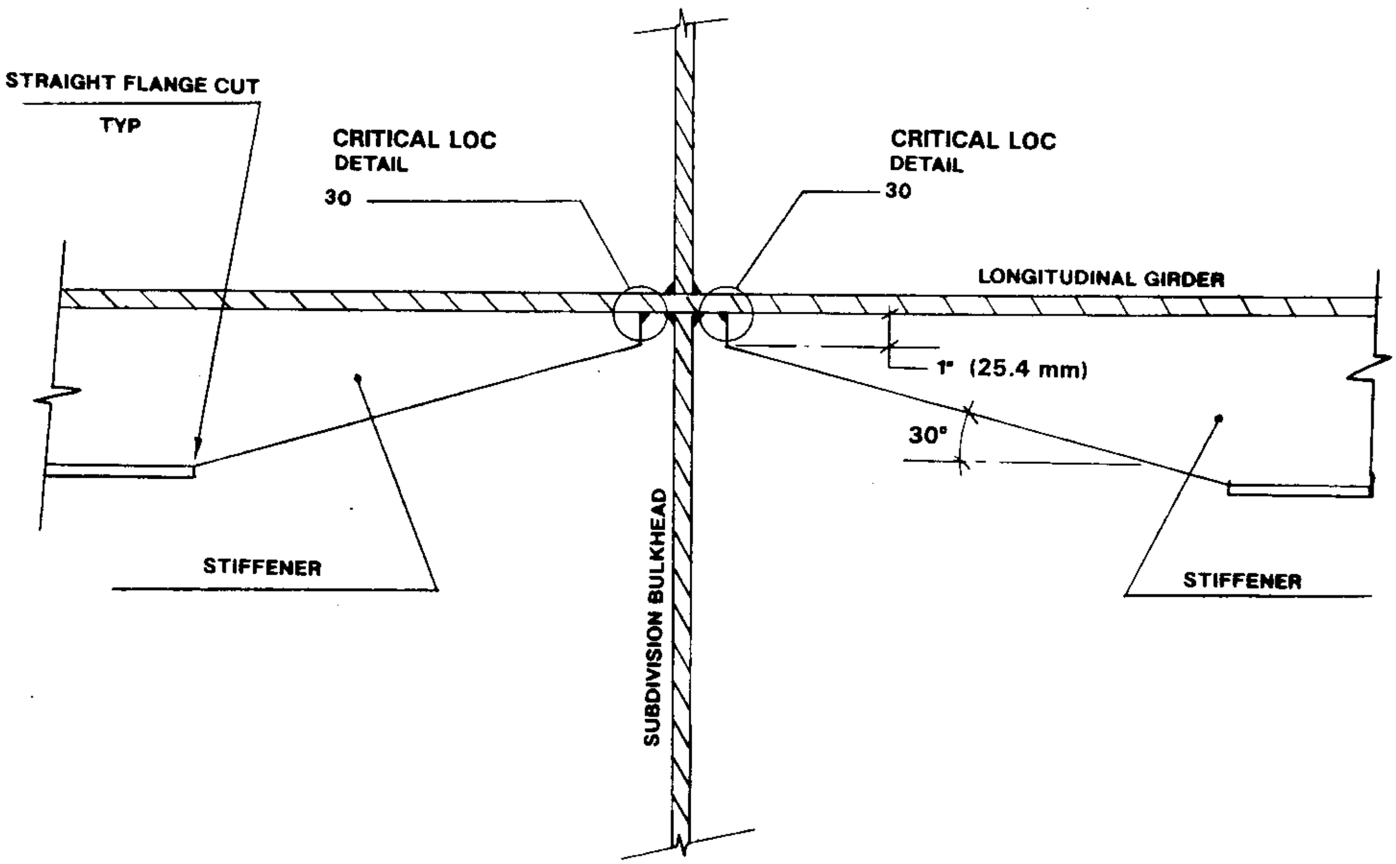

Note: Detail 30 taken from Reference (g)

FIGURE 2-27. CRITICAL STRESS LOCATIONS FOR NAVAL COMBATANT DETAIL

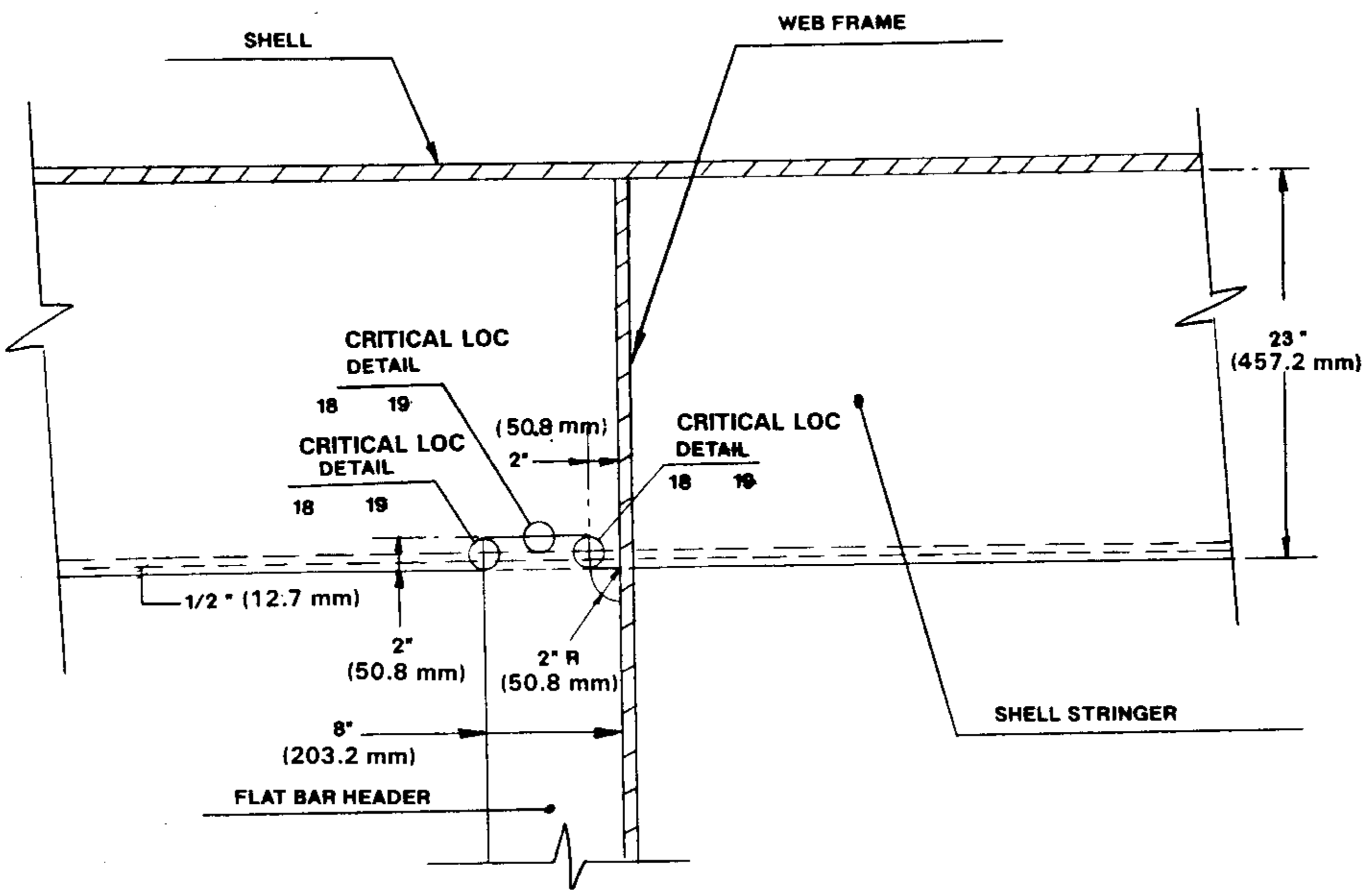

Note: Details 18 and 19 are taken from Reference (g)

FIGURE 2-28. CRITICAL STRESS LOCATIONS FOR TANKER DETAIL

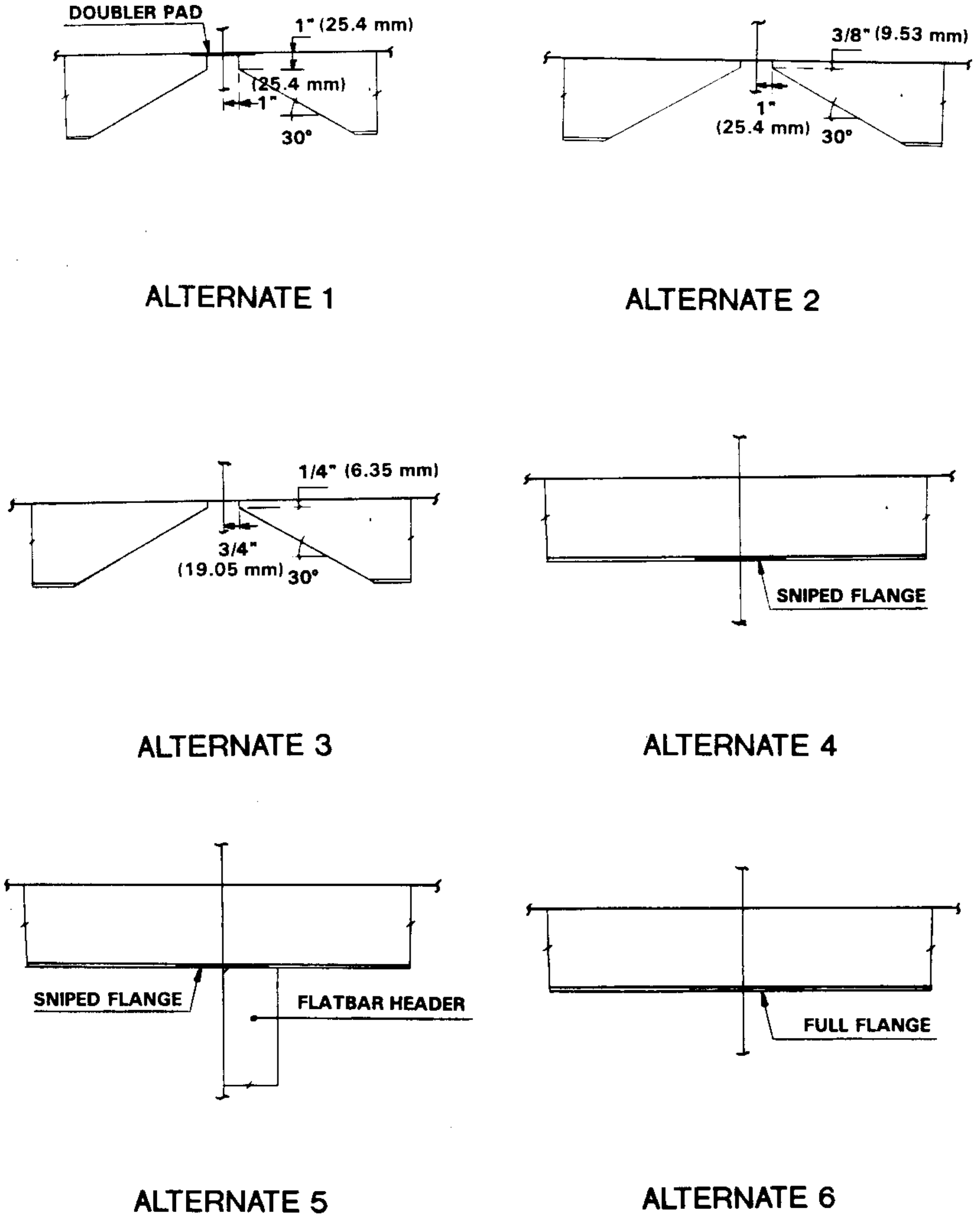

FIGURE 2-29. NAVAL COMBATANT ALTERNATIVE DETAILS

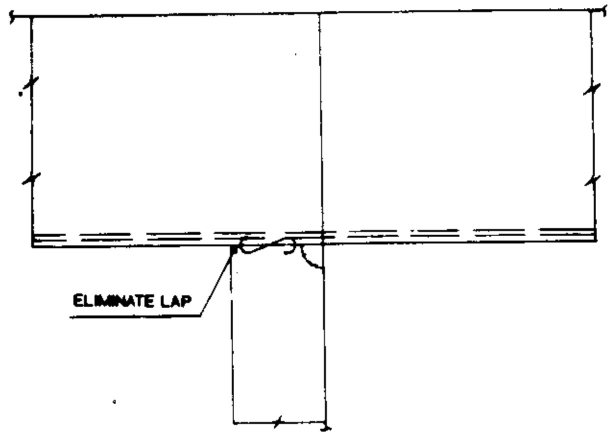

ALTERNATE 1

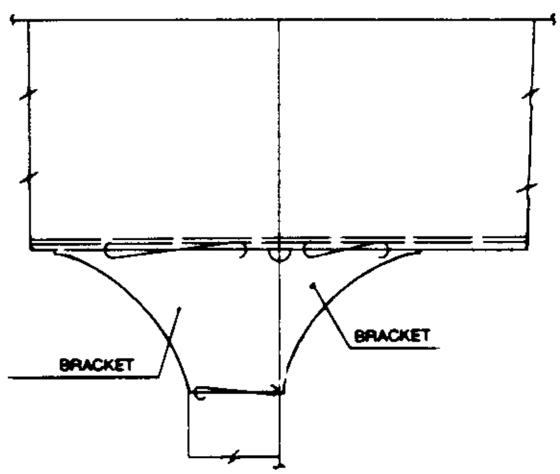

ALTERNATE 2

FIGURE 2-30. TANKER ALTERNATIVE DETAILS

TABLE 2-1. CRITICAL INSPECTION PLANS REVIEWED

Class	Vessel	Operator
American Sun	AMERICAN TRADER	American Trading Trans. Co.
	GLACIER BAY	Trinidad Corp.
	ADMIRALTY BAY	Trinidad Corp.
	ASPEN	Trinidad Corp.
ARCO Anchorage	ARCO ANCHORAGE	ARCO Marine, Inc.
	ARCO FAIRBANKS	ARCO Marine, Inc.
	OVERSEAS JUNEAU	Maritime Overseas, Corp.
Atigun Pass	ATIGUN PASS	Keystone Shipping
	KEYSTONE CANYON	Keystone Shipping
	BROOKS RANGE	Interocean Management
	THOMPSON PASS	Interocean Management
	EXXON NORTH SLOPE	Exxon Shipping
Chevron GT	CHEVRON OREGON	Chevron Shipping
	CHEVRON WASHINGTON	Chevron Shipping
	CHEVRON LOUISIANA	Chevron Shipping
Exxon Houston	EXXON NEW ORLEANS	Exxon Shipping
Exxon San Francisco	EXXON SAN FRANCISCO	Exxon Shipping
	EXXON BATON ROUGE	Exxon Shipping
	EXXON PHILADELPHIA	Exxon Shipping
Exxon Valdez	EXXON LONG BEACH	Exxon Shipping
Massachusetts	ARCO SPIRIT	ARCO Marine, Inc.
San Clemente	OVERSEAS NEW YORK	Maritime Overseas Corp.
	OVERSEAS WASHINGTON	Maritime Overseas Corp.

TABLE 2-1. CRITICAL INSPECTION PLANS REVIEWED (Cont'd)

Class	Vessel	Operator
San Diego	B.T. SAN DIEGO	Marine Transport Lines
	B.T. ALASKA	Marine Transport Lines
Sansinena	SANSINENA II	West Coast Shipping
	ARCO PRUDHOE BAY	ARCO Marine, Inc.
	CHEVRON CALIFORNIA	Chevron Shipping
	CHEVRON MISSISSIPPI	Chevron Shipping
Sunship TAPS	PRINCE WILLIAM SOUND	Sun Transport
	TONSINA	Keystone Shipping
	KENAI	Keystone Shipping
Reflagged	OVERSEAS BOSTON	Cambridge Tankers, Inc.
Not in a Class	ARCO TEXAS	ARCO Marine, Inc.
	EXXON BAYTOWN	Exxon Shipping
	OVERSEAS ALASKA	Maritime Overseas Corp.
	OVERSEAS PHILADELPHIA	Maritime Overseas Corp.
	OVERSEAS NEW ORLEANS	Maritime Overseas Corp.
	OVERSEAS OHIO	Maritime Overseas Corp.
	OVERSEAS CHICAGO	Maritime Overseas Corp.
	OVERSEAS ARCTIC	Maritime Overseas Corp.

TABLE 2-2. RANDOM LOAD FACTORS FOR WEIBULL DISTRIBUTED LOADING

Slope	WEIBULL SHAPE FACTORS, k														
m	0.5	0.6	0.7	0.8	0.9	1.0[1]	1.1	1.2	1.3	1.4	1.5	1.6	1.7	1.8	1.9	2.0[2]
2.0	69.26	42.22	28.63	20.93	16.17	13.02	10.83	9.24	8.05	7.12	6.39	5.80	5.32	4.92	4.58	4.29
2.5	49.99	32.55	23.12	17.49	13.86	11.39	9.63	8.33	7.33	6.55	5.92	5.41	4.99	4.64	4.34	4.08
3.0	37.86	26.05	19.23	14.96	12.12	10.14	8.69	7.60	6.75	6.08	5.54	5.09	4.72	4.40	4.13	3.90
3.5	29.70	21.42	16.35	13.04	10.77	9.14	7.93	7.00	6.27	5.69	5.21	4.81	4.48	4.20	3.96	3.75
4.0	23.94	18.00	14.15	11.53	9.68	8.32	7.30	6.50	5.86	5.35	4.93	4.58	4.28	4.02	3.80	3.61
4.5	19.73	15.39	12.41	10.31	8.79	7.64	6.76	6.07	5.52	5.06	4.68	4.37	4.10	3.86	3.66	3.49
5.0	16.54	13.34	11.01	9.31	8.04	7.07	6.31	5.71	5.21	4.81	4.47	4.18	3.94	3.72	3.54	3.38
5.5	14.03	11.70	9.87	8.48	7.41	6.58	5.92	5.39	4.95	4.58	4.28	4.02	3.79	3.60	3.43	3.28
6.0	12.13	10.36	8.91	7.77	6.87	6.15	5.58	5.10	4.71	4.38	4.11	3.87	3.66	3.48	3.32	3.18
6.5	10.56	9.26	8.11	7.16	6.40	5.78	5.27	4.85	4.50	4.21	3.95	3.73	3.54	3.38	3.23	3.10
7.0	9.28	8.33	7.42	6.64	5.99	5.45	5.00	4.63	4.31	4.04	3.81	3.61	3.44	3.28	3.14	3.02
7.5	8.22	7.55	6.83	6.18	5.62	5.16	4.76	4.43	4.14	3.90	3.68	3.50	3.34	3.19	3.07	2.95
8.0	7.34	6.87	6.31	5.78	5.30	4.89	4.54	4.24	3.98	3.76	3.57	3.40	3.24	3.11	2.99	2.88
8.5	6.59	6.29	5.86	5.42	5.01	4.66	4.35	4.08	3.84	3.64	3.46	3.30	3.16	3.04	2.92	2.82
9.0	5.95	5.79	5.46	5.10	4.75	4.44	4.17	3.92	3.71	3.52	3.36	3.21	3.08	2.96	2.86	2.76
9.5	5.40	5.35	5.11	4.81	4.52	4.25	4.00	3.78	3.59	3.42	3.26	3.13	3.01	2.90	2.80	2.71
10.0	4.92	4.95	4.79	4.55	4.30	4.07	3.85	3.65	3.48	3.32	3.18	3.05	2.94	2.84	2.74	2.66

Notes:

1. Values for exponential distribution.
2. Values for Rayleigh distribution.
3. Values are based on a life of 10^8 cycles. For any other life N the values in this table would be multiplied by:

$$\frac{(\ln N)^{1/k}}{(18.42)^{1/k}}$$

4. Table 2-2 was reprinted from Reference (g).

TABLE 2-3. RELIABILITY FACTORS FOR TYPICAL WELDED DETAILS, R_F

	Reliability, L(n)				Reliability, L(n)		
DETAIL NO.	0.90	0.95	0.99	DETAIL NO.	0.90	0.95	0.99
1 (all steels)	0.655	0.578	0.431	16(G)	0.643	0.567	0.422
1M	0.732	0.671(M)	0.549(M)	17	0.694	0.617	0.468
1H	0.719	0.660	0.540	17(S)	0.725	0.657	0.523
1Q	0.657	0.578	0.430	17A	0.670	0.588	0.435
1F	0.666	0.587	0.438	17A(S)	0.725	0.657	0.523
2	0.690	0.617	0.475	18	0.615	0.530	0.374
3	0.692	0.619	0.478	18(S)	0.715	0.649	0.519
3(G)	0.674	0.600	0.457	19	0.658	0.583	0.441
4	0.690	0.616	0.474	19(S)	0.659	0.585	0.444
5	0.629	0.542	0.384	20	0.639	0.557	0.405
6	0.690	0.616	0.474	20(S)	0.644	0.567	0.422
7(B)	0.640	0.557	0.402	21 (1/4")	--	--	--
7(P)	0.668	0.589	0.438	21 (3/8")	--	--	--
8	0.663	0.587	0.444	21(S)	0.676	0.604	0.464
9	0.694	0.626	0.494	22	0.670	0.587	0.432
10M	0.670	0.597	0.457	23	0.600	0.535	0.411
10H	0.707	0.644	0.518	24	0.600	0.535	0.411
10Q	0.634	0.553	0.403	25	0.681	0.608	0.468
10(G)	0.650	0.575	0.431	25A	0.679	0.609	0.472
10A	0.639	0.559	0.410	25B	0.709	0.640	0.504
10A(G)	--	--	--	26	0.586(m)	0.496	0.336
11	0.674	0.599	0.454	27	0.586(m)	0.495(m)	0.335(m)
12	0.695	0.619	0.474	27(s)	0.694	0.620	0.477
12G	0.690	0.616	0.474	28	0.687	0.616	0.478
13	0.685	0.608	0.460	28(F)	--	--	--
14	0.662	0.588	0.447	30	0.671	0.589	0.434
14A	--	--	--	30A	0.724	0.650	0.506
15	0.688	0.610	0.463				
16	0.667	0.589	0.440				

TABLE 2-3. RELIABILITY FACTORS FOR TYPICAL WELDED DETAILS (CONTD)

Notes:

1. Table 2-3 was reprinted from Reference (g).

2. M = maximum value.

3. m = minimum value.

TABLE 2-4. PITCH MOTION PARAMETERS FOR CALCULATION OF LOADING FACTORS FOR CONVENTIONAL SURFACE SHIPS

Sea State	Length Between Perpendiculars (LBP) meters (feet)	Pitch Angle, Degrees (Note 1)	Pitch Period, Seconds
4	Less than 46 (150)	2	3.5
	46-76 (150-250)	2	4
	76-107 (250-350)	1	5
	107-152 (350-500)	1	6
	152-213 (500-700)	1	7
	Greater than 213 (700)	1	8
5	Less than 46 (150)	3	3.5
	46-76 (150-250)	3	4
	76-107 (250-350)	2	5
	107-152 (350-500)	2	6
	152-213 (500-700)	2	7
	Greater than 213 (700)	1	8
6	Less than 46 (150)	5	3.5
	46-76 (150-250)	4	4
	76-107 (250-350)	4	5
	107-152 (350-500)	3	6
	152-213 (500-700)	3	7
	Greater than 213 (700)	2	8
7	Less than 46 (150)	7	3.5
	46-76 (150-250)	6	4
	76-107 (250-350)	6	5
	107-152 (350-500)	5	6
	152-213 (500-700)	4	7
	Greater than 213 (700)	3	8
8	Less than 46 (150)	11	3.5
	46-76 (150-250)	10	4
	76-107 (250-350)	9	5
	107-152 (350-500)	7	6
	152-213 (500-700)	6	7
	Greater than 213 (700)	5	8

Notes:

1. Pitch angle is measured from horizontal to bow up or down.
2. Table 2-4 was reprinted from Reference (k).

TABLE 2-5. ROLL MOTION PARAMETERS FOR CALCULATION OF LOADING FACTORS FOR CONVENTIONAL SURFACE SHIPS (NOTE 1)

Sea State	Beam, Meters (Feet)	Roll Angle, Degrees (Note 2)	Roll Period, Seconds
4	Less than 15 (50) 15-23 (50-75) 23-32 (75-105) Greater than 32 (105)	7 6 6 5	See note 3 for determination of roll period
5	Less than 15 (50) 15-23 (50-75) 23-32 (75-105) Greater than 32 (105)	12 10 10 9	See note 3 for determination of roll period
6	Less than 15 (50) 15-23 (50-75) 23-32 (75-105) Greater than 32 (105)	19 16 15 13	See note 3 for determination of roll period
7	Less than 15 (50) 15-23 (50-75) 23-32 (75-105) Greater than 32 (105)	28 24 22 20	See note 3 for determination of roll period
8	Less than 15 (50) 15-23 (50-75) 23-32 (75-105) Greater than 32 (105)	42 37 34 31	See note 3 for determination of roll period

Notes:

1. This table excludes multi-hulls, surface effect ships, and all craft supported principally by hydrodynamic lift.
2. Roll angle is measured from vertical to starboard or port.
3. Full roll period is to be calculated from:

   $Tr = (C \times B) / (GM)^{1/2}$

   Where:

   Tr - is the full roll period (seconds).

   C - is a roll constant based upon experimental results from similar ships - usual range 0.69 to 0.89 (sec/$\sqrt{m}$) (0.38 to 0.49 (sec/$\sqrt{ft}$)).

   B - is the maximum beam at or below the waterline (m or ft).

   GM - is the maximum metacentric height (m or ft).
4. Table 2-5 was reprinted from Reference (k).

TABLE 2-6. HEAVE AND SURGE MOTION PARAMETERS FOR CALCULATION OF LOADING FACTORS FOR CONVENTIONAL SURFACE SHIPS

Sea State	LBP meters (feet)	Heave Acceleration (g's)	Surge Acceleration (g's)
4	Less than 46 (150)	0.10	0.06
	46-76 (150-250)	0.10	0.05
	76-107 (250-350)	0.10	0.05
	107-152 (350-500)	0.08	0.04
	152-213 (500-700)	0.06	0.04
	Greater than 213 (700)	0.04	0.02
5	Less than 46 (150)	0.17	0.10
	46-76 (150-250)	0.17	0.10
	76-107 (250-350)	0.17	0.10
	107-152 (350-500)	0.14	0.05
	152-213 (500-700)	0.10	0.05
	Greater than 213 (700)	0.07	0.05
6	Less than 46 (150)	0.27	0.15
	46-76 (150-250)	0.27	0.15
	76-107 (250-350)	0.27	0.15
	107-152 (350-500)	0.21	0.10
	152-213 (500-700)	0.16	0.10
	Greater than 213 (700)	0.11	0.05
7	Less than 46 (150)	0.4	0.25
	46-76 (150-250)	0.4	0.20
	76-107 (250-350)	0.4	0.20
	107-152 (350-500	0.3	0.15
	152-213 (500-700)	0.2	0.15
	Greater than 213 (700)	0.2	0.10
8	Less than 46 (150)	0.6	0.35
	46-76 (150-250)	0.6	0.30
	76-107 (250-350)	0.6	0.30
	107-152 (350-500)	0.5	0.25
	152-213 (500-700)	0.4	0.25
	Greater than 213 (700)	0.2	0.10

Note:

1. Table 2-6 was reprinted from Reference (k).

3.0 RESULTS

This section presents the numerical results of the study. The results are presented in the form of stress summary tables and stress contour plots. The SXX stress (normal stress in the global X direction) contour plots are presented to provide a graphical indication of the stress concentrations which exist in each detail. Stress results for the longitudinal girder stiffener ending detail for the naval combatant are presented in Section 3.1. Stress results for the shell longitudinal to web frame connection for the tanker are presented in Section 3.2. Section 3.3 discusses the analyses of the alternative details which were described in Section 2.9. Stress results for the modified longitudinal girder stiffener ending detail for the naval combatant are presented in Section 3.4. Finally, stress results for the modified shell longitudinal to web frame connection for the tanker are presented in Section 3.5.

To obtain the stresses representative of the maximum state of stress expected during the lifetime of the ship, the unit load case stresses are multiplied by the design loads specified in Section 2.6, summed and then averaged at the critical node. Principal stresses are then calculated in the plane of potential crack propagation. The maximum stress range is the summation of the maximum principal stresses in the hogging and sagging conditions. These maximum stress ranges are then compared to the allowable stress ranges calculated in Appendix A.

It should be noted that buckling calculations for the structural elements of the details being considered indicate that panting will not occur in the operating stress ranges considered. Therefore, no additional loading is assumed for the buckled state.

3.1 NAVAL COMBATANT DETAIL

Figures B-1 through B-4 of Appendix B show the SXX stress contour plots for the unit load cases defined in Section 2.6. Tables 3-1 and 3-2 present stress summaries of the four elements surrounding the critical node as depicted in Figure 2-24, for the unit load cases. Table 3-3 presents a summary of the maximum expected stresses for the hogging and sagging conditions. Due to the symmetry of the problem, only the results for one stiffener snipe are presented.

It should be noted that for the hogging condition, the stress in the web is at the material yield stress. The maximum stress range is 80.3 ksi (553.7 N/mm^2). This stress range greatly exceeds the allowable stress range of 18.1 ksi (124.8 N/mm^2) for Detail No. 18. Based on the design loads used, and assuming a Weibull distribution factor of 1.7, it would be expected that this detail will experience cracking within one year of service.

3.2 TANKER DETAIL

Figures B-5 through B-7 of Appendix B show the SXX stress contour plots for the HSS detail for the unit load cases defined in Section 2.6. Tables 3-4 through 3-7 present stress summaries of the elements surrounding the two critical nodes as depicted in Figure 2-26, for the unit load cases. Tables 3-8 and 3-9 present a summary of the maximum stresses expected for the "design" loads defined in Section 2.6.

The maximum stress range occurred for the Full Load Departure condition and is 47.0 ksi (324.07 N/mm^2). Based on the design loads used, and assuming a Weibull distribution factor of 1.0, it would be expected that this detail will experience cracking within three years of service.

In contrast, Tables 3-10 and 3-11 present stress summaries for the elements surrounding critical node 81 of the comparable MS detail, depicted in Figure 2-26, for the unit load cases. It should be noted that the general shape of the stress contours for the comparable MS detail are similar in nature to those for the HSS detail. They vary in magnitude only. Table 3-12 presents a summary of the maximum stresses expected for the "design" loads as defined in Section 2.6, and modified in Section 2.10.

The maximum stress range occurred for the Full Load Departure condition and is 33.0 ksi (227.54 N/mm^2). Based on the design load used, and assuming a Weibull distribution factor of 1.0, it would be expected that the comparable MS detail will experience cracking within thirteen years of service. This is more than four times the service life of the equivalent HSS detail.

3.3 ALTERNATIVE DETAILS

As discussed in Section 2.9, alternative details were chosen for evaluation. The relative merit of the alternate details was evaluated by considering the relative stress concentrations for a specified loading condition. For the naval combatant, the uniform 1.0 ksi (6.895 N/mm^2) tensile stress was chosen since it has the greatest influence on the overall stress in the detail. For the tanker, the 1.0 kip (4.448 N) internal stiffener shear case was chosen to evaluate the relative merit of the details.

Figures B-8 through B-13 of Appendix B show the SXX stress contour plots for the naval combatant alternative details as described in Section 2.9. The table below lists the average nodal stress at the critical node for each alternative.

Alternate	Maximum SXX Stress, psi (N/mm^2)
Original	2929.0 (20.195)
1	2317.0 (15.976)
2	2677.0 (18.458)
3	2480.0 (17.000)
4	2907.0 (20.044)
5	2713.0 (18.706)
6	1121.0 (7.729)

As can be seen from the above table, all attempts at providing minor modifications to improve the stress concentration in the detail proved unsuccessful. The stress concentration did not reduce to a reasonable level until the stiffener was fully welded to the bulkhead (i.e., no snipe). The stresses for the fully welded detail (Alternative 6) will be evaluated and compared to the original. Figure 3-1 shows the modified naval combatant detail, indicating the locations of critical stress. Figures 3-2 and 3-3 show the updated fine mesh finite element model for the modified naval combatant detail, including the locations of critical stress.

Figures B-14 and B-15 of Appendix B show the SXX stress contour plots for the tanker alternatives as described in Section 2.9. The table below lists the average nodal stress at the critical nodes for each alternative.

Alternate	Maximum SXX Stress, psi (N/mm^2)
Original	-276.0 (-1.903)
1	-268.3 (-1.850)
2	- 85.2 (-0.587)

As can be seen from the above table, the addition of the brackets on either side of the header is the better alternative. The stresses for the detail with the additional brackets (Alternative 2) will be evaluated and compared to the original detail. Figure 3-4 shows the modified tanker detail. Figures 3-5 and 3-6 show the updated fine mesh finite element model, including the locations of critical stress.

Attempts were made to reduce stress concentrations in the tanker detail through minor changes in bracket contour, snipe geometry and relief cuts. For the tanker detail under investigation, these changes did not result in a significant improvement. Other authors, however, have demonstrated the effectiveness of these minor changes in improving similar details. Figure 3-7, taken from Reference (p), shows various side longitudinal end connections from a VLCC. As can be seen, the structural stress concentration (K_{STRUCT}), which includes the effects of both global and local discontinuities, is reduced by approximately 35% when going from a quarter circle to a semi-circle scallop.

3.4 MODIFIED NAVAL COMBATANT DETAIL

Figures B-16 through B-19 of Appendix B show the SXX stress contour plots for the unit load cases as defined in Section 2.6. Table 3-13 presents a stress summary of the elements surrounding the critical node, as depicted in Figure 3-3, for the unit load cases. Table 3-14 presents a summary of the maximum expected stresses for the "design" loads specified in Section 2.6. The maximum stress range for the modified detail is 31.70 ksi (218.57 N/mm^2). Based on the design loads considered, and a Weibull distribution factor of 1.7, it would be expected that this detail will experience cracking within 9 years of service. This is more than a ten fold improvement in the fatigue life. Additional life can be obtained by making the longitudinal continuous through the transverse bulkhead and providing collars as required. Although this detail is more costly to fabricate, it may be warranted for longitudinal strength members. Careful consideration should be given when using the original sniped detail on longitudinal strength structure carrying high primary stresses.

3.5 MODIFIED TANKER DETAIL

Figures B-20 through B-22 of Appendix B depict the SXX stress contour plots for the unit load cases defined in Section 2.6. Tables 3-15 and 3-16 present a stress summary for the elements surrounding the critical nodes, as depicted in Figure 3-6, for the unit load cases. Tables 3-17 and 3-18 present summaries of the maximum expected stresses for the "design" loads specified in Section 2.6. The maximum stress range occurring in the Full Load Departure condition is 45.0 ksi (310.28 N/mm^2). Based on the design loads considered, and a Weibull distribution factor of 1.0, it would be expected that this detail will experience cracking after 14 years of service. This modification has increased the expected service life to 5 times that of the original lapped detail. It should be noted that although the stress levels between the original and modified details are not markedly different, the choice of a better fatigue detail (seam vs. lapped connection) has significantly increased the life of the detail.

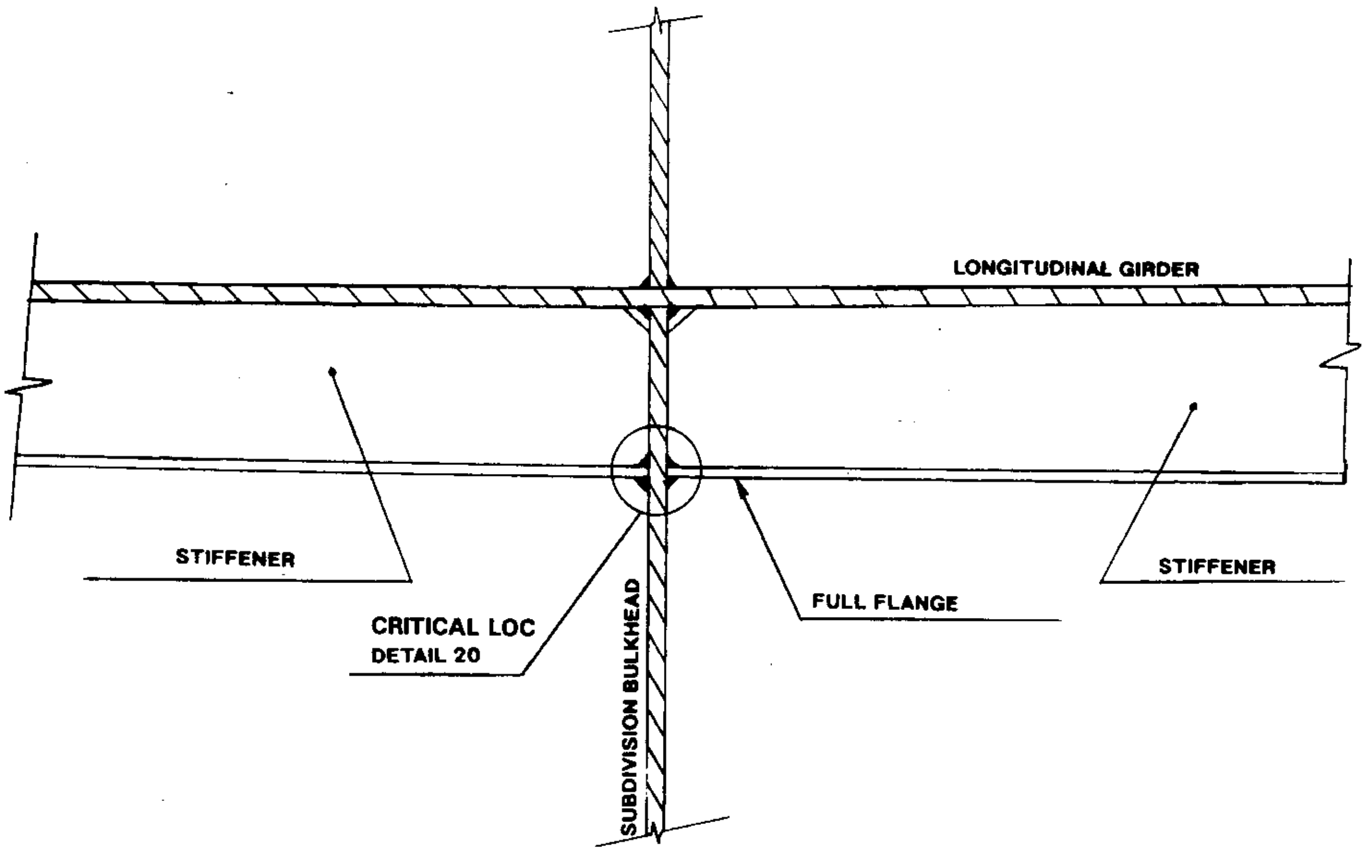

Note: Detail 20 taken from Reference (g)

FIGURE 3-1. MODIFIED NAVAL COMBATANT DETAIL SHOWING CRITICAL STRESS LOCATIONS

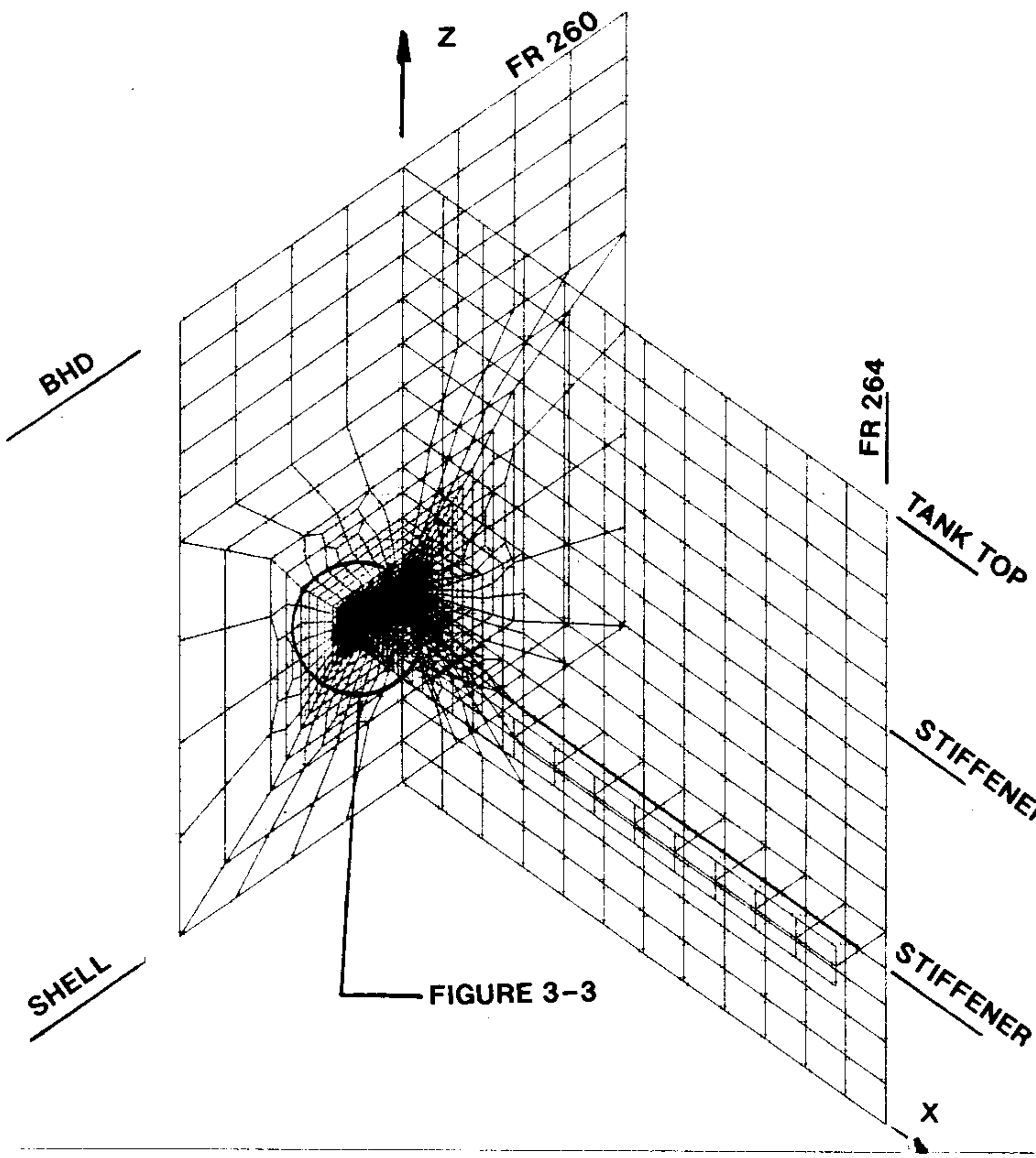

FIGURE 3-2. ISOMETRIC OF MODIFIED NAVAL COMBATANT FINE MESH MODEL

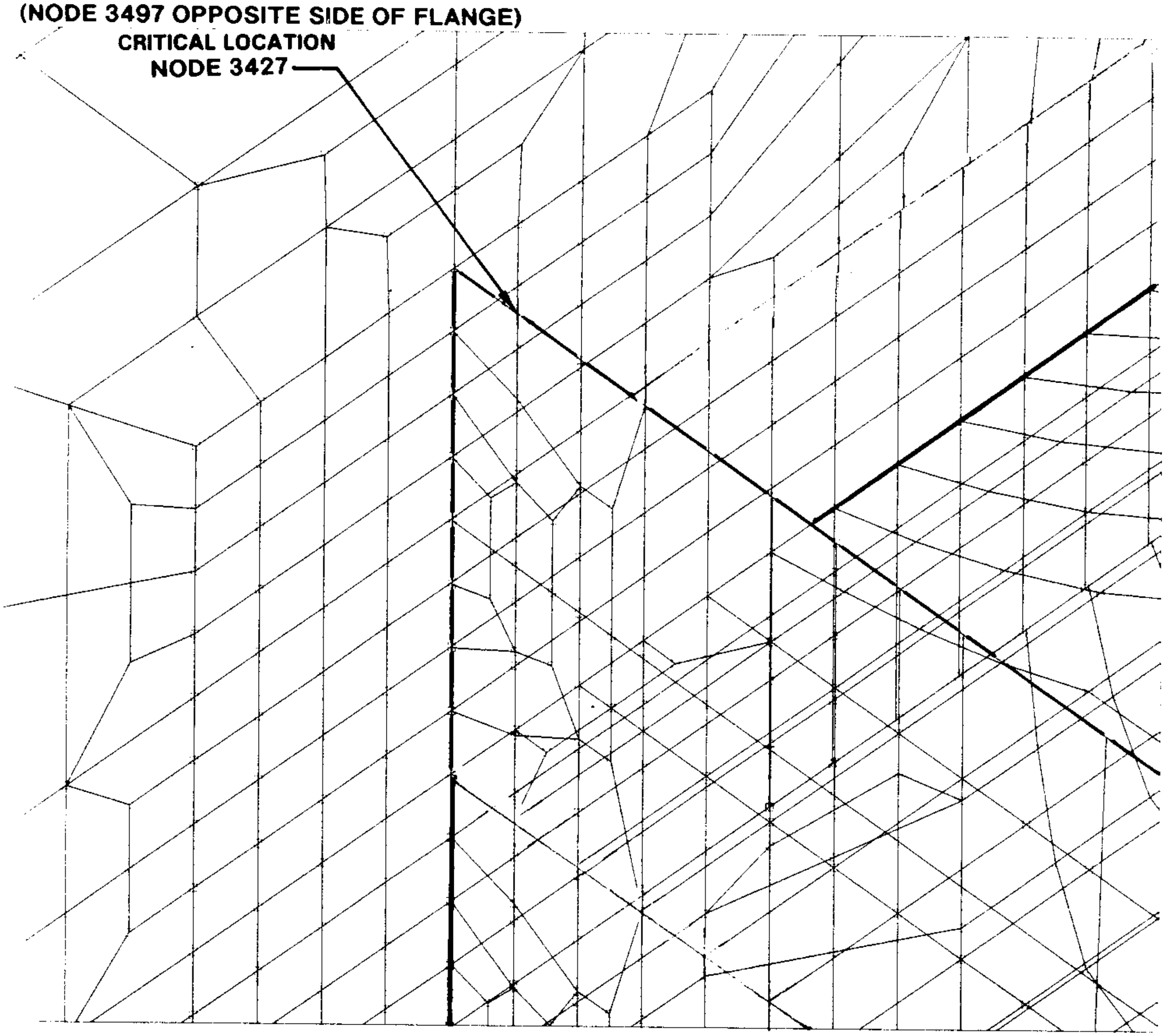

FIGURE 3-3. MESHING CONFIGURATION AT CRITICAL NODE - MODIFIED NAVAL COMBATANT

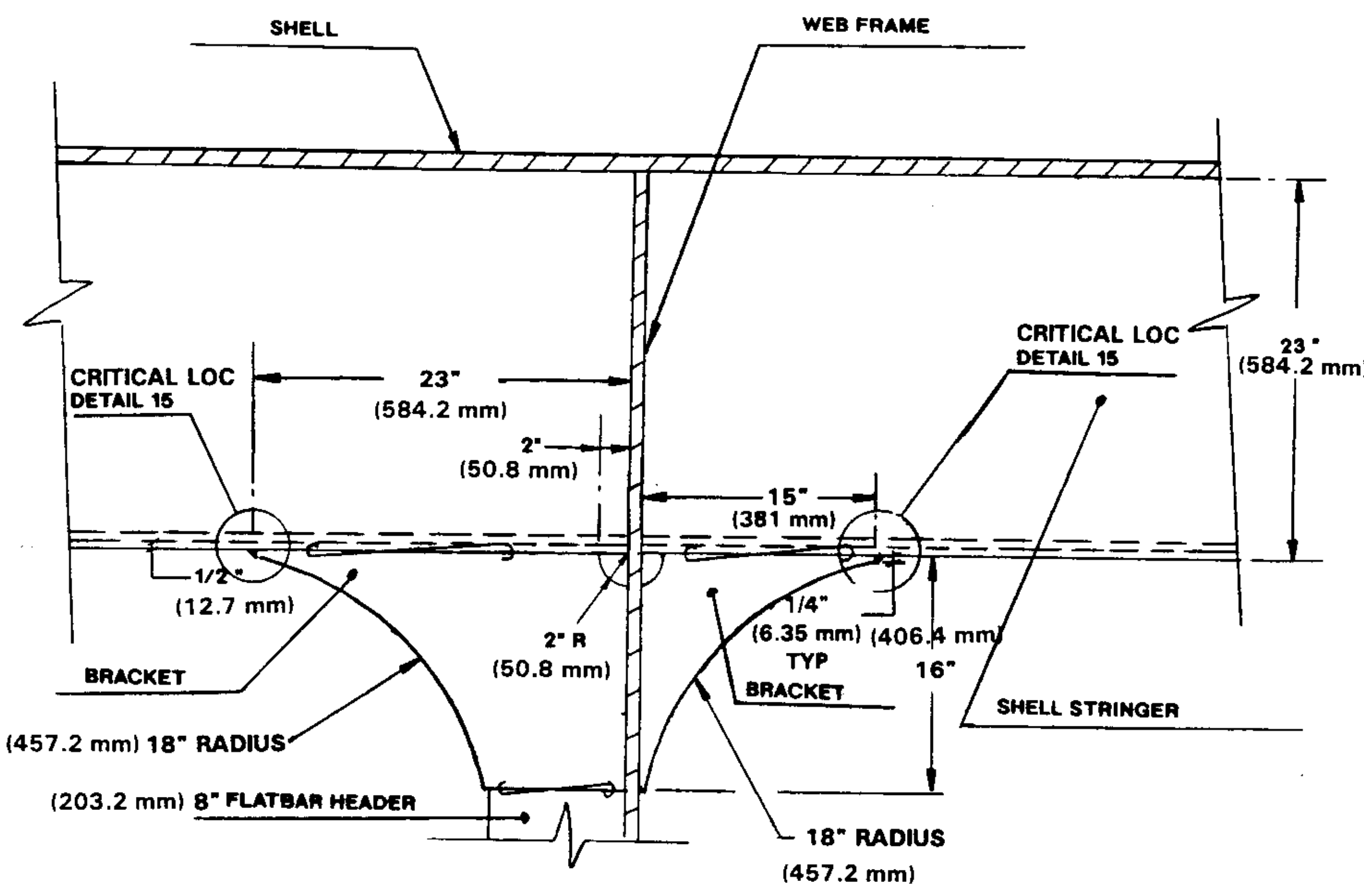

Note: Detail 15 taken from Reference (g)

FIGURE 3-4. MODIFIED TANKER DETAIL SHOWING CRITICAL STRESS LOCATIONS

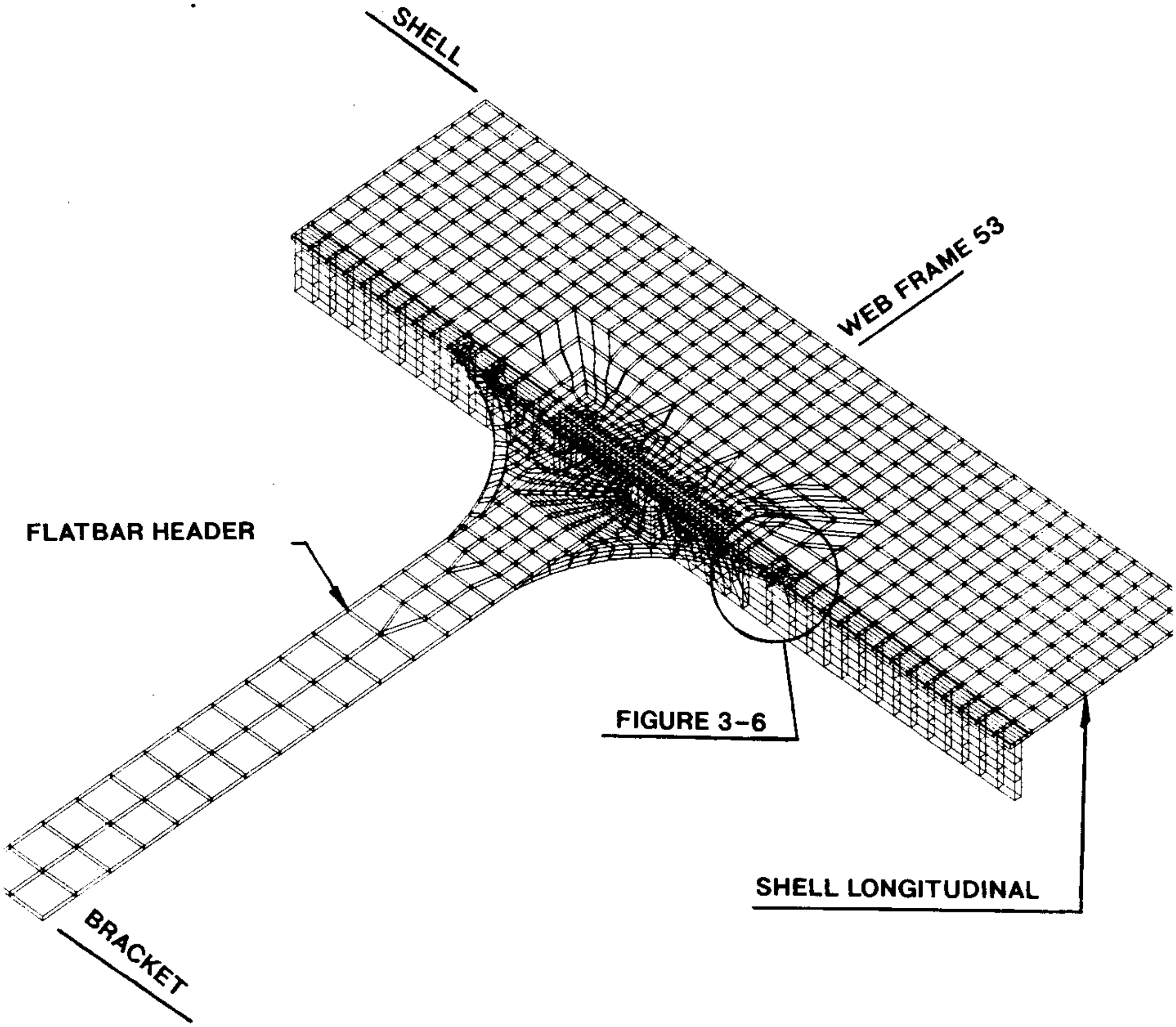

FIGURE 3-5. ISOMETRIC OF MODIFIED TANKER FINE MESH MODEL

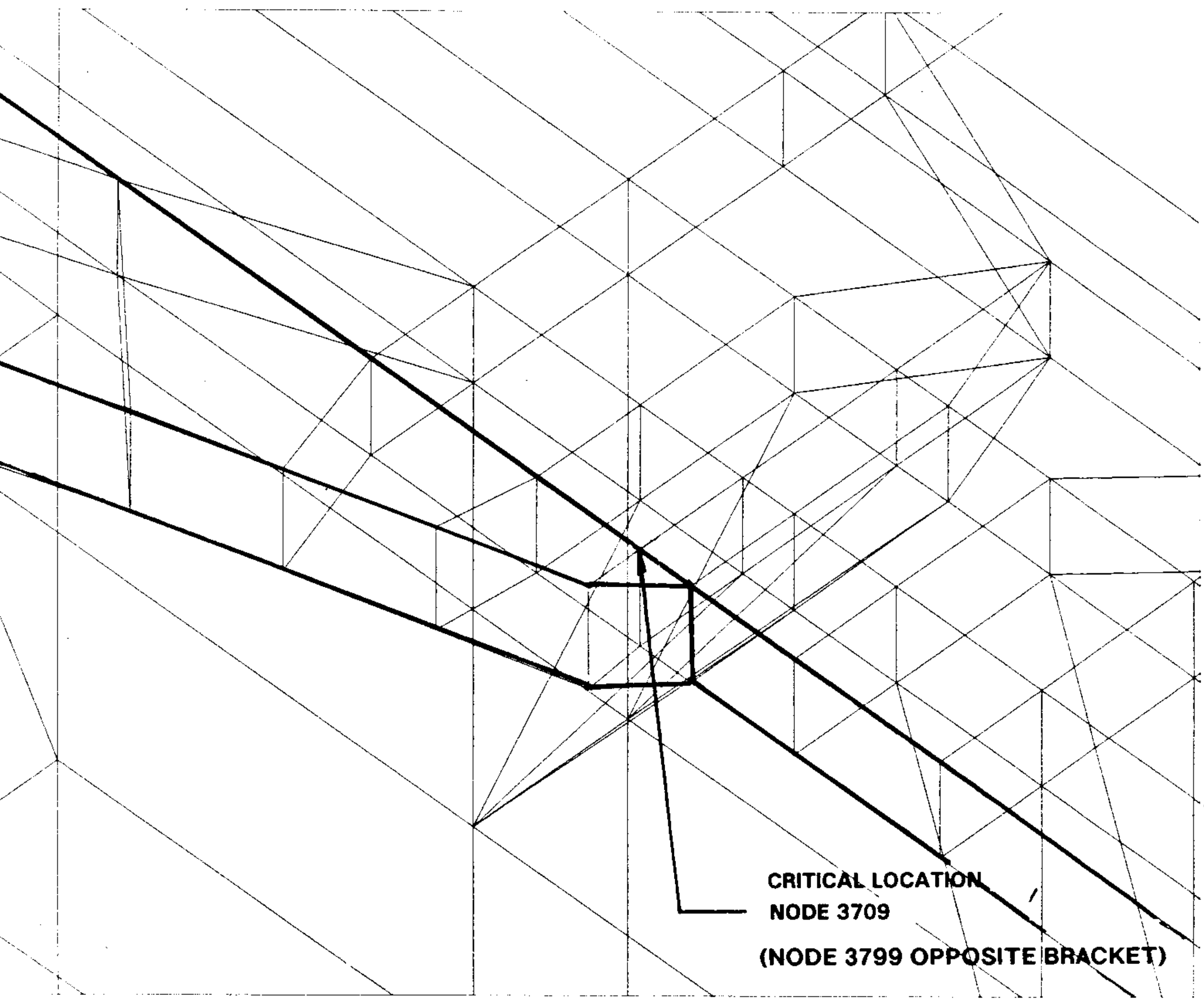

FIGURE 3-6 MESHING CONFIGURATION AT CRITICAL AREA - MODIFIED TANKER DETAIL

Flatbar stiffener		
Type of intersection		K_{STRUCT}
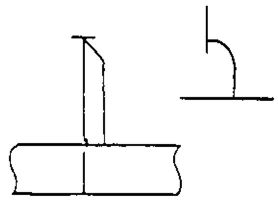		2.7
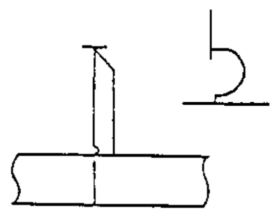		1.8
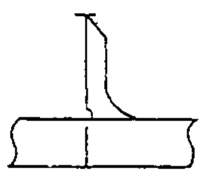		2.8
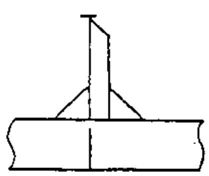		2.3
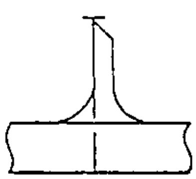		1.1

FIGURE 3-7. EXAMPLES OF STRESS CONCENTRATION FACTORS FOR VARIOUS SIDE LONGITUDINAL END CONNECTIONS

TABLE 3-1. UNIT LOAD STRESS SUMMARY FOR CRITICAL NODE 56 - NAVAL COM

ELEMENT 35 NODE 56

	SXX (PSI)	SYY (PSI)	SZZ (PSI)	SXY (PSI)	SYZ
PRIMARY STR.	2834.40	0.0	897.10	0.0	0
GRDR MOMENT	0.44	0.0	0.19	0.0	0
GRDR SHEAR	32.77	0.0	11.96	0.0	0
EXT PRESSURE	-1.43	0.0	-1.61	0.0	0

ELEMENT 36 NODE 56

	SXX (PSI)	SYY (PSI)	SZZ (PSI)	SXY (PSI)	SY
PRIMARY STR.	2970.80	0.0	937.95	0.0	0
GRDR MOMENT	0.47	0.0	0.20	0.0	0
GRDR SHEAR	30.67	0.0	11.33	0.0	0
EXT PRESSURE	2.01	0.0	-0.58	0.0	0

NOTE: FOR METRIC UNITS SEE PAGE 3-15.

TABLE 3-1. UNIT LOAD STRESS SUMMARY FOR CRITICAL NODE 56 - NAVAL COMBAT

ELEMENT 35 NODE 56

	SXX (N/mm^2)	SYY (N/mm^2)	SZZ (N/mm^2)	SXY (N/mm^2)	SY
PRIMARY STR.	1.954E+1	0.0	6.186E+0	0.0	0
GRDR MOMENT	3.014E-3	0.0	1.299E-3	0.0	0
GRDR SHEAR	2.259E-1	0.0	8.245E-2	0.0	0
EXT PRESSURE	-9.839E-3	0.0	-1.109E-2	0.0	0

ELEMENT 36 NODE 56

	SXX (N/mm^2)	SYY (N/mm^2)	SZZ (N/mm^2)	SXY (N/mm^2)	S
PRIMARY STR.	2.048E+1	0.0	6.467E+0	0.0	(
GRDR MOMENT	3.213E-3	0.0	1.353E-3	0.0	(
GRDR SHEAR	2.115E-1	0.0	7.812E-2	0.0	(
EXT PRESSURE	1.385E-2	0.0	-3.984E-3	0.0	(

NOTE: FOR ENGLISH UNITS SEE PAGE 3-14.

TABLE 3-2. UNIT LOAD STRESS SUMMARY FOR CRITICAL NODE 56 - NAVAL COMBATANT

ELEMENT 27 NODE 56

	SXX (PSI)	SYY (PSI)	SZZ (PSI)	SXY (PSI)	SYZ (PSI)	SXZ (PSI)
PRIMARY STR.	2834.5	0.0	897.40	0.0	0.0	-66.35
GRDR MOMENT	0.44	0.0	0.19	0.0	0.0	-0.049
GRDR SHEAR	32.78	0.0	12.00	0.0	0.0	37.28
EXT PRESSURE	-1.42	0.0	-1.56	0.0	0.0	64.29

ELEMENT 28 NODE 56

	SXX (PSI)	SYY (PSI)	SZZ (PSI)	SXY (PSI)	SYZ (PSI)	SXZ (PSI)
PRIMARY STR.	2970.8	0.0	938.30	0.0	0.0	-151.41
GRDR MOMENT	0.47	0.0	0.20	0.0	0.0	-0.061
GRDR SHEAR	30.68	0.0	11.37	0.0	0.0	36.67
EXT PRESSURE	2.02	0.0	-0.53	0.0	0.0	64.11

NOTE: FOR METRIC UNITS SEE PAGE 3-17.

TABLE 3-2. UNIT LOAD STRESS SUMMARY FOR CRITICAL NODE 56 - NAVAL COMBATANT (CONTD)

ELEMENT 27 NODE 56

	SXX (N/mm^2)	SYY (N/mm^2)	SZZ (N/mm^2)	SXY (N/mm^2)	SYZ (N/mm^2)	SXZ (N/mm^2)
PRIMARY STR.	1.954E+1	0.0	6.188E+0	0.0	0.0	-4.575E-1
GRDR MOMENT	3.015E-3	0.0	1.298E-3	0.0	0.0	-3.351E-4
GRDR SHEAR	2.260E-1	0.0	8.274E-2	0.0	0.0	2.570E-1
EXT PRESSURE	-9.756E-3	0.0	-1.076E-2	0.0	0.0	4.433E-1

ELEMENT 28 NODE 56

	SXX (N/mm^2)	SYY (N/mm^2)	SZZ (N/mm^2)	SXY (N/mm^2)	SYZ (N/mm^2)	SXZ (N/mm^2)
PRIMARY STR.	2.048E+1	0.0	6.470E+0	0.0	0.0	-1.044E+0
GRDR MOMENT	3.214E-3	0.0	1.358E-3	0.0	0.0	-4.171E-4
GRDR SHEAR	2.115E-1	0.0	7.840E-2	0.0	0.0	2.528E-1
EXT PRESSURE	1.394E-2	0.0	-3.652E-3	0.0	0.0	4.420E-1

NOTE: FOR ENGLISH UNITS SEE PAGE 3-16.

TABLE 3-3. STRESS SUMMARY FOR DESIGN LOADS - NAVAL COMBATANT

HOGGING CONDITION

	SXX (PSI)	SYY (PSI)	SZZ (PSI)	SXY (PSI)	SYZ (PSI)	SXZ (PSI)
PRIMARY STR.	-53260.0	0.0	-16840.0	0.0	0.0	1970.0
GRDR MOMENT	1510.0	0.0	643.0	0.0	0.0	-128.0
GRDR SHEAR	242.0	0.0	89.0	0.0	0.0	292.0
EXT PRESSURE	23.4	0.0	-23.1	0.0	0.0	876.0
TOTAL	-51484.6	0.0	-1613.0	0.0	0.0	3010.0

PRINCIPAL STRESSES (PSI) - S1 = -15880.0, S2 = -51730.0

SAGGING CONDITION

	SXX (PSI)	SYY (PSI)	SZZ (PSI)	SXY (PSI)	SYZ (PSI)	SXZ (PSI)
PRIMARY STR.	28160.0	0.0	8900.0	0.0	0.0	1040.0
GRDR MOMENT	264.0	0.0	115.0	0.0	0.0	-22.3
GRDR SHEAR	42.0	0.0	16.0	0.0	0.0	51.0
EXT PRESSURE	4.1	0.0	-2.5	0.0	0.0	86.0
TOTAL	28470.0	0.0	9030.0	0.0	0.0	1155.0

PRINCIPAL STRESSES (PSI) - S1 = 28540.0, S2 = 8960.0

NOTE: FOR METRIC UNITS SEE PAGE 3-19.

TABLE 3-3. STRESS SUMMARY FOR DESIGN LOADS - NAVAL COMBATANT (CONTD)

HOGGING CONDITION

	SXX (N/mm^2)	SYY (N/mm^2)	SZZ (N/mm^2)	SXY (N/mm^2)	SYZ (N/mm^2)	SXZ (N/mm^2)
PRIMARY STR.	-3.672E+2	0.0	-1.161E+2	0.0	0.0	1.358E+1
GRDR MOMENT	1.041E+1	0.0	4.433E+0	0.0	0.0	-8.826E-1
GRDR SHEAR	1.669E+0	0.0	6.137E-1	0.0	0.0	2.013E+0
EXT PRESSURE	1.613E-1	0.0	-1.593E-1	0.0	0.0	6.040E+0
TOTAL	-3.550E+2	0.0	-1.112E+2	0.0	0.0	2.075E+1

PRINCIPAL STRESSES (N/mm^2) - S1 = -109.5, S2 = 356.7

SAGGING CONDITION

	SXX (N/mm^2)	SYY (N/mm^2)	SZZ (N/mm^2)	SXY (N/mm^2)	SYZ (N/mm^2)	SXZ (N/mm^2)
PRIMARY STR.	1.942E+2	0.0	6.137E+1	0.0	0.0	7.171E+0
GRDR MOMENT	1.820E+0	0.0	7.929E-1	0.0	0.0	-1.538E-1
GRDR SHEAR	2.896E-1	0.0	1.103E-1	0.0	0.0	3.516E-1
EXT PRESSURE	2.027E-2	0.0	-1.724E-2	0.0	0.0	5.930E-1
TOTAL	1.963E+2	0.0	6.226E+1	0.0	0.0	7.964E+0

PRINCIPAL STRESSES (N/mm^2) - S1 = 196.78, S2 = 61.78

NOTE: FOR ENGLISH UNITS SEE PAGE 3-18.

TABLE 3-4. UNIT LOAD STRESS SUMMARY FOR CRITICAL NODE 81 - TANKER DETAIL (HSS)

ELEMENT 28 NODE 81

	SXX (PSI)	SYY (PSI)	SZZ (PSI)	SXY (PSI)	SYZ (PSI)	SXZ (PSI)
PRIMARY STR.	1041.15	451.95	63.26	-190.56	-32.72	-63.91
EXT PRESSURE	-198.63	-106.30	-16.35	82.01	6.21	7.87
INT. SHEAR	-132.15	-104.06	-15.01	52.40	2.11	7.93

ELEMENT 37 NODE 81

	SXX (PSI)	SYY (PSI)	SZZ (PSI)	SXY (PSI)	SYZ (PSI)	SXZ (PSI)
PRIMARY STR.	1027.0	452.05	8.93	-88.27	-67.59	-19.06
EXT PRESSURE	-202.87	-129.94	-8.85	92.69	16.69	-3.04
INT. SHEAR	-137.81	-128.83	-4.48	47.58	11.53	-2.75

NOTE: FOR METRIC UNITS SEE PAGE 3-21.

TABLE 3-4. UNIT LOAD STRESS SUMMARY FOR CRITICAL NODE 81 - TANKER DETAIL (HSS) (CONTD)

ELEMENT 28 NODE 81

	SXX (N/mm^2)	SYY (N/mm^2)	SZZ (N/mm^2)	SXY (N/mm^2)	SYZ (N/mm^2)	SXZ (N/mm^2)
PRIMARY STR.	7.179E+0	3.116E+0	4.362E-1	-1.314E+0	-2.256E-1	-4.407E-1
EXT PRESSURE	-1.370E+0	-7.329E-1	-1.127E-1	5.655E-1	3.593E-2	5.426E-2
INT. SHEAR	-9.112E-1	7.175E-1	1.035E-1	3.613E-1	1.455E-2	5.468E-2

ELEMENT 37 NODE 81

	SXX (N/mm^2)	SYY (N/mm^2)	SZZ (N/mm^2)	SXY (N/mm^2)	SYZ (N/mm^2)	SXZ (N/mm^2)
PRIMARY STR.	7.081E+0	3.117E+0	6.157E-2	-6.086E-1	-4.660E-1	-1.314E-1
EXT PRESSURE	-1.399E+0	-8.959E-1	-6.102E-2	6.391E-1	1.151E-1	-2.096E-2
INT. SHEAR	-9.502E-1	-8.883E-1	-3.089E-2	3.281E-1	7.950E-2	-1.896E-2

NOTE: FOR ENGLISH UNITS SEE PAGE 3-20.

TABLE 3-5. UNIT LOAD STRESS SUMMARY FOR CRITICAL NODE 81 - TANKER DETAIL (HSS)

ELEMENT 505 NODE 81

	SXX (PSI)	SYY (PSI)	SZZ (PSI)	SXY (PSI)	SYZ (PSI)	SXZ (PSI)
PRIMARY STR.	1424.70	581.72	-0.22	-266.17	-78.30	-28.280
EXT PRESSURE	-262.76	-126.26	-1.63	108.46	15.37	-2.50
INT. SHEAR	-178.13	-118.60	-6.31	77.33	8.00	-3.14

ELEMENT 513 NODE 81

	SXX (PSI)	SYY (PSI)	SZZ (PSI)	SXY (PSI)	SYZ (PSI)	SXZ (PSI)
PRIMARY STR.	1466.99	611.46	136.03	-169.88	-79.59	59.49
EXT PRESSURE	-276.57	-157.71	-32.80	110.49	23.61	-15.500
INT. SHEAR	-191.79	-152.58	-28.88	68.43	21.76	-12.32

NOTE: FOR METRIC UNITS SEE PAGE 3-23.

TABLE 3-5. UNIT LOAD STRESS SUMMARY FOR CRITICAL NODE 81 - TANKER DETAIL (HSS) (CONTD)

ELEMENT 505 NODE 81

	SXX (N/mm^2)	SYY (N/mm^2)	SZZ (N/mm^2)	SXY (N/mm^2)	SYZ (N/mm^2)	SXZ (N/mm^2)
PRIMARY STR.	9.823E+0	4.011E+0	-1.517E-3	-1.835E+0	-5.399E-1	-1.950E-1
EXT PRESSURE	-1.812E+0	-8.706E-1	-1.124E-2	7.478E-1	1.060E-1	-1.724E-2
INT. SHEAR	-1.228E+0	-8.173E-1	-4.351E-2	5.332E-1	5.516E-2	-2.165E-2

ELEMENT 513 NODE 81

	SXX (N/mm^2)	SYY (N/mm^2)	SZZ (N/mm^2)	SXY (N/mm^2)	SYZ (N/mm^2)	SXZ (N/mm^2)
PRIMARY STR.	1.012E+1	4.216E+0	9.379E-1	-1.171E+0	-5.488E-1	4.102E-1
EXT PRESSURE	-1.907E+0	-1.087E+0	-2.262E-1	7.628E-1	1.628E-1	-1.069E-1
INT. SHEAR	-1.322E+0	-1.052E+0	-1.991E-1	4.718E-1	1.500E-1	-8.495E-2

NOTE: FOR ENGLISH UNITS SEE PAGE 3-22.

TABLE 3-6. UNIT LOAD STRESS SUMMARY FOR CRITICAL NODE 82 - TANKER DETAIL (HSS)

ELEMENT 137 NODE 82

	SXX (PSI)	SYY (PSI)	SZZ (PSI)	SXY (PSI)	SYZ (PSI)	SXZ (PSI)
PRIMARY STR.	1105.40	269.24	-43.87	38.86	-62.40	34.94
EXT PRESSURE	-285.77	-117.91	14.80	42.42	18.65	-18.14
INT. SHEAR	-178.46	-85.06	1.93	-16.63	9.69	-4.29

ELEMENT 152 NODE 82

	SXX (PSI)	SYY (PSI)	SZZ (PSI)	SXY (PSI)	SYZ (PSI)	SXZ (PSI)
PRIMARY STR.	1117.00	254.62	71.380	-9.590	-32.02	-49.49
EXT PRESSURE	-293.81	-131.52	-21.15	85.61	6.46	5.04
INT. SHEAR	-184.96	-98.47	-24.78	1.33	13.39	12.42

NOTE: FOR METRIC UNITS SEE PAGE 3-25.

TABLE 3-6. UNIT LOAD STRESS SUMMARY FOR CRITICAL NODE 82 - TANKER DETAIL (HSS) (CONTD)

ELEMENT 137 NODE 82

	SXX (N/mm^2)	SYY (N/mm^2)	SZZ (N/mm^2)	SXY (N/mm^2)	SYZ (N/mm^2)	SXZ (N/mm^2)
PRIMARY STR.	7.622E+0	1.856E+0	-3.025E-1	2.679E-1	-4.302E-1	2.409E-1
EXT PRESSURE	-1.970E+0	-8.130E-1	1.021E-1	2.925E-1	1.286E-1	-1.251E-1
INT. SHEAR	-1.231E+0	-5.865E-1	1.331E-2	-1.147E-1	6.681E-2	2.958E-1

ELEMENT 152 NODE 82

	SXX (N/mm^2)	SYY (N/mm^2)	SZZ (N/mm^2)	SXY (N/mm^2)	SYZ (N/mm^2)	SXZ (N/mm^2)
PRIMARY STR.	7.702E+0	1.756E+0	4.922E-1	-6.612E-2	-2.208E-1	-3.412E-1
EXT PRESSURE	-2.026E+0	-9.068E-1	-1.458E-1	5.903E-1	4.454E-2	3.475E-2
INT. SHEAR	-1.275E+0	-6.790E-1	-1.709E-1	9.170E-3	9.232E-2	8.564E-2

NOTE: FOR ENGLISH UNITS SEE PAGE 3-24.

TABLE 3-7 UNIT LOAD STRESS SUMMARY FOR CRITICAL NODE 82 - TANKER DETAIL (HSS)

ELEMENT 36 NODE 82

	SXX (PSI)	SYY (PSI)	SZZ (PSI)	SXY (PSI)	SYZ (PSI)	SXZ (PSI)
PRIMARY STR.	840.75	179.37	12.33	64.95	-28.68	40.62
EXT PRESSURE	-202.59	-89.63	-1.52	26.33	6.63	-19.55
INT. SHEAR	-131.81	-69.46	-7.74	-13.82	3.64	-10.11

ELEMENT 47 NODE 82

	SXX (PSI)	SYY (PSI)	SZZ (PSI)	SXY (PSI)	SYZ (PSI)	SXZ (PSI)
PRIMARY STR.	823.62	173.97	-0.71	-4.92	-37.42	20.24
EXT PRESSURE	-201.67	-104.36	6.27	84.48	7.77	-8.57
INT. SHEAR	-131.58	-78.65	-1.39	6.94	9.14	-2.15

NOTE: FOR METRIC UNITS SEE PAGE 3-27.

TABLE 3-7 UNIT LOAD STRESS SUMMARY FOR CRITICAL NODE 82 - TANKER DETAIL (HSS) (CONT'D)

ELEMENT 36 NODE 82

	SXX (N/mm²)	SYY (N/mm²)	SZZ (N/mm²)	SXY (N/mm²)	SYZ (N/mm²)	SXZ (N/mm²)
PRIMARY STR.	5.797E+0	1.237E+0	8.502E-2	4.478E-1	-1.977E-1	2.801E-1
EXT PRESSURE	-1.397E+0	-6.180E-1	-1.048E-2	1.816E-1	4.571E-3	-1.348E-1
INT. SHEAR	-9.088E-1	-4.789E-1	-5.337E-2	-9.529E-2	2.510E-2	-6.971E-1

ELEMENT 47 NODE 82

	SXX (N/mm²)	SYY (N/mm²)	SZZ (N/mm²)	SXY (N/mm²)	SYZ (N/mm²)	SXZ (N/mm²)
PRIMARY STR.	5.679E+0	1.200E+0	-4.895E-3	-3.392E-2	-2.580E-1	1.396E-1
EXT PRESSURE	-1.391E+0	-7.196E-1	4.323E-2	5.825E-1	5.357E-2	-5.909E-2
INT. SHEAR	-9.072E-1	-5.423E-1	-9.584E-3	4.785E-2	6.302E-2	-1.482E-2

NOTE: FOR ENGLISH UNITS SEE PAGE 3-26.

TABLE 3-8. STRESS SUMMARY FOR DESIGN LOADS AT CRITICAL NODE 81 - TANKER DETAIL (HSS)

							PRINCIPAL STRESSES	
LOADING	SXX(PSI)	SYY(PSI)	SZZ(PSI)	SXY(PSI)	SYZ(PSI)	SXZ(PSI)	S1(PSI)	S2(PSI)
F.L.DEPART. HOG.	-31570.0	-17710.0	-1880.0	8710.0	1890.0	-880.0	-13509.5	-35770.5
F.L.DEPART. SAG.	11160.0	2490.0	360.0	730.0	-460.0	-498.0	11221.0	2428.96
F.L.ARRIVL. HOG.	-30940.0	-17440.0	-1860.0	8620.0	1860.0	-860.0	-13241.6	-35138.4
F.L.ARRIVL. SAG.	11240.0	2520.0	360.0	730.0	463.0	-500.0	11300.7	2459.3
N.B.DEPART. HOG. DN	-15790.0	-4910.0	550.0	910.0	723.0	640.0	-4834.4	-15865.5
N.B.DEPART. SAG. DN	19280.0	12050.0	1310.0	-6500.0	-1220.0	610.0	23102.6	8227.3
N.B.DEPART. HOG. UP	-23290.0	-9980.0	-995.0	3590.0	1220.0	790.0	-9073.4	-24196.6
N.B.DEPART. SAG. UP	11770.0	6980.0	750.0	-3500.0	720.0	340.0	13616.0	5134.0
N.B.ARRIVL. HOG. DN	-15170.0	-4640.0	530.0	960.0	690.0	613.0	-4553.2	-15256.8
N.B.ARRIVL. SAG. DN	19300.0	12060.0	1310.0	-6510.0	-1220.0	610.0	23128.8	8231.2
N.B.ARRIVL. HOG UP	-22675.0	-9720.0	970.0	3498.0	1190.0	770.0	-8836.0	-23560.0
N.B.ARRIVL. SAG. UP	11800.0	6990.0	750.0	-3500.0	720.0	340.0	13641.6	5148.4

NOTE: FOR METRIC UNITS SEE PAGE 3-29.

TABLE 3-8. STRESS SUMMARY FOR DESIGN LOADS AT CRITICAL NODE 81 - TANKER DETAIL (HSS) (CONT'D)

							PRINCIPAL STRESSES	
LOADING	SXX(N/mm²)	SYY(N/mm²)	SZZ(N/mm²)	SXY(N/mm²)	SYZ(N/mm²)	SXZ(N/mm²)	S1(Nmm²)	S2(N/mm²)
F.L.DEPART. HOG.	-217.68	-122.11	-12.96	60.06	13.03	-6.07	-93.15	-246.69
F.L.DEPART. SAG.	76.95	17.17	2.482	5.033	-3.172	-3.434	77.37	16.75
F.L.ARRIVL. HOG.	-213.33	-120.25	-12.82	59.43	12.82	-5.930	-91.30	-242.3
F.L.ARRIVL. SAG.	77.50	17.38	2.482	5.03 3	3.192	-3.448	77.92	16.96
N.B.DEPART. HOG. DN	-108.87	-33.85	3.792	6.274	4.985	4.413	-33.33	-109.39
N.B.DEPART. SAG. DN	132.94	83.08	9.032	-44.82	-8.412	4.206	159.29	56.73
N.B.DEPART. HOG. UP	-160.58	-68.812	-6.86	24.75	8.412	5.447	-62.56	-166.84
N.B.DEPART. SAG. UP	81.154	48.127	5.171	-24.131	4.964	2.344	93.88	35.40
N.B.ARRIVL. HOG. DN	-104.60	-31.993	3.654	6.619	4.758	4.227	-31.39	-105.20
N.B.ARRIVL. SAG. DN	133.07	83.154	9.032	-44.89	-8.412	4.206	159.47	56.75
N.B.ARRIVL. HOG UP	-156.34	-67.019	6.688	24.119	8.205	5.309	-60.924	-162.45
N.B.ARRIVL. SAG. UP	81.361	48.196	5.171	-24.133	4.964	2.344	94.059	35.498

NOTE: FOR ENGLISH UNITS SEE PAGE 3-28.

TABLE 3-9. STRESS SUMMARY FOR DESIGN LOADS AT CRITICAL NODE 82 - TANKER DETAIL (HSS)

							PRINCIPAL STRESSES	
LOADING	SXX(PSI)	SYY(PSI)	SZZ(PSI)	SXY(PSI)	SYZ(PSI)	SXZ(PSI)	S1(PSI)	S2(PSI)
F.L.DEPART. HOG.	-28390.0	-10840.0	1200.0	1680.0	1210.0	1250.0	-10680.6	-28549.4
F.L.DEPART. SAG.	6613.0	-780.0	138.0	1070.0	-260.0	150.0	6764.7	-931.7
F.L.ARRIVL. HOG.	-27890.0	-10730.0	1190.0	1660.0	1180.0	1230.0	-10570.8	-28049.1
F.L.ARRIVL. SAG.	6940.0	-700.0	143.0	1073.0	700.0	163.0	7088.0	-847.8
N.B.DEPART. HOG. DN	-10890.0	-650.0	265.0	-975.0	435.0	330.0	-558.0	-10982.0
N.B.DEPART. SAG. DN	18380.0	8120.0	845.0	1325.0	788.0	3420.0	18548.3	7951.6
N.B.DEPART. HOG. UP	-18470.0	-4370.0	618.0	623.0	763.0	703.0	-4342.5	-18497.5
N.B.DEPART. SAG. UP	10800.0	4400.0	473.0	665.0	-463.0	480.0	10868.4	4331.6
N.B.ARRIVL. HOG. DN	-10400.0	-583.0	-250.0	-965.0	420.0	313.0	-489.0	-10493.9
N.B.ARRIVL. SAG. DN	18400.0	8123.0	845.0	1320.0	790.0	860.0	18566.8	7956.2
N.B.ARRIVL. HOG UP	-17990.0	-4270.0	610.0	610.0	740.0	685.0	-4242.9	-18017.1
N.B.ARRIVL. SAG. UP	10820.0	4400.0	480.0	680.0	470.0	480.0	10891.2	4328.7

NOTE: FOR METRIC UNITS SEE PAGE 3-31.

TABLE 3-9. STRESS SUMMARY FOR DESIGN LOADS AT CRITICAL NODE 82 - TANKER DETAIL (HSS) (CONT'D)

							PRINCIPAL STRESSES	
LOADING	SXX(N/mm^2)	SYY(N/mm^2)	SZZ(N/mm^2)	SXY(N/mm^2)	SYZ(N/mm^2)	SXZ(N/mm^2)	S1(N/mm^2)	S2(N/mm^2)
F.L.DEPART. HOG.	-195.75	-74.74	8.274	11.584	8.343	8.619	-73.64	-195.85
F.L.DEPART. SAG.	45.60	-5.378	-0.952	+7.378	-1.793	1.034	46.64	-6.424
F.L.ARRIVL. HOG.	-192.30	-73.983	8.205	11.446	8.136	8.481	-72.89	-193.40
F.L.ARRIVL. SAG.	47.85	-4.827	0.986	7.398	4.827	1.124	48.87	-5.846
N.B.DEPART. HOG. DN	-75.066	-4.482	1.827	-6.723	2.999	2.275	-3.847	-75.721
N.B.DEPART. SAG. DN	126.73	55.987	5.826	9.136	5.433	23.581	127.89	54.826
N.B.DEPART. HOG. UP	-127.35	-30.131	4.261	4.296	5.261	4.847	-29.941	-127.54
N.B.DEPART. SAG. UP	74.466	30.338	3.261	4.585	-3.182	3.3096	74.938	29.866
N.B.ARRIVL. HOG. DN	-71.708	-4.020	-1.724	-6.654	2.896	2.158	-3.369	-72.355
N.B.ARRIVL. SAG. DN	126.868	56.008	5.826	9.101	5.447	5.920	128.02	54.86
N.B.ARRIVL. HOG UP	-124.041	-29.442	4.206	4.206	5.102	4.723	-29.255	-124.23
N.B.ARRIVL. SAG. UP	74.604	30.338	3.310	4.689	3.241	3.310	75.095	29.846

NOTE: FOR ENGLISH UNITS SEE PAGE 3-30.

TABLE 3-10. UNIT LOAD STRESS SUMMARY FOR CRITICAL NODE 81 - TANKER DETAIL (MS)

ELEMENT 28 NODE 81

	SXX (PSI)	SYY (PSI)	SZZ (PSI)	SXY (PSI)	SYZ (PSI)	SXZ (PSI)
PRIMARY STR.	1037.97	380.52	63.96	-191.79	-50.62	-23.07
EXT. PRESSURE	-140.06	-62.08	-12.15	57.50	6.65	-0.35
INT. SHEAR	-123.34	-86.04	-14.82	44.48	4.89	0.66

ELEMENT 37 NODE 81

	SXX (PSI)	SYY (PSI)	SZZ (PSI)	SXY (PSI)	SYZ (PSI)	SXZ (PSI)
PRIMARY STR.	1041.66	389.15	35.09	-70.12	-61.54	-14.39
EXT. PRESSURE	-144.50	-76.77	-10.31	60.61	9.95	-2.05
INT. SHEAR	-128.15	-101.97	-8.44	41.74	9.41	-2.61

NOTE: FOR METRIC UNITS SEE PAGE 3-33.

TABLE 3-10 UNIT LOAD STRESS SUMMARY FOR CRITICAL NODE 81 - TANKER DETAIL (MS) (CONTD)

ELEMENT 28 NODE 81

	SXX (N/mm^2)	SYY (N/mm^2)	SZZ (N/mm^2)	SXY (N/mm^2)	SYZ (N/mm^2)	SXZ (N/mm^2)
PRIMARY STR.	7.157E+0	2.624E+0	4.410E-1	-1.322E+0	-3.490E-1	-1.591E-1
EXT. PRESSURE	-9.657E-1	-4.280E-1	-8.377E-2	3.965E-1	4.585E-2	-2.413E-3
INT. SHEAR	-8.504E-1	-5.932E-1	-1.022E-1	3.343E-1	3.372E-2	4.551E-3

ELEMENT 37 NODE 81

	SXX (N/mm^2)	SYY (N/mm^2)	SZZ (N/mm^2)	SXY (N/mm^2)	SYZ (N/mm^2)	SXZ (N/mm^2)
PRIMARY STR.	7.182E+0	2.683E+0	2.419E-1	-4.835E-1	-4.243E-1	-9.922E-2
EXT. PRESSURE	-9.963E-1	-5.293E-1	-7.109E-2	4.179E-1	6.861E-2	-1.413E-2
INT. SHEAR	-8.336E-1	-7.031E-1	-5.819E-2	2.878E-1	6.488E-2	-1.800E-2

NOTE: FOR ENGLISH UNITS SEE PAGE 3-32.

TABLE 3-11. UNIT LOAD STRESS SUMMARY FOR CRITICAL NODE 81 - TANKER DETAIL (MS)

ELEMENT 505 NODE 81

	SXX (PSI)	SYY (PSI)	SZZ (PSI)	SXY (PSI)	SYZ (PSI)	SXZ (PSI)
PRIMARY STR.	1302.30	479.30	23.25	-268.11	-59.11	-11.77
EXT. PRESSURE	-168.20	-71.95	-4.63	72.99	7.84	-2.80
INT. SHEAR	-153.39	-97.81	-11.10	68.17	4.30	-4.69

ELEMENT 513 NODE 81

	SXX (PSI)	SYY (PSI)	SZZ (PSI)	SXY (PSI)	SYZ (PSI)	SXZ (PSI)
PRIMARY STR.	1345.08	502.7	129.04	-151.7	-70.64	64.21
EXT. PRESSURE	-177.26	-89.72	-21.89	71.81	13.37	-11.59
INT. SHEAR	-162.85	-118.70	-26.24	58.84	16.01	-12.55

NOTE: FOR METRIC UNITS SEE PAGE 3-35.

TABLE 3-11 UNIT LOAD STRESS SUMMARY FOR CRITICAL NODE 81 - TANKER DETAIL (MS) (CONTD)

ELEMENT 505 NODE 81

	SXX (N/mm^2)	SYY (N/mm^2)	SZZ (N/mm^2)	SXY (N/mm^2)	SYZ (N/mm^2)	SXZ (N/mm^2)
PRIMARY STR.	8.979E+0	3.305E+0	1.603E-1	-1.849E+0	-4.076E-1	-8.115E-2
EXT. PRESSURE	-1.160E+0	-4.961E-1	-3.192E-2	5.033E-1	5.406E-2	-1.931E-2
INT. SHEAR	-1.058E+0	-6.744E-1	-1.653E-2	4.700E-1	2.965E-2	-3.234E-2

ELEMENT 513 NODE 81

	SXX (N/mm^2)	SYY (N/mm^2)	SZZ (N/mm^2)	SXY (N/mm^2)	SYZ (N/mm^2)	SXZ (N/mm^2)
PRIMARY STR.	9.274E+0	3.466E+0	8.897E-1	-1.046E+0	-4.871E-1	-4.427E-1
EXT. PRESSURE	-1.222E+0	-6.186E-1	-1.509E-1	4.951E-1	9.212E-2	-7.991E-2
INT. SHEAR	-1.123E+0	-8.818E-1	-1.809E-1	4.057E-1	1.104E-1	-8.653E-2

NOTE: FOR ENGLISH UNITS SEE PAGE 3-34.

TABLE 3-12. STRESS SUMMARY FOR DESIGN LOADS AT CRITICAL NODE 81 - TANKER DETAIL (MS)

							PRINCIPAL STRESSES	
LOADING	SXX(PSI)	SYY(PSI)	SZZ(PSI)	SXY(PSI)	SYZ(PSI)	SXZ(PSI)	S1(PSI)	S2(PSI)
F.L.DEPART.HOG.	-23460.0	-12060.0	-1813.0	6643.0	1320.0	-560.0	-9010.6	-26510.0
F.L.DEPART. SAG.	6510.0	-688.0	-140.0	730.0	-270.0	-250.0	6600.0	600.0
F.L.ARRIVL. HOG.	-23030.0	-11903.0	1790.0	6583.0	1300.0	-550.0	-8850.8	-26090.0
F.L.ARRIVL. SAG.	6810.0	-793.0	150.0	690.0	-288.0	-260.0	6880.0	720.0
N.B.DEPART. HOG. DN	-10105.0	-2373.0	-318.0	-585.0	468.0	315.0	-2320.0	-10160.0
N.B.DEPART. SAG. DN	14838.0	8518.0	1293.0	-5060.0	-870.0	418.0	17650.0	5710.0
N.B.DEPART. HOG. UP	-15990.0	-6010.0	-868.0	2463.0	823.0	375.0	-5440.0	-16560.0
N.B.DEPART. SAG. UP	8950.0	4880.0	735.0	2725.0	513.0	233.0	10316.0	3514.0
N.B.ARRIVL. HOG. DN	-9680.0	-2220.0	-300.0	663.0	443.0	305.0	-2160.0	-9740.0
N.B.ARRIVL. SAG. DN	14350.0	8523.0	1295.0	-5063.0	-870.0	418.0	17657.0	5717.0
N.B.ARRIVL. HOG UP	-15570.0	-5850.0	-845.0	2403.0	810.0	365.0	-5290.0	-16132.0
N.B.ARRIVL. SAG. UP	8970.0	4890.0	738.0	-2730.0	-513.0	233.0	10340.0	3520.0

NOTE: FOR METRIC UNITS SEE PAGE 3-37.

TABLE 3-12. STRESS SUMMARY FOR DESIGN LOADS AT CRITICAL NODE 81 - TANKER DETAIL (MS) (CONTD)

							PRINCIPAL STRESSES	
LOADING	SXX(N/mm^2)	SYY(N/mm^2)	SZZ(N/mm^2)	SXY(N/mm^2)	SYZ(N/mm^2)	SXZ(N/mm^2)	S1(N/mm^2)	S2(N/mm^2)
F.L.DEPART. HOG.	-161.76	-83.15	-12.50	45.80	9.10	-3.861	-62.124	-182.79
F.L.DEPART. SAG.	44.89	-4.744	-0.952	5.033	-1.862	-1.724	45.51	4.137
F.L.ARRIVL. HOG.	-158.79	-82.07	-12.34	45.39	8.964	-3.792	-61.02	-179.87
F.L.ARRIVL. SAG.	46.95	5.468	1.034	4.758	-1.986	-1.793	47.44	4.964
N.B.DEPART. HOG. DN	-69.67	-16.36	-2.193	-4.723	3.227	2.172	-15.996	-70.05
N.B.DEPART. SAG. DN	102.31	58.73	8.913	-54.89	-5.999	2.882	121.70	39.37
N.B.DEPART. HOG. UP	-110.25	-41.44	-5.895	16.98	5.675	2.586	-37.51	-114.18
N.B.DEPART. SAG. UP	61.71	33.65	5.068	18.79	3.537	1.607	71.13	24.23
N.B.ARRIVL. HOG. DN	-66.74	-15.31	-2.069	4.571	3.054	2.103	-14.89	-67.16
N.B.ARRIVL. SAG. DN	102.39	58.77	8.929	-34.91	-5.999	2.882	121.75	39.42
N.B.ARRIVL. HOG UP	-107.36	-40.34	-5.826	16.57	5.585	2.517	-36.47	-111.23
N.B.ARRIVL. SAG. UP	61.85	33.72	5.089	-18.82	-3.537	1.607	71.29	24.27

NOTE: FOR ENGLISH UNITS SEE PAGE 3-36.

TABLE 3-13. UNIT LOAD STRESS SUMMARY FOR CRITICAL NODES 3427 AND 3497 - MODIFIED NAVAL COMBATANT

ELEMENT 2652 NODE 3427

	SXX (PSI)	SYY (PSI)	SZZ (PSI)	SXY (PSI)	SYZ (PSI)	SXZ (PSI)
PRIMARY STR.	936.60	0.0	-37.72	0.0	0.0	-8.29
GRDR MOMENT	0.12	0.0	-0.010	0.0	0.0	0.0
GRDR SHEAR	-15.64	0.0	4.81	0.0	0.0	0.92
EXT. PRESSURE	-15.18	0.0	14.89	0.0	0.0	4.30

ELEMENT 2679 NODE 3497

	SXX (PSI)	SYY (PSI)	SZZ (PSI)	SXY (PSI)	SYZ (PSI)	SXZ (PSI)
PRIMARY STR.	1125.6	0.0	-6.58	0.0	0.0	22.11
GRDR MOMENT	0.21	0.0	-0.002	0.0	0.0	0.006
GRDR SHEAR	6.62	0.0	-1.46	0.0	0.0	-5.76
EXT. PRESSURE	-4.96	0.0	-2.17	0.0	0.0	-17.79

NOTE: FOR METRIC UNITS SEE PAGE 3-39.

TABLE 3-13. UNIT LOAD STRESS SUMMARY FOR CRITICAL NODES 3427 AND 3497 - MODIFIED NAVAL COMBATANT (CONT'D)

ELEMENT 2652 NODE 3427

	SXX (PSI)	SYY (PSI)	SZZ (PSI)	SXY (PSI)	SYZ (PSI)	SXZ (PSI)
PRIMARY STR.	6.458E+0	0.0	2.601E-1	0.0	0.0	-5.716E-2
GRDR MOMENT	8.274E-4	0.0	-6.206E-5	0.0	0.0	0.0
GRDR SHEAR	-1.078E-1	0.0	3.317E-2	0.0	0.0	6.337E-3
EXT. PRESSURE	1.047E-1	0.0	1.027E-1	0.0	0.0	2.965E-2

ELEMENT 2679 NODE 3497

	SXX (PSI)	SYY (PSI)	SZZ (PSI)	SXY (PSI)	SYZ (PSI)	SXZ (PSI)
PRIMARY STR.	7.761E+0	0.0	-4.537E-2	0.0	0.0	1.524E-1
GRDR MOMENT	1.420E-3	0.0	1.689E-5	0.0	0.0	4.206E-5
GRDR SHEAR	4.564E-2	0.0	-1.007E-2	0.0	0.0	3.972E-2
EXT. PRESSURE	3.420E-2	0.0	1.496E-2	0.0	0.0	1.227E-1

NOTE: FOR ENGLISH UNITS SEE PAGE 3-38.

TABLE 3-14. STRESS SUMMARY FOR DESIGN LOADS- MODIFIED NAVAL COMBATANT

HOGGING CONDITION

	SXX (PSI)	SYY (PSI)	SZZ (PSI)	SXY (PSI)	SYZ (PSI)	SXZ (PSI)
PRIMARY STR.	-20655.0	0.0	-692.0	0.0	0.0	-152.0
GRDR MOMENT	401.0	0.0	-29.0	0.0	0.0	0.0
GRDR SHEAR	-193.0	0.0	37.0	0.0	0.0	7.0
EXT PRESSURE	-207.0	0.0	203.0	0.0	0.0	59.0
TOTAL	-20654.0	0.0	-481.0	0.0	0.0	-86.0

PRINCIPAL STRESSES (PSI) - S1 = -481.0, S2 = -20654.0

SAGGING CONDITION

	SXX (PSI)	SYY (PSI)	SZZ (PSI)	SXY (PSI)	SYZ (PSI)	SXZ (PSI)
PRIMARY STR.	10920.0	0.0	-64.0	0.0	0.0	215.0
GRDR MOMENT	120.3	0.0	-1.4	0.0	0.0	3.6
GRDR SHEAR	8.8	0.0	-1.9	0.0	0.0	-7.7
EXT. PRESSURE	-11.8	0.0	-5.2	0.0	0.0	-42.3
TOTAL	11037.0	0.0	-72.6	0.0	0.0	168.1

PRINCIPAL STRESSES (PSI) S1 = 11040.0, S2 = -80.0

NOTE: FOR METRIC UNITS SEE PAGE 3-41.

TABLE 3-14. STRESS SUMMARY FOR DESIGN LOADS- MODIFIED NAVAL COMBATANT (CONT'D)

HOGGING CONDITION

	SXX (N/mm^2)	SYY (N/mm^2)	SZZ (N/mm^2)	SXY (N/mm^2)	SYZ (N/mm^2)	SXZ (N/mm^2)
PRIMARY STR.	-1.424E+2	0.0	-4.771E+0	0.0	0.0	1.048E+0
GRDR MOMENT	2.765E+0	0.0	-1.999E-1	0.0	0.0	0.0
GRDR SHEAR	-1.331E+0	0.0	2.551E-1	0.0	0.0	4.823E-2
EXT PRESSURE	-1.427E+0	0.0	1.400E+0	0.0	0.0	4.068E-1
TOTAL	-1.424E+2	0.0	-3.316E+0	0.0	0.0	5.930E-1

PRINCIPAL STRESSES (PSI) - S1 = -3.316E+0, S2 = -1.424E+2

SAGGING CONDITION

	SXX (N/mm^2)	SYY (N/mm^2)	SZZ (N/mm^2)	SXY (N/mm^2)	SYZ (N/mm^2)	SXZ (N/mm^2)
PRIMARY STR.	7.529E+1	0.0	-4.413E-1	0.0	0.0	1.482E+0
GRDR MOMENT	8.295E-1	0.0	-9.653E-3	0.0	0.0	2.482E-2
GRDR SHEAR	6.068E-2	0.0	-1.310E-2	0.0	0.0	-5.309E-2
EXT. PRESSURE	8.136E-2	0.0	-3.585E-2	0.0	0.0	-4.754E-2
TOTAL	7.610E+1	0.0	-5.006E-1	0.0	0.0	1.159E+0

PRINCIPAL STRESSES (PSI) S1 = 7.612E+1, S2 = -5.516E-1

NOTE: FOR ENGLISH UNITS SEE PAGE 3-40.

TABLE 3-15. UNIT LOAD STRESS SUMMARY FOR CRITICAL NODE 3709 - MODIFIED TANKER DETAIL (HHS)

ELEMENT 1828 NODE 3709

	SXX (PSI)	SYY (PSI)	SZZ (PSI)	SXY (PSI)	SYZ (PSI)	SXZ (PSI)
PRIMARY STR.	1387.80	108.63	-57.20	-290.90	13.81	4.53
EXT. PRESSURE	-108.70	-18.60	0.63	32.77	-0.62	-0.41
INT. SHEAR	-62.80	-7.69	1.93	16.37	-0.628	-0.482

ELEMENT 1829 NODE 3709

	SXX (PSI)	SYY (PSI)	SZZ (PSI)	SXY (PSI)	SYZ (PSI)	SXZ (PSI)
PRIMARY STR.	1493.89	165.45	6.86	-248.50	-13.60	11.11
EXT. PRESSURE	-109.91	-19.51	-1.95	26.51	0.493	0.625
INT. SHEAR	-65.34	-9.128	-0.198	13.238	0.3410	0.032

NOTE: FOR METRIC UNITS SEE PAGE 3-43.

TABLE 3-15. UNIT LOAD STRESS SUMMARY FOR CRITICAL NODE 3709 - MODIFIED TANKER DETAIL (HSS) (CONTD)

ELEMENT 1828 NODE 3709

	SXX (N/mm^2)	SYY (N/mm^2)	SZZ (N/mm^2)	SXY (N/mm^2)	SYZ (N/mm^2)	SXZ (N/mm^2)
PRIMARY STR.	9.569E+0	7.490E-1	-3.944E-1	-2.006E+0	9.522E-2	3.123E+0
EXT. PRESSURE	-7.495E-1	1.283E-1	4.323E-3	2.259E-1	-4.275E-3	-2.827E-3
INT. SHEAR	-4.330E-1	-5.302E-2	1.331E-2	1.129E-1	-4.330E-3	-3.330E-3

ELEMENT 1829 NODE 3709

	SXX (N/mm^2)	SYY (N/mm^2)	SZZ (N/mm^2)	SXY (N/mm^2)	SYZ (N/mm^2)	SXZ (N/mm^2)
PRIMARY STR.	1.030E+1	1.141E+0	4.732E-2	-1.713E+0	-9.377E-2	7.660E-2
EXT. PRESSURE	-7.578E-1	-1.345E-1	-1.342E-2	1.828E-1	3.399E-3	4.309E-3
INT. SHEAR	-4.505E-1	-6.294E-2	-1.365E-3	9.128E-2	2.351E-3	2.206E-4

NOTE: FOR ENGLISH UNITS SEE PAGE 3-42.

TABLE 3-16. UNIT LOAD STRESS SUMMARY FOR CRITICAL NODE 3799 - MODIFIED TANKER DETAIL (HSS)

ELEMENT 1859 NODE 3799

	SXX (PSI)	SYY (PSI)	SZZ (PSI)	SXY (PSI)	SYZ (PSI)	SXZ (PSI)
PRIMARY STR.	1197.59	101.50	-48.45	238.98	12.61	-2.64
EXT. PRESSURE	-269.29	-41.22	8.58	-77.71	-1.96	-0.367
INT. SHEAR	-69.98	-8.34	2.82	-17.734	-0.632	0.116

ELEMENT 1860 NODE 3799

	SXX (PSI)	SYY (PSI)	SZZ (PSI)	SXY (PSI)	SYZ (PSI)	SXZ (PSI)
PRIMARY STR.	1313.28	153.70	9.3970	221.33	-8.127	-8.59
EXT. PRESSURE	-274.86	-41.070	8.5500	-64.73	-2.66	-5.647
INT. SHEAR	-74.00	-9.55	1.368	-15.275	-0.257	-0.628

NOTE: FOR METRIC UNITS SEE PAGE 3-45.

TABLE 3-16. UNIT LOAD STRESS SUMMARY FOR CRITICAL NODE 3799 - MODIFIED TANKER DETAIL (HSS) (CONTD)

ELEMENT 1859 NODE 3799

	SXX (N/mm^2)	SYY (N/mm^2)	SZZ (N/mm^2)	SXY (N/mm^2)	SYZ (N/mm^2)	SXZ (N/mm^2)
PRIMARY STR.	8.257E+0	6.998E-1	-3.341E-1	1.648E+0	8.696E-2	-1.819E-2
EXT. PRESSURE	-1.858E+0	-2.842E-1	5.916E-2	-5.358E-1	-1.348E-2	-2.530E-3
INT. SHEAR	-4.825E-1	-5.750E-2	1.943E-2	-1.223E-1	-4.358E-3	7.998E-4

ELEMENT 1860 NODE 3799

	SXX (N/mm^2)	SYY (N/mm^2)	SZZ (N/mm^2)	SXY (N/mm^2)	SYZ (N/mm^2)	SXZ (N/mm^2)
PRIMARY STR.	9.055E+0	1.060E+0	6.479E-2	1.526E+0	5.6036E-2	-5.923E-2
EXT. PRESSURE	-1.895E+0	-2.832E-1	5.895E-2	-4.463E-1	-1.834E-2	-3.894E-2
INT. SHEAR	-5.102E-1	-6.585E-2	9.432E-1	-1.0532E-1	-1.772E+0	-4.330E-3

NOTE: FOR ENGLISH UNITS SEE PAGE 3-44.

TABLE 3-17. STRESS SUMMARY FOR DESIGN LOADS FOR CRITICAL NODE 3709 - MODIFIED TANKER DETAIL (HSS)

							PRINCIPAL STRESSES	
LOADING	SXX(PSI)	SYY(PSI)	SZZ(PSI)	SXY(PSI)	SYZ(PSI)	SXZ(PSI)	S1(PSI)	S2(PSI)
F.L.DEPART. HOG.	-24680.0	-2740.0	495.0	5060.0	-220.0	-110.0	-1629.3	-25790.7
F.L.DEPART. SAG.	18730.0	1580.0	-820.0	3290.0	-190.0	120.0	19339.5	970.5
F.L.ARRIVL. HOG.	-23940.0	-2670.0	810.0	4920.0	-220.0	-100.0	-1587.0	-25023.0
F.L.ARRIVL. SAG.	19210.0	1630.0	-840.0	-3370.0	-200.0	120.0	19833.4	1006.2
N.B.DEPART. HOG. DN	-23240.0	-2050.0	440.0	4170.0	NIL	-140.0	-1258.9	-24032.0
N.B.DEPART. SAG. DN	11260.0	1420.0	-120.0	-2540.0	10.0	35.0	11877.0	803.0
N.B.DEPART. HOG. UP	-26470.0	-2550.0	460.0	4990.0	NIL	-140.0	-1550.8	-27469.2
N.B.DEPART. SAG. UP	8030.0	925.0	-105.0	-1530.0	10.0	30.0	8345.6	609.5
N.B.ARRIVL. HOG. DN	-22530.0	-1990.0	430.0	4040.0	10.0	-130.0	-1223.9	-23296.5
N.B.ARRIVL. SAG. DN	11690.0	1460.0	-120.0	-2580.0	10.0	35.0	12303.8	846.2
N.B.ARRIVL. HOG UP	-25760.0	2480.0	440.0	4860.0	-10.0	-140.0	3293.0	-26572.98
N.B.ARRIVL. SAG. UP	8450.0	970.0	-120.0	-1760.0	-10.0	35.0	8843.4	576.5

NOTE: FOR METRIC UNITS SEE PAGE 3-47.

TABLE 3-17. STRESS SUMMARY FOR DESIGN LOADS FOR CRITICAL NODE 3709 - MODIFIED TANKER DETAIL (HSS) (CONTD)

							PRINCIPAL STRESSES	
LOADING	SXX (N/mm^2)	SYY (N/mm^2)	SZZ (N/mm^2)	SXY (N/mm^2)	SYZ (N/mm^2)	SXZ (N/mm^2)	S1 (N/mm^2)	S2 (N/mm^2)
F.L.DEPART. HOG.	-170.17	-18.89	3.413	34.89	-1.517	-0.76	-11.234	-177.83
F.L.DEPART. SAG.	129.14	10.89	-5.654	22.68	-1.310	+0.827	133.35	6.692
F.L.ARRIVL. HOG.	-165.07	-18.41	5.585	33.92	-1.517	-0.690	-10.94	-172.53
F.L.ARRIVL. SAG.	132.45	11.24	-5.792	-23.24	-1.379	+0.827	136.751	6.938
N.B.DEPART. HOG. DN	-160.24	-14.14	3.034	28.75	0.0	-0.965	-8.680	-165.70
N.B.DEPART. SAG. DN	77.64	9.791	-0.827	17.53	0.6895	+0.241	81.892	5.537
N.B.DEPART. HOG. UP	-182.51	-17.58	3.172	34.41	0.0	-0.965	-10.692	-189.40
N.B.DEPART. SAG. UP	55.37	6.378	-0.724	-10.55	0.6895	0.207	57.54	4.203
N.B.ARRIVL. HOG. DN	-155.34	-13.72	2.965	27.86	0.6895	-0.896	-8.439	-160.63
N.B.ARRIVL. SAG. DN	80.60	10.07	-0.827	-17.79	0.6895	0.241	84.835	5.835
N.B.ARRIVL. HOG UP	-177.62	-17.10	3.034	33.51	-0.6895	-0.965	22.705	-183.21
N.B.ARRIVL. SAG. UP	58.26	6.688	-0.827	-12.14	-0.6895	0.241	60.975	3.975

NOTE: FOR ENGLISH UNITS SEE PAGE 3-46.

TABLE 3-18. STRESS SUMMARY FOR DESIGN LOADS FOR CRITICAL NODE 3799 - MODIFIED TANKER DETAIL (HSS)

							PRINCIPAL STRESSES	
LOADING	SXX(PSI)	SYY(PSI)	SZZ(PSI)	SXY(PSI)	SYZ(PSI)	SXZ(PSI)	S1(PSI)	S2(PSI)
F.L.DEPART. HOG.	-27600.0	-3300.0	610.0	5880.0	-250.0	-110.0	-1951.9	-28948.0
F.L.DEPART. SAG.	13190.0	1090.0	-540.0	2000.0	-170.0	-140.0	13512.0	767.9
F.L.ARRIVL. HOG.	-26970.0	-32320.0	610.0	-5770.0	-120.0	-100.0	-1901.9	-28298.1
F.L.ARRIVL. SAG.	13620.0	1140.0	-550.0	2075.0	-180.0	-140.0	13955.9	804.0
N.B.DEPART. HOG. DN	-17770.0	-1610.0	210.0	-2930.0	NIL	150.0	-1095.2	-18284.8
N.B.DEPART. SAG. DN	15270.0	1990.0	-400.0	3540.0	90.0	70.0	16154.7	1105.3
N.B.DEPART. HOG. UP	-23640.0	-2450.0	390.0	-4410.0	-50.0	95.0	-1568.8	-24521.1
N.B.DEPART. SAG. UP	9395.0	1150.0	-220.0	-2050.0	45.0	20.0	9876.6	668.4
N.B.ARRIVL. HOG. DN	-17140.0	-1550.0	190.0	-2810.0	NIL	140.0	-1058.9	-17631.0
N.B.ARRIVL. SAG. DN	15660.0	2030.0	-410.0	3600.0	90.0	70.0	16552.4	1137.6
N.B.ARRIVL. HOG UP	-23020.0	-2380.0	370.0	-4290.0	-50.0	90.0	-1523.8	-23876.2
N.B.ARRIVL. SAG. UP	9770.0	1190.0	-230.0	2120.0	50.0	20.0	10265.24	694.8

NOTE: FOR METRIC UNITS SEE PAGE 3-49

TABLE 3-18. STRESS SUMMARY FOR DESIGN LOADS FOR CRITICAL NODE 3799 - MODIFIED TANKER DETAIL (HSS) (CONTD)

							PRINCIPAL STRESSES	
LOADING	SXX (N/mm^2)	SYY (N/mm^2)	SZZ (N/mm^2)	SXY (N/mm^2)	SYZ (N/mm^2)	SXZ (N/mm^2)	S1 (N/mm^2)	S2 (N/mm^2)
F.L.DEPART. HOG.	-190.30	-22.754	4.206	40.54	-1.724	-0.758	-13.46	-199.60
F.L.DEPART. SAG.	90.95	7.516	-3.723	13.79	-1.172	-0.965	93.17	5.295
F.L.ARRIVL. HOG.	-185.96		4.206	-39.78	-0.827	-0.689	-13.11	-195.12
F.L.ARRIVL. SAG.	93.91	7.860	-3.792	14.31	-1.241	-0.965	96.23	5.544
N.B.DEPART. HOG. DN	-122.52	-11.101	1.448	-20.20	NIL	1.034	-7.551	-126.07
N.B.DEPART. SAG. DN	105.29	18.783	-2.758	24.41	0.621	0.483	111.39	7.621
N.B.DEPART. HOG. UP	-162.99	-16.893	2.689	-30.407	-0.345	0.655	-10.82	-169.07
N.B.DEPART. SAG. UP	64.78	7.929	-1.517	-14.135	0.310	0.138	68.10	4.609
N.B.ARRIVL. HOG. DN	-118.18	-10.687	1.3101	-19.375	NIL	0.965	-7.301	-121.57
N.B.ARRIVL. SAG. DN	107.976	13.997	-2.827	24.822	0.621	0.483	114.13	7.844
N.B.ARRIVL. HOG UP	-158.72	-16.410	2.551	-29.588	-0.345	0.621	-10.51	-164.63
N.B.ARRIVL. SAG. UP	67.364	8.205	-1.586	14.617	0.345	0.138	70.78	4.791

NOTE: FOR ENGLISH UNITS SEE PAGE 3-48.

4.0 CONCLUSIONS AND RECOMMENDATIONS

This paper demonstrated a fatigue analysis methodology using readily available "design" loads and current fatigue documentation. This methodology was then used to improve two high strength steel details which have potential cracking problems. This was accomplished to call attention to the problems of cracking in high strength steel details. The fatigue methodology chosen is that outlined in SSC Report No. 318 entitled "Fatigue Characterization of Fabricated Ship Details for Design". This method was chosen for several reasons. The general nature by which the effects of the long term load factor are introduced allows any ship, who's loading history can be described by a Weibull probability density function, to be easily accommodated. The effects of the long term load factor are applied to the allowable stress, rather than the applied load. This provides the analyst the freedom to choose from many analysis procedures to develop the actual maximum stress range. Reliability factors (safety factors) are provided for 90%, 95% and 99% reliability for each detail. This allows the designer a range of reliabilities so that more critical details can be afforded greater safety factors. Also, the details reviewed in the method correspond to many of the most frequently used details in the U.S. shipbuilding industry.

From a design standpoint, there are some draw-backs to the methodology. Since the description of the long term loading factor is general, there is little guidance for the choice of the Weibull parameter (k) for various ship types. Several tankers and cargo ships were reviewed in the method, however, little correlation can be drawn between the Weibull shape parameter (k) and the basic hull characteristics. It is evident that the Weibull shape parameter is very dependent on the basic ship characteristics of length, width and weight. In order to make the method a more viable design tool, correlation between the Weibull shape parameter and the basic hull characteristics for various classes of ships will be needed. ABS has taken a step in this direction with their "Guide for the Fatigue Strength Assessment of Tankers". The long term load factors are developed as a function of the length of the tanker. However, the simplification of the parameters limits the usefulness of the method.

A second problem arises in the S-N data. This data is based upon "Hot Spot" S-N curves for each detail. The basic problem is that there is no widely accepted or complete collection of S-N data. Several key details reviewed in the methodology do not have S-N data available or the data is inconclusive. This forces the analyst to choose another detail or to try and fit non "Hot Spot" data into the design methodology. Care must also be taken to evaluate the stresses at the correct location in the detail consistent with the S-N data. It may be worthwhile to incorporate a more consistent set of S-N data into the methodology. Several other existing methodologies use the welding classification and associated S-N curves of the British Welding Institute. This system empirically includes the stress concentration factor which occurs as the result of the welded joint.

Recent reports by the U.S. Coast Guard have highlighted a high percentage of class III (i.e., nuisance) cracking in the TAPS tankers. One of the key factors sited as the cause of this high percentage is the use of high strength steel. It should be noted that during an independent study by ABS, there was no conclusion regarding the effects of high strength steel on the frequency of cracking in TAPS tankers.

Current fatigue design methodologies do not consider the effects of material on the S-N data used. Highly polished coupons of high strength steel (HSS) and mild steel (MS) in air show a marked difference in fatigue strength. However, welded HSS and MS details in a corrosive environment do not exhibit this pronounced difference in fatigue strength. The statistical evaluation of the S-N data (data scatter), also reduces this difference between the two materials. From this perspective, there is little difference if the detail is fabricated from HSS or MS. Fatigue becomes strictly a consideration of stress state. Classification societies allow for reduced HSS scantlings based upon strength considerations. In some cases, standard details previously used in MS construction are also used for the reduced HSS scantlings without due consideration for fatigue. The increased stress state produced by the use of thinner HSS scantlings may be aggravating initially poor details. Therefore, placing the blame for the cracking problems experienced by the TAPS tankers on the material alone seems unjustified. With proper consideration for connection detailing, HSS can still be a source of weight and cost savings.

During this study an attempt was made to obtain Response Amplitude Operator (RAO) data for the vessels being considered. It was learned that in many cases this data did not exist or that only partial data was available. Although the classification societies are tending towards longitudinal strength calculations based upon a first principles approach, this type of data seems to be the exception rather than the rule. A need exists for empirical type formulas for the evaluation of long term ship forces based on basic ship parameters.
This type of data would make the fatigue assessment of details more cost effective for the design office.

5.0 REFERENCES

(a) Jordon, C. R. and Cochran, C. S., "In-Service Performance of Structural Details", SSC-272, 1978

(b) Jordon, C. R. and Knight, L. T., "Further Survey of In-Service Performance of Structural Details", SSC-294, 1980

(c) "Guidance Manual for the Inspection and Condition Assessment of Tanker Structures", Tanker Co-Operative Forum, 1986

(d) "Report on the Trans-Alaska Pipeline Service (TAPS) Tanker Structural Failure Study", U.S. Department of Transportation/U.S. Coast Guard, June 25, 1990

(e) "Trans-Alaska Pipeline Service (TAPS) Tanker Structural Failure Study - Follow-Up Report", U.S. Department of Transportation/U.S Coast Guard, May 1991

(f) "ABS Service History of Trans-Alaskan Pipeline Service (TAPS) Vessels", ABS Americas, February 1991

(g) Munse, W.H.; Wilbur, T.W.; Tellalian, M.L.; Nicoll, K. and Wilson, K.; "Fatigue Characterization of Fabricated Ship Details for Design", SSC-318, 1983

(h) "A Method for Estimating Lifetime Loads and Fatigue Lives for SWATH and Conventional Monohull Ships", Sikora, Disenbacher and Beach, Naval Engineers Journal, May 1983

(i) "A Probabilistic Analysis of Hull Girder Slamming Loads", Jerome P. Sikora, Naval Surface Warfare Center, SSPD-93-173-30, December 1992

(j) E.F. Bruhn, "Analysis and Design of Flight Vehicle Structures", S.R. Jacobs & Associates, Inc.

(k) DOD-STD-1339(Navy), Section 301A, Ship Motion and Attitude (Metric), dated July 21, 1986

(l) Ochi, M.K., "Marine Environment Applied to the Design of Ships and Marine Structures" (Draft)

(m) "Guide for the Fatigue Strength Assessment of Tankers", ABS June 1992

(n) Bleich, F. and Ramsey, L.B. "A Design Manual on the Buckling Strength of Metal Structures", SNAME 1965

(o) Timoshenko and Gere, "Theory of Elastic Stability", McGraw-Hill Book Co., 1961

(p) "Cracking of HTS Longitudinals of VLCC", Nippon Kaiji Kyokai, TSCF Work Group Meeting #14

APPENDIX A

CALCULATIONS FOR THE MAXIMUM ALLOWABLE FATIGUE STRESS RANGE FOR THE SELECTED DETAILS

Naval Combatant

Weibull Shape Factor = 1.7

Detail 30 (Figure 2-13)

Mean Fatigue Stress Range (S_N) (from Figure 2-13) = 3.9 ksi (26.89 N/mm^2)

Slope m = 3.159

Random Load Factor (ξ) for k=1.7 and m=3.159 (from Table 2-2)

Interpolating:

$$4.72 - \frac{3.159 - 3.0}{3.5 - 3.0} x (4.72 - 4.48) = 4.64$$

Reliability Factor (R_F) (from Table 2-3) (0.90) = 0.671

S_D = 3.9 ksi x 4.64 x 0.671 = 12.14 ksi (83.71 N/mm^2) (New Design)

S_D = 3.9 ksi x 4.64 x 1.0 = 18.10 ksi (124.8 N/mm^2) (Existing Detail)

Detail 20 (Figure 2-12)

Mean Fatigue Stress Range (S_N) (from Figure 2-12) = 5.9 ksi (40.68 N/mm^2)

Slope m = 4.619

Random Load Factor (ξ) for k=1.7 and m=4.619 (from Table 2-2)

Interpolating:

$$4.1 - \frac{4.619 - 4.5}{5.0 - 4.5} x (4.1 - 3.94) = 4.06$$

Reliability Factor (R_F) (from Table 2-3) (0.90) = 0.671

S_D = 5.9 ksi x 4.06 x = 12.14 ksi (83.71 N/mm^2) (New Design)

S_D = 5.9 ksi x 4.06 x 1.0 = 23.95 ksi (165.1 N/mm^2) (Existing Detail)

Tanker

Weibull Shape Factor k = 1.0

Detail 18 (Figure 2-10)

Mean Fatigue Stress Range (S_N) (from Figure 2-10) = 3.6 ksi (24.82 N/mm^2)

Slope m = 4.027

Random Load Factor (ξ) for k=1.0 and m=4.027 (from Table 2-2)

Interpolating:

$$8.32 - \frac{4.027 - 4.0}{4.5 - 4.0} x (8.32 - 7.64) = 8.28$$

Reliability Factor (R_F) (from Table 2-3) (0.90) = 0.615

S_D = 3.6 ksi x 8.28 x 0.615 = 18.33 ksi (126.39 N/mm^2) (New Design)

S_D = 3.6 ksi x 8.28 x 1.0 = 29.81 ksi (205.54 N/mm^2) (Existing Detail)

Detail 19 (Figure 2-11)

Mean Fatigue Stress Range (S_N) (from Figure 2-11) = 9.2 ksi (63.43 N/mm^2)

Slope m = 7.472

Random Load Factor (ξ) for k=1.0 and m=7.472 (from Table 2-2)

Interpolating:

$$5.45-\frac{7.472-7.0}{7.5-7.0}x(5.45-5.16)=5.18$$

Reliability Factor (R_F) (from Table 2-3) (0.90) = 0.658

S_D = 9.2 ksi x 5.18 x 0.658 = 31.36 ksi (216.23 N/mm^2) (New Design)

S_D = 9.2 ksi x 5.18 = 47.66 ksi (321.72 N/mm^2) (Existing Detail)

<u>Detail 15</u> (Figure 2-9)

Mean Fatigue Stress Range (S_N) (from Figure 2-9) = 4.7 ksi (32.41 N/mm^2)

Slope m = 4.2

Random Load Factor (ξ) for k=1.0 and m=4.2 (from Table 2-2)

Interpolating:

$$8.32-\frac{4.2-4.0}{4.5-4.0}x(8.32-7.64)=8.05$$

Reliability Factor (R_F) (from Table 2-3) (0.90) = 0.688

S_D = 4.7 ksi x 8.05 x 0.688 = 26.03 ksi (174.48 N/mm^2) ksi (New Design)

S_D = 4.7 ksi x 8.05 x 1.0 = 37.84 ksi (260.91 N/mm^2) (Existing Detail)

APPENDIX B

STRESS CONTOUR PLOTS FOR THE SELECTED DETAILS (EXISTING AND MODIFIED)

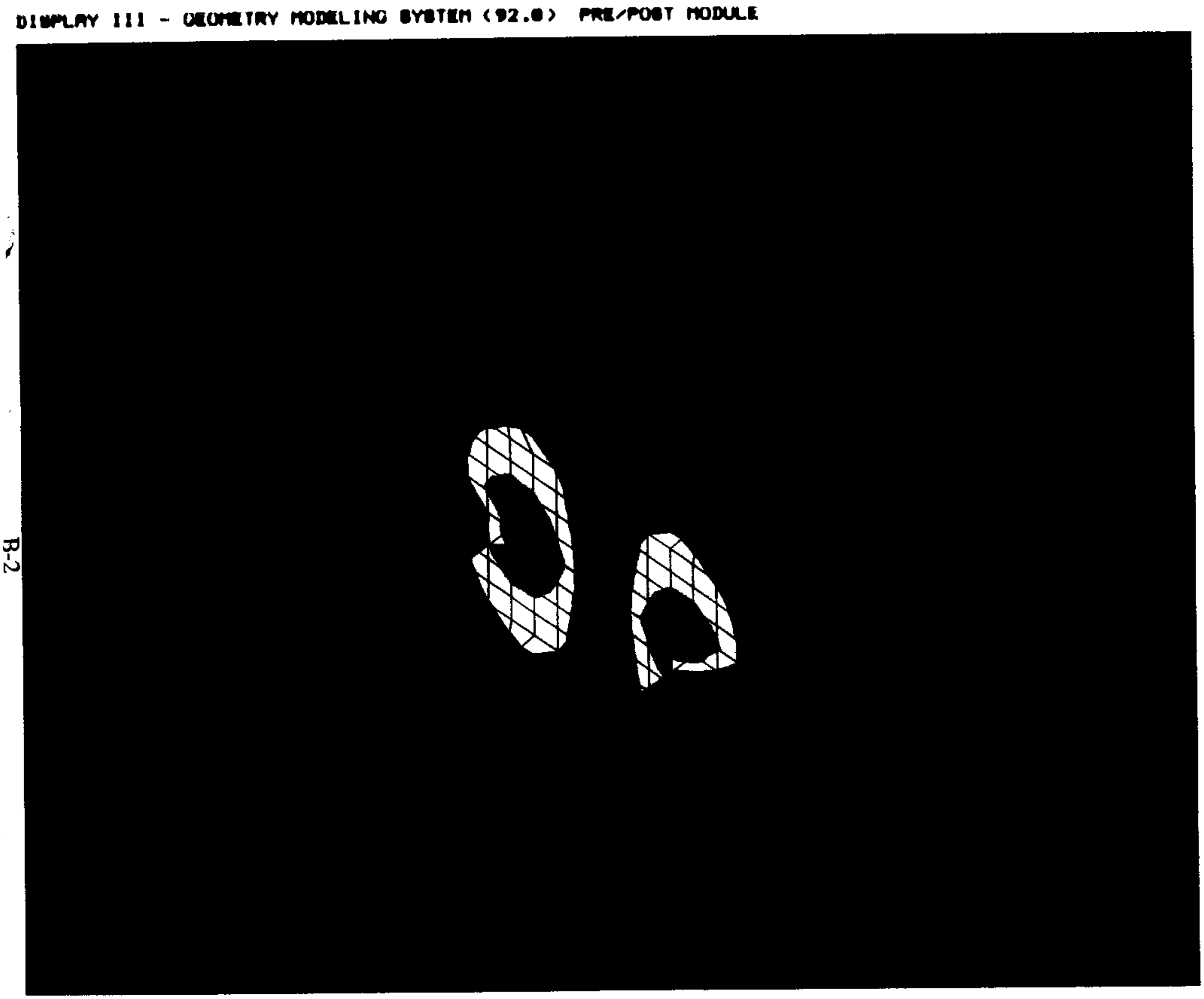

FIGURE B-1. UNIT LOAD STRESS CONTOUR PLOT FOR VERTICAL HULL PRIMARY STRESS - NAVAL COMBATANT

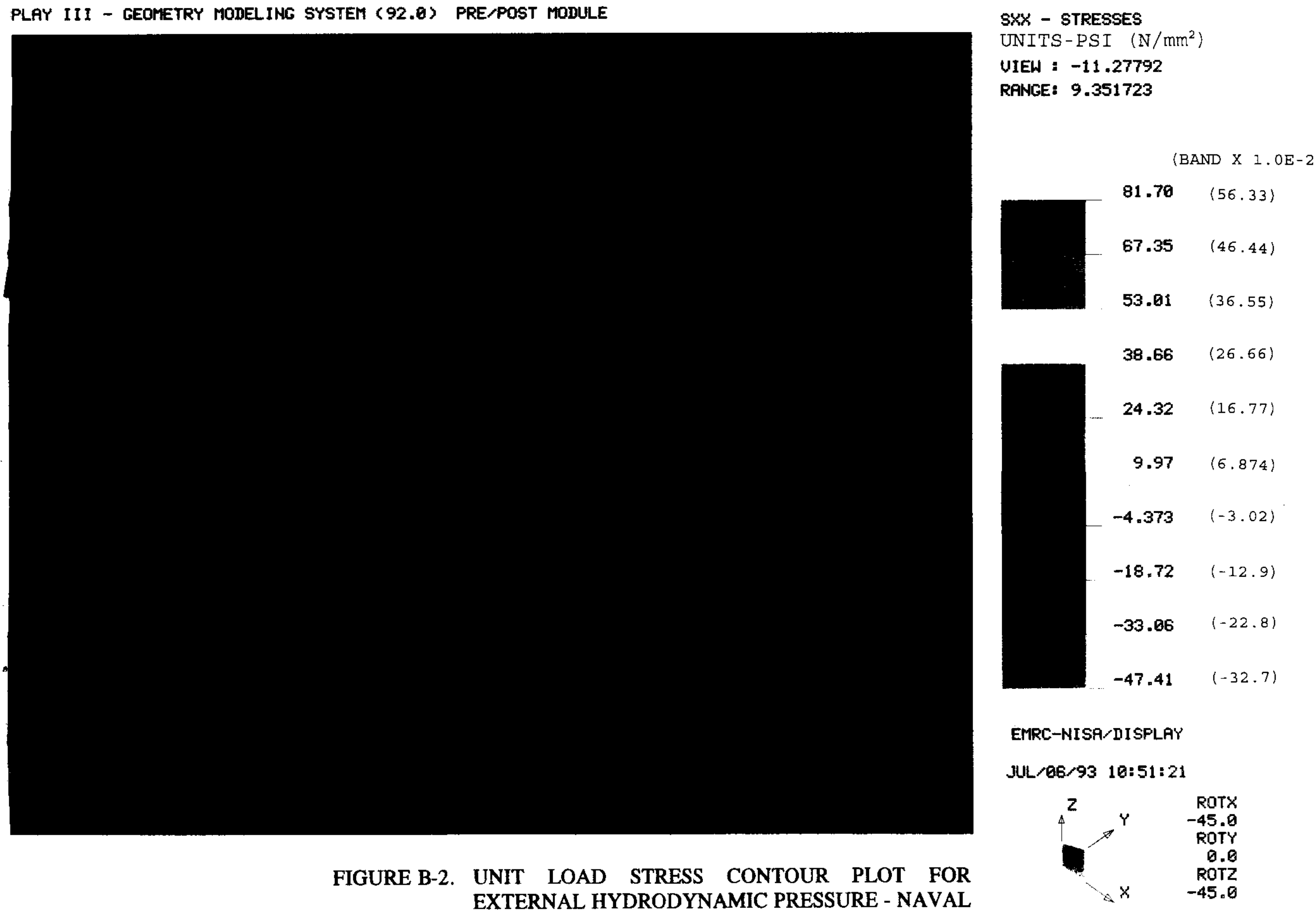

FIGURE B-2. UNIT LOAD STRESS CONTOUR PLOT FOR EXTERNAL HYDRODYNAMIC PRESSURE - NAVAL COMBATANT

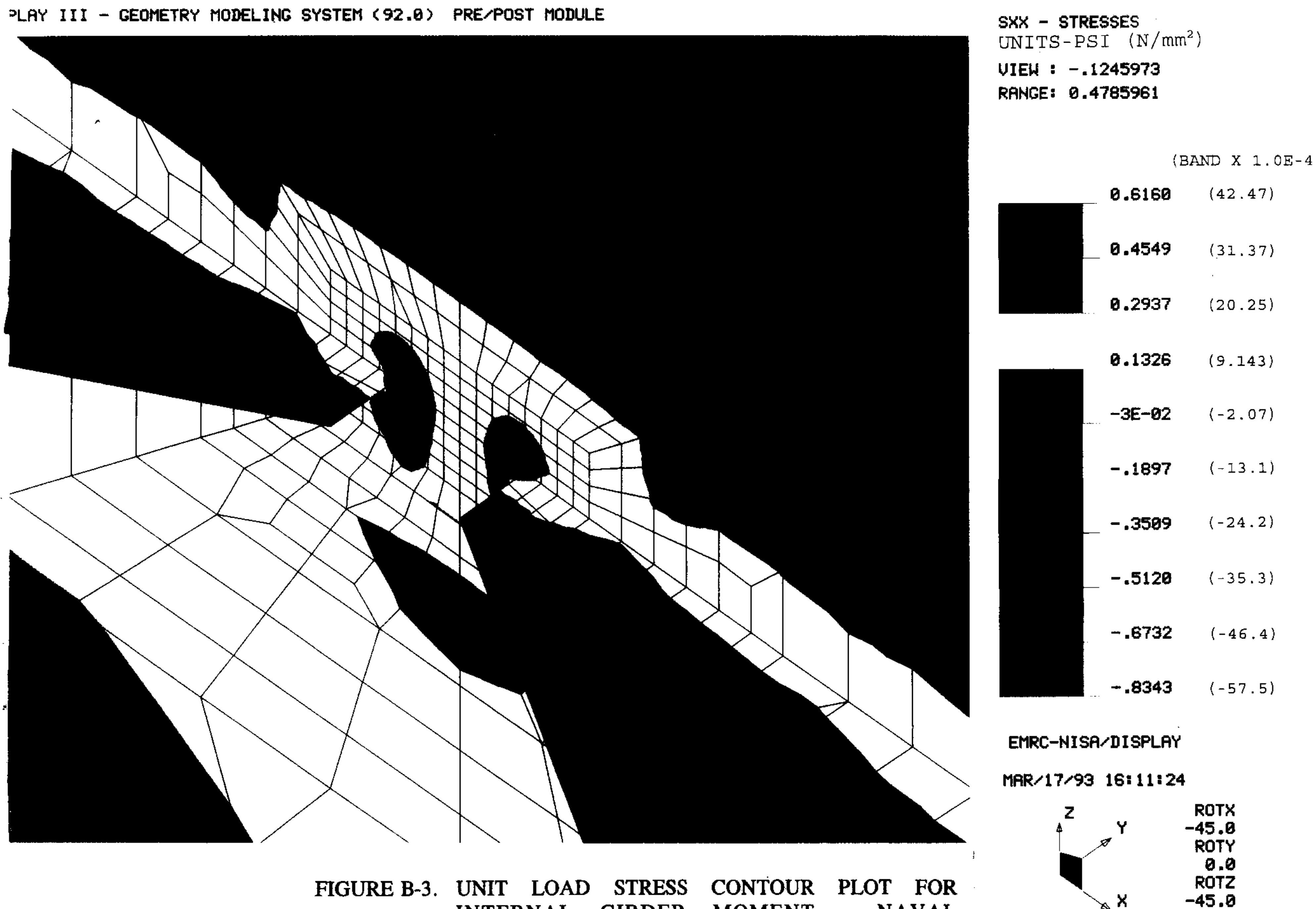

FIGURE B-3. UNIT LOAD STRESS CONTOUR PLOT FOR INTERNAL GIRDER MOMENT - NAVAL COMBATANT

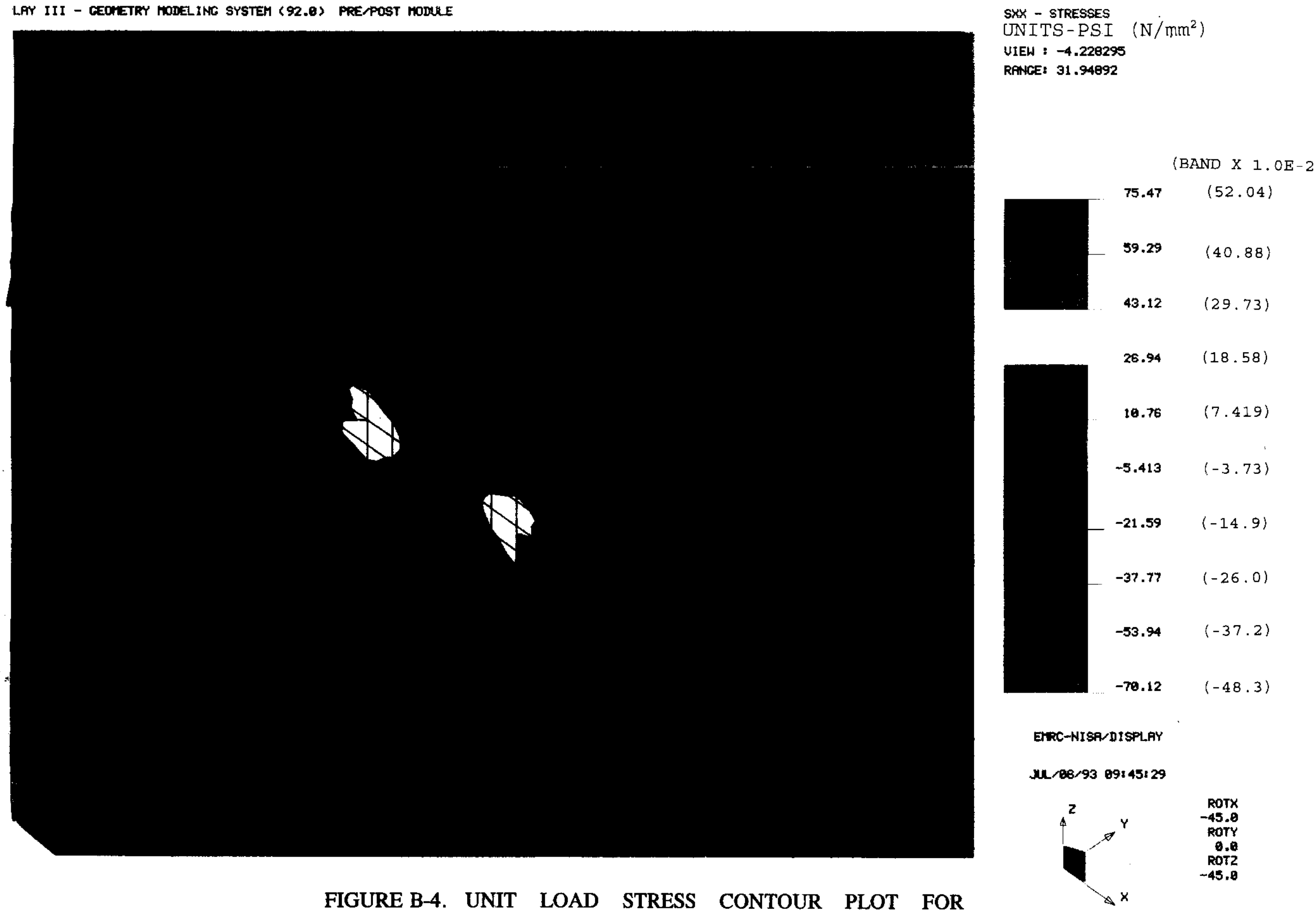

FIGURE B-4. UNIT LOAD STRESS CONTOUR PLOT FOR INTERNAL GIRDER SHEAR - NAVAL COMBATANT

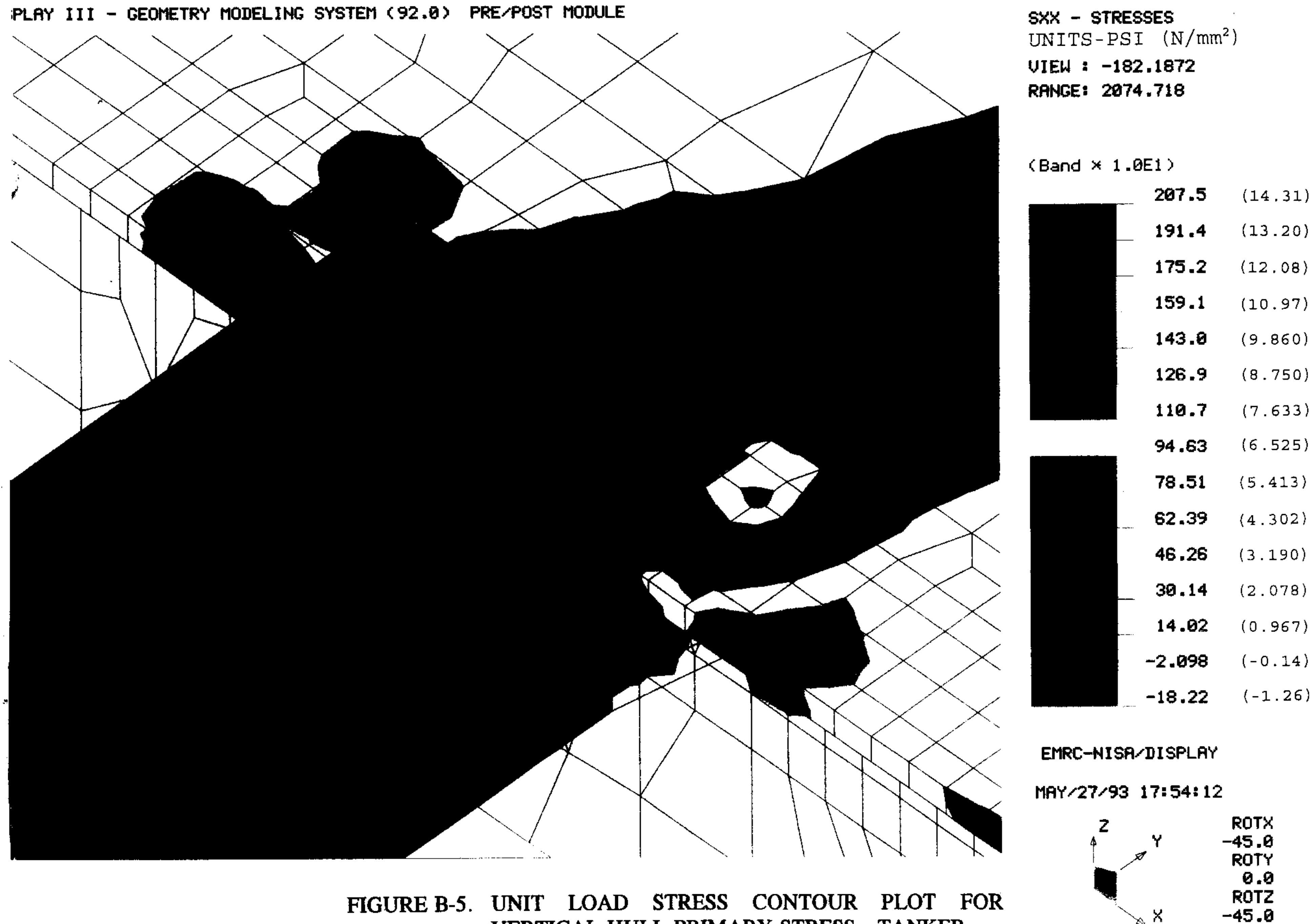

FIGURE B-5. UNIT LOAD STRESS CONTOUR PLOT FOR VERTICAL HULL PRIMARY STRESS - TANKER

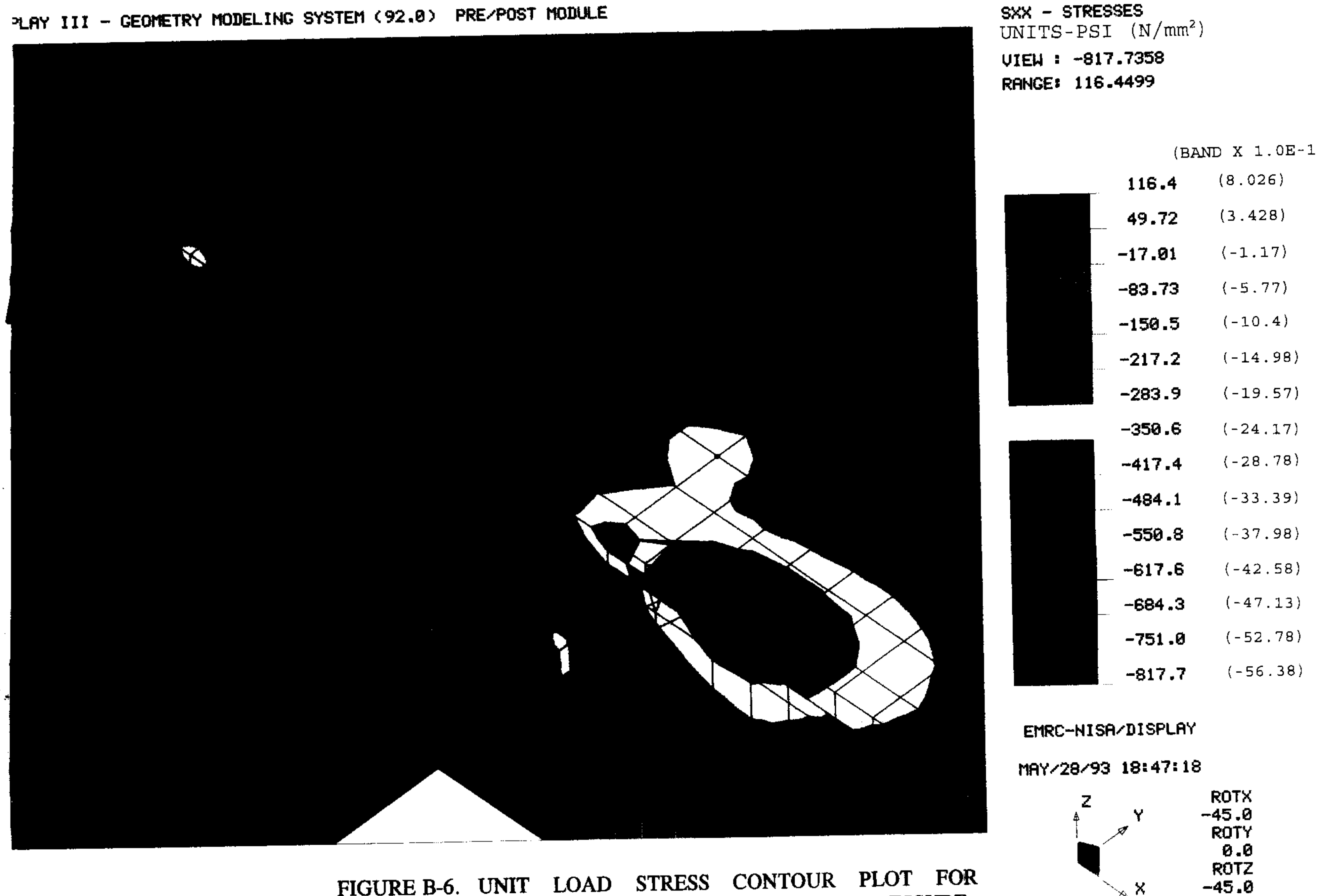

FIGURE B-6. UNIT LOAD STRESS CONTOUR PLOT FOR EXTERNAL/INTERNAL HYDROSTATIC PRESSURE - TANKER

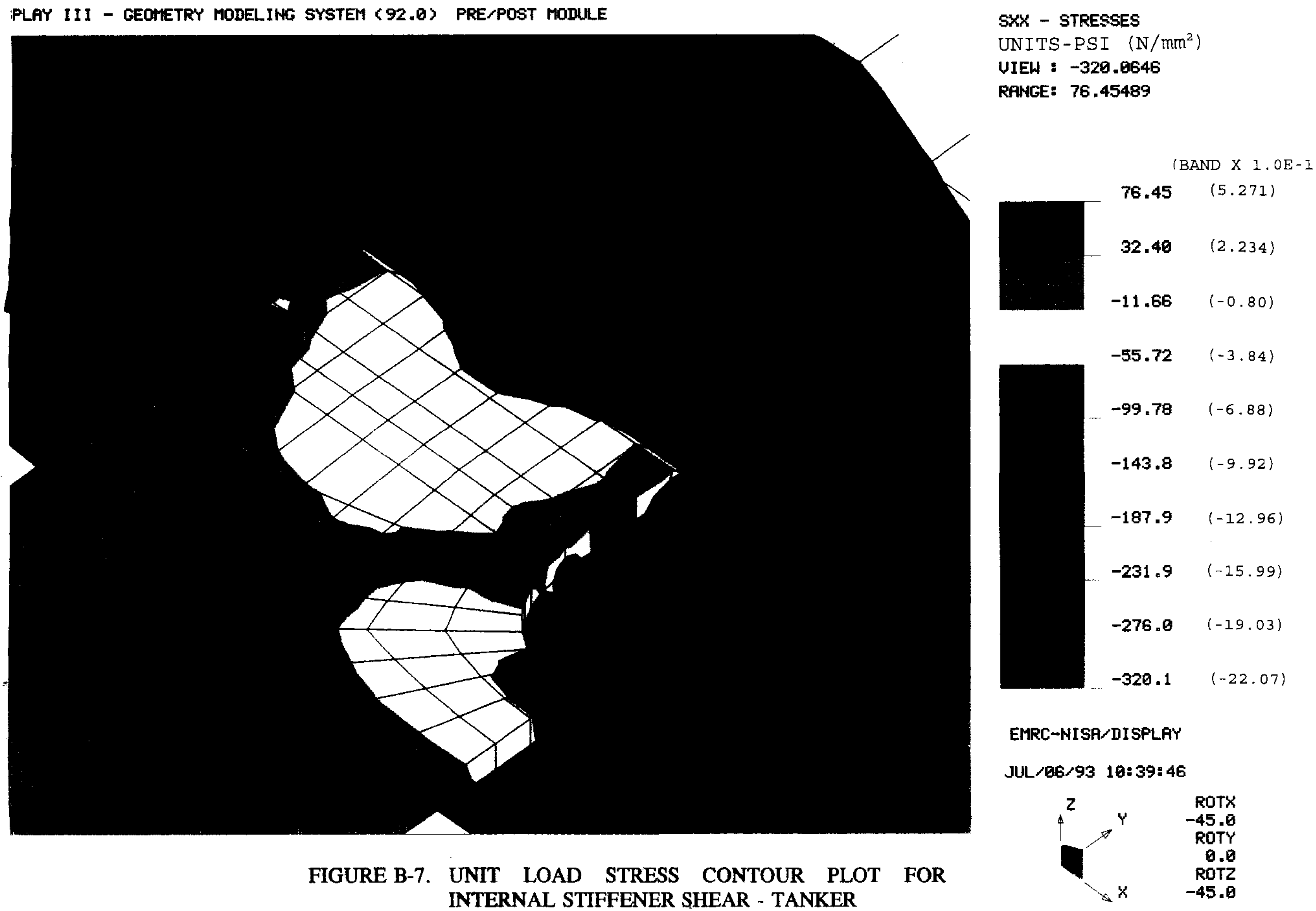

FIGURE B-7. UNIT LOAD STRESS CONTOUR PLOT FOR INTERNAL STIFFENER SHEAR - TANKER

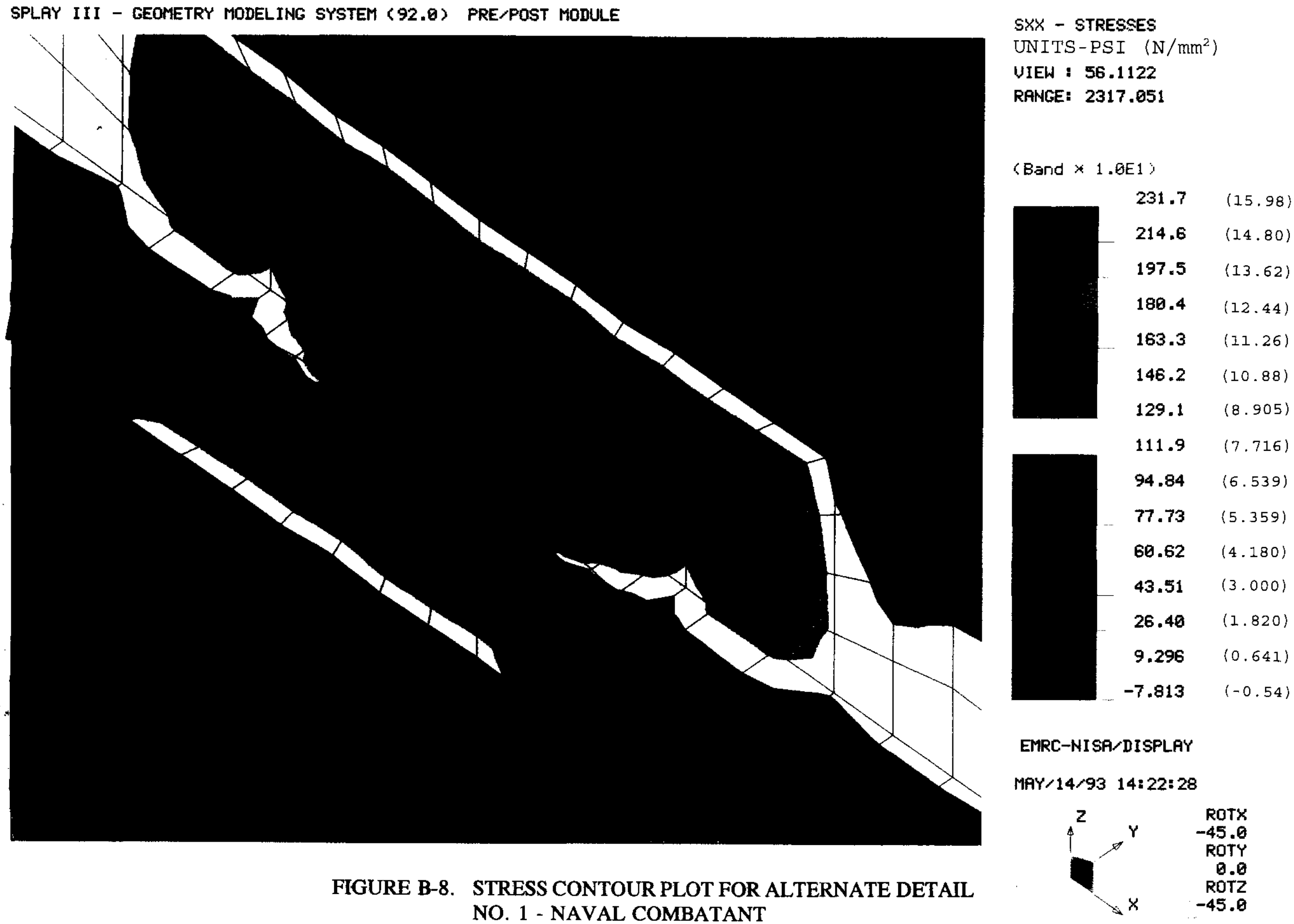

FIGURE B-8. STRESS CONTOUR PLOT FOR ALTERNATE DETAIL NO. 1 - NAVAL COMBATANT

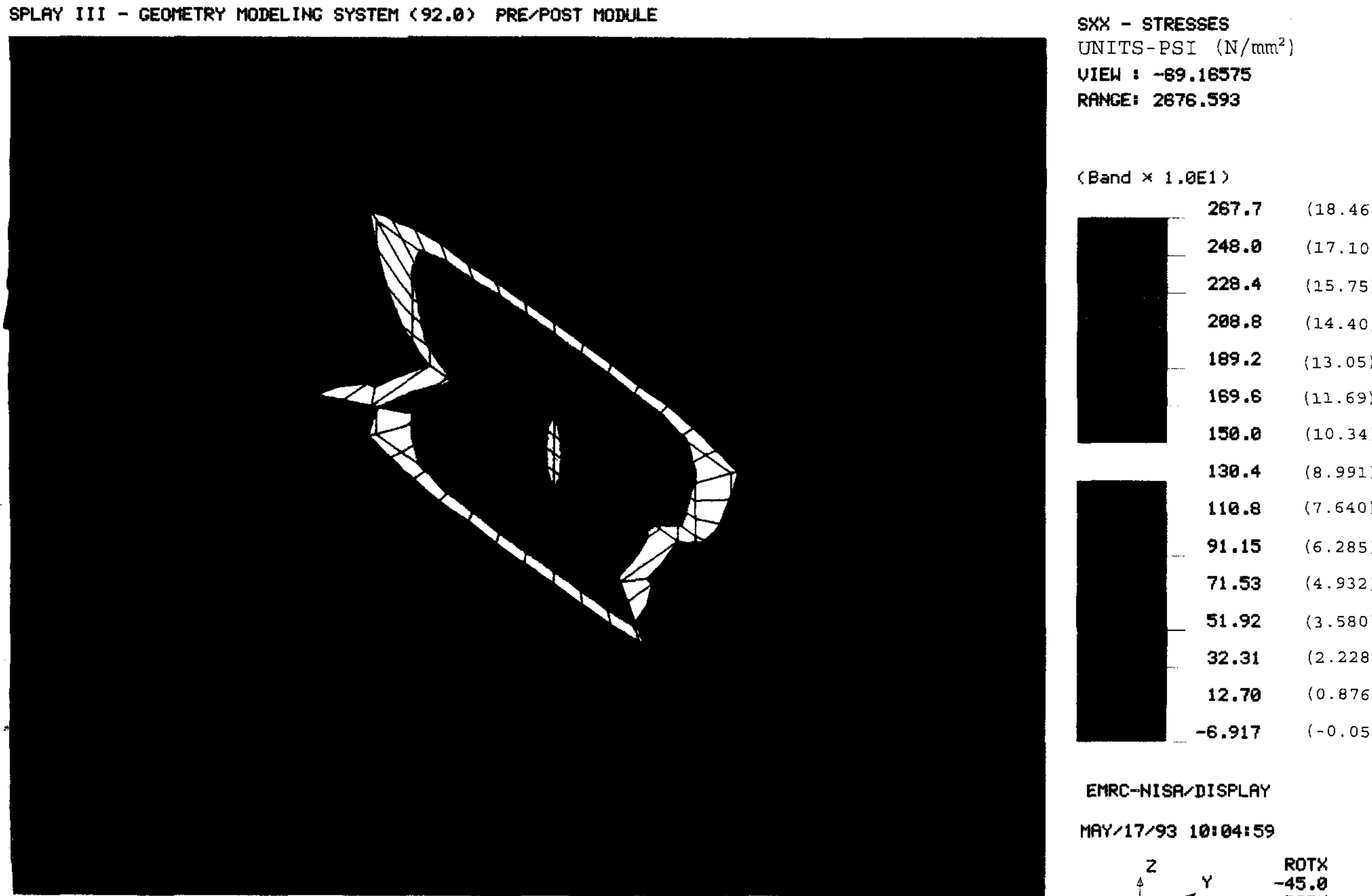

FIGURE B-9. STRESS CONTOUR PLOT FOR ALTERNATE DETAIL NO. 2 - NAVAL COMBATANT

PLAY III - GEOMETRY MODELING SYSTEM (92.0) PRE/POST MODULE

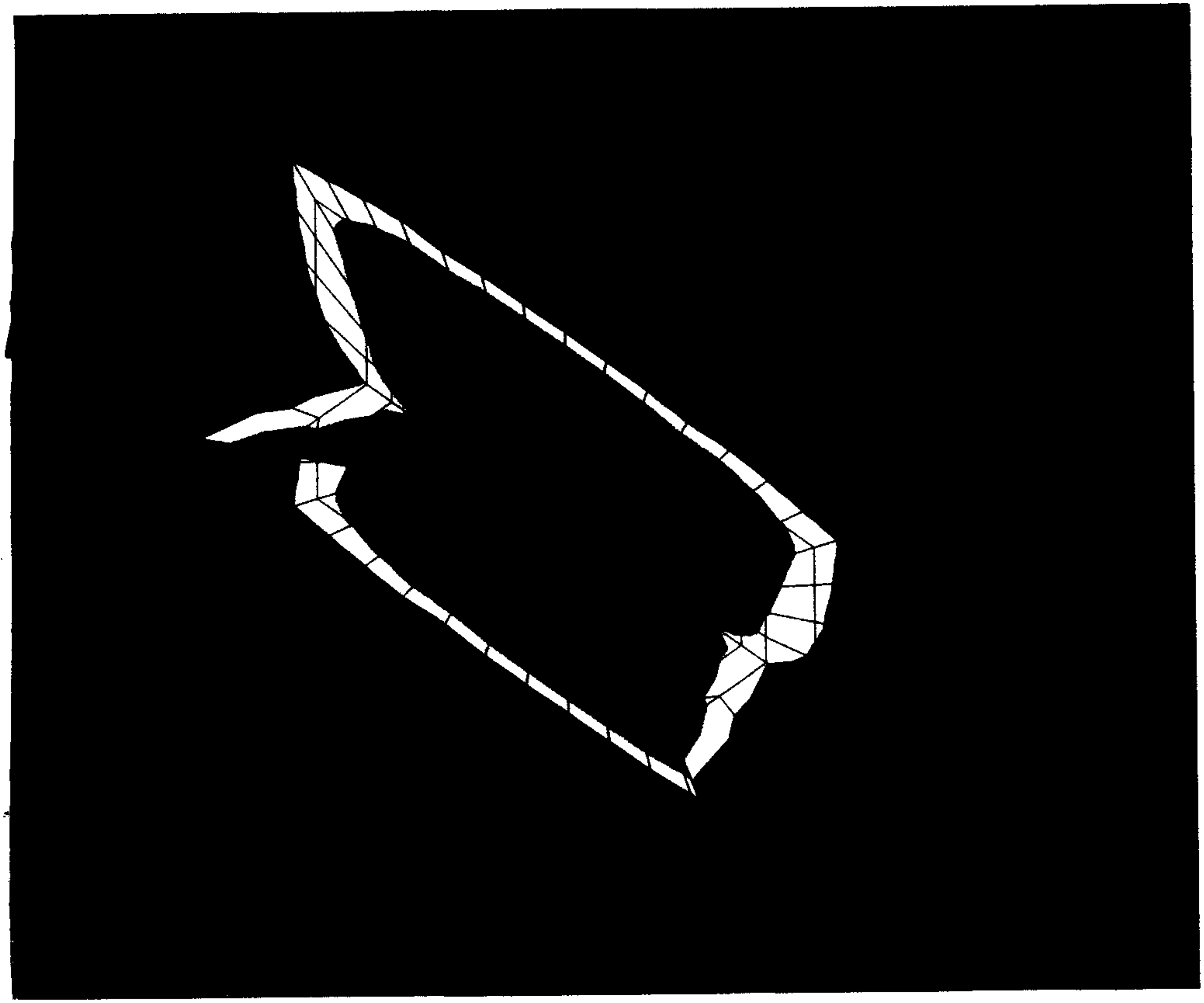

SXX - STRESSES
UNITS-PSI (N/mm²)
VIEW : 39.81051
RANGE: 2480.288

(Band × 1.0E1)

248.0	(17.10)
229.9	(15.85)
211.7	(14.60)
193.5	(13.34)
175.4	(12.09)
157.2	(10.84)
139.0	(9.584)
120.9	(8.336)
102.7	(7.081)
84.53	(5.820)
66.37	(4.576)
48.20	(3.323)
30.03	(2.071)
11.87	(0.818)
-6.299	(-0.43)

EMRC-NISA/DISPLAY

MAY/17/93 12:45:00

Z Y X

ROTX -45.0
ROTY 0.0
ROTZ -45.0

FIGURE B-10. STRESS CONTOUR PLOT FOR ALTERNATE DETAIL NO. 3 - NAVAL COMBATANT

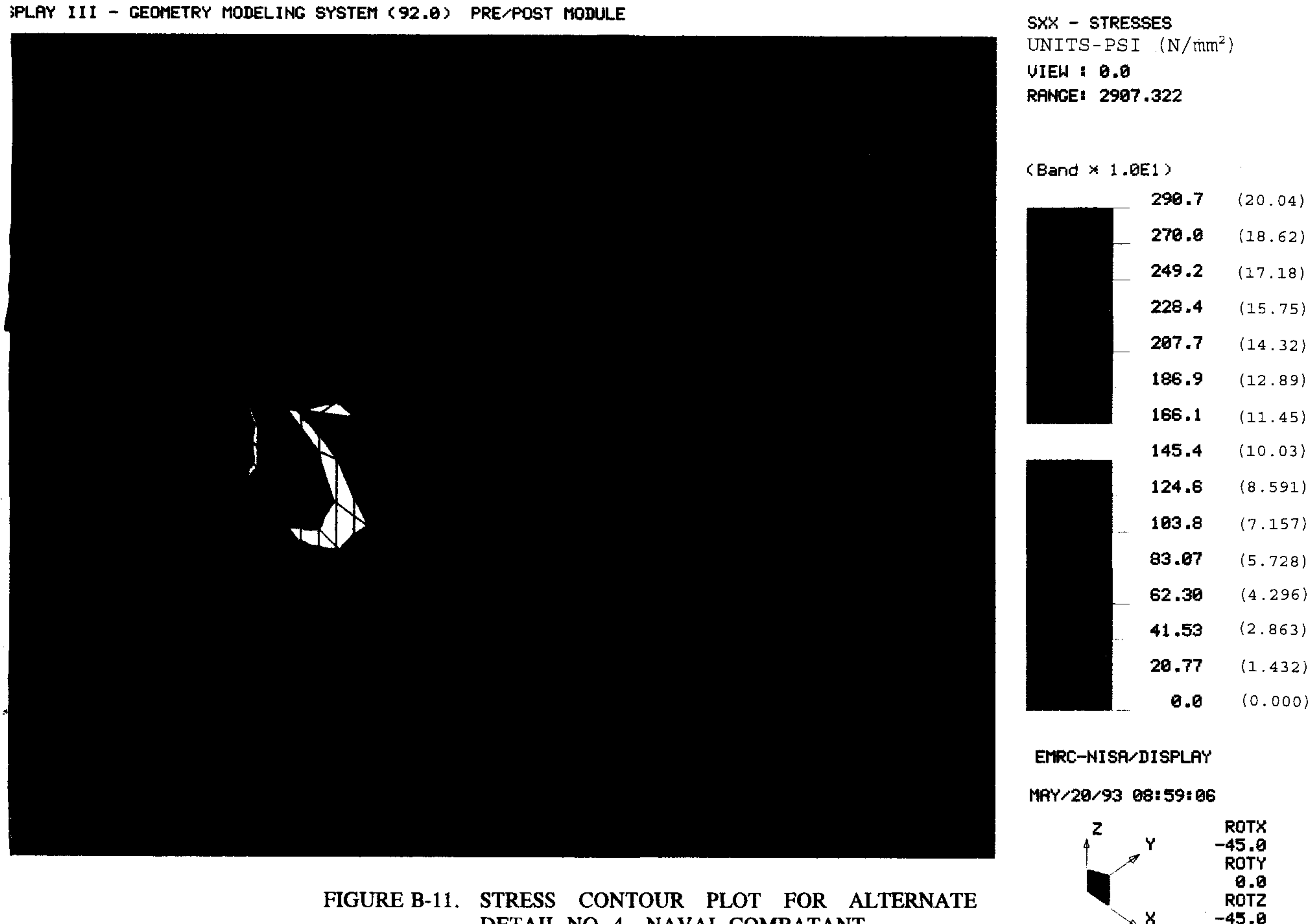

FIGURE B-11. STRESS CONTOUR PLOT FOR ALTERNATE DETAIL NO. 4 - NAVAL COMBATANT

PLAY III - GEOMETRY MODELING SYSTEM (92.0) PRE/POST MODULE

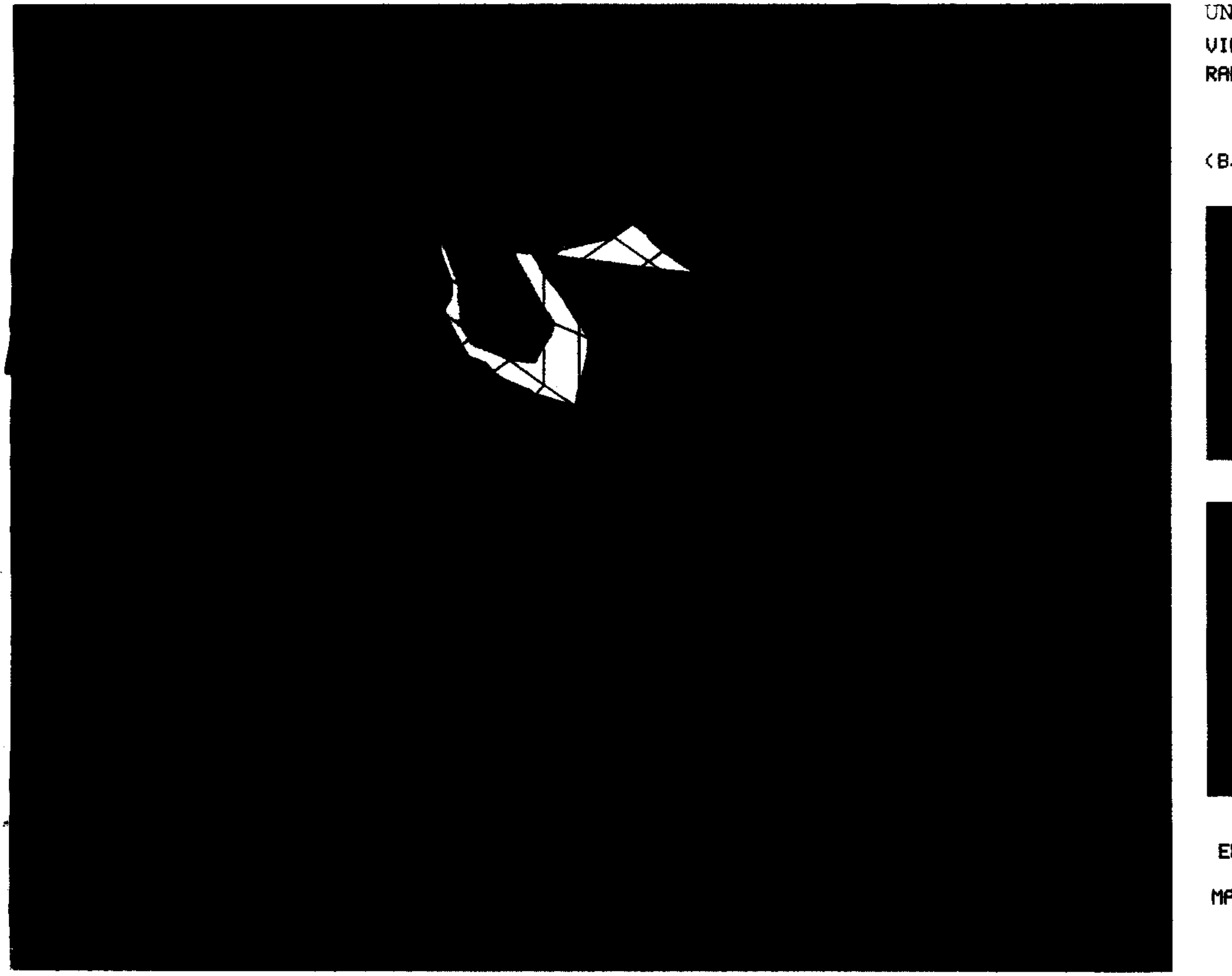

FIGURE B-12. STRESS CONTOUR PLOT FOR ALTERNATE DETAIL NO. 5 - NAVAL COMBATANT

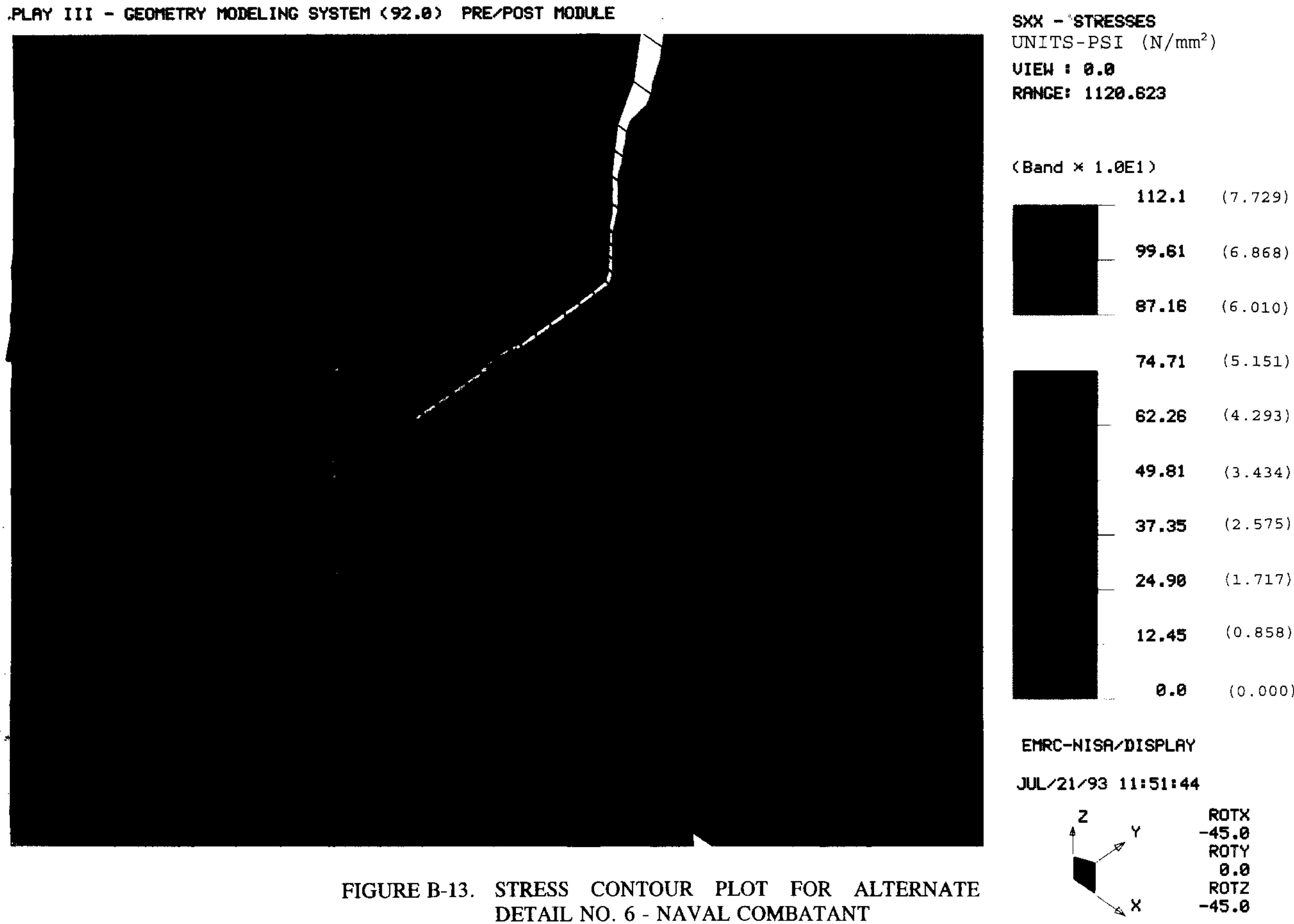

FIGURE B-13. STRESS CONTOUR PLOT FOR ALTERNATE DETAIL NO. 6 - NAVAL COMBATANT

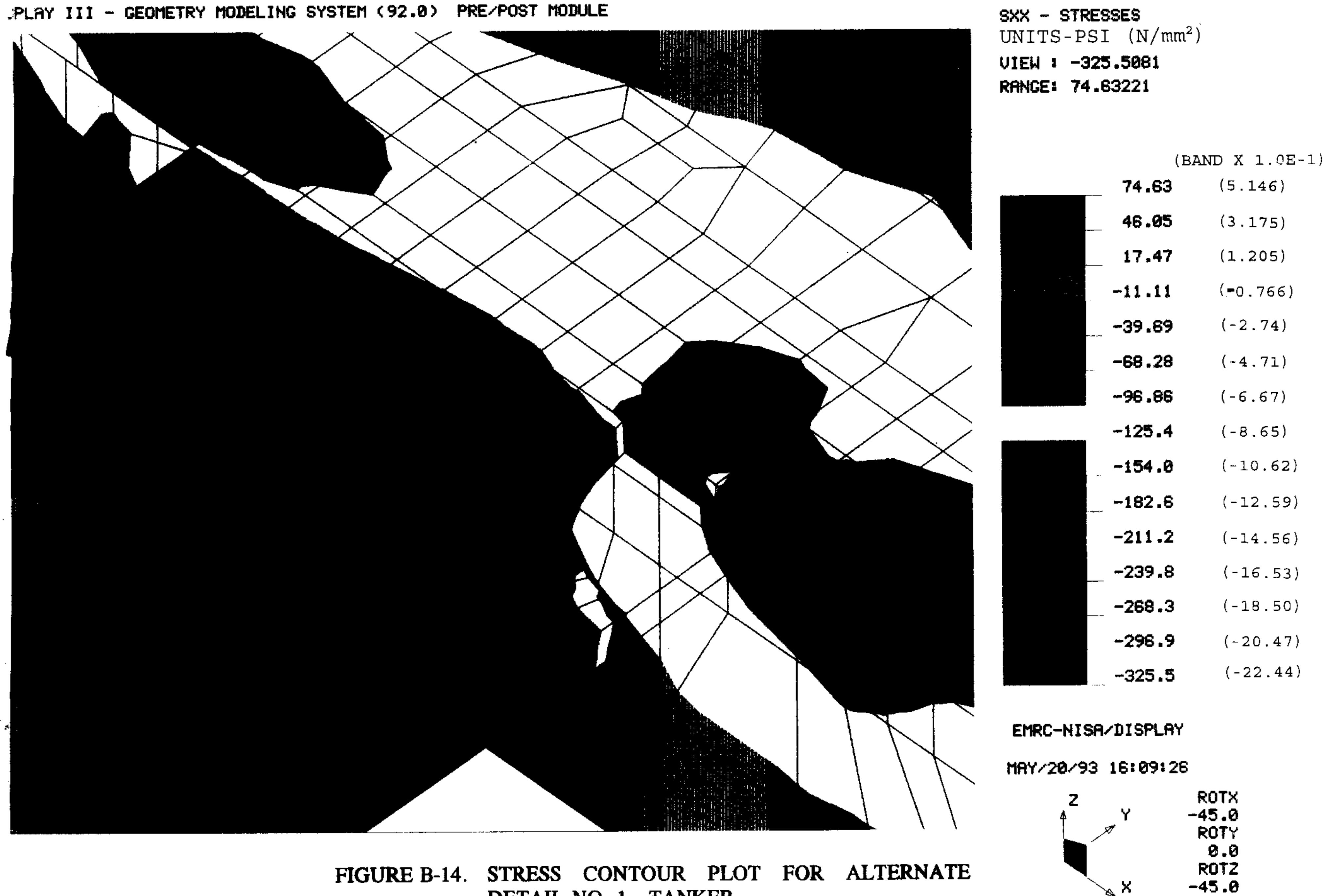

FIGURE B-14. STRESS CONTOUR PLOT FOR ALTERNATE DETAIL NO. 1 - TANKER

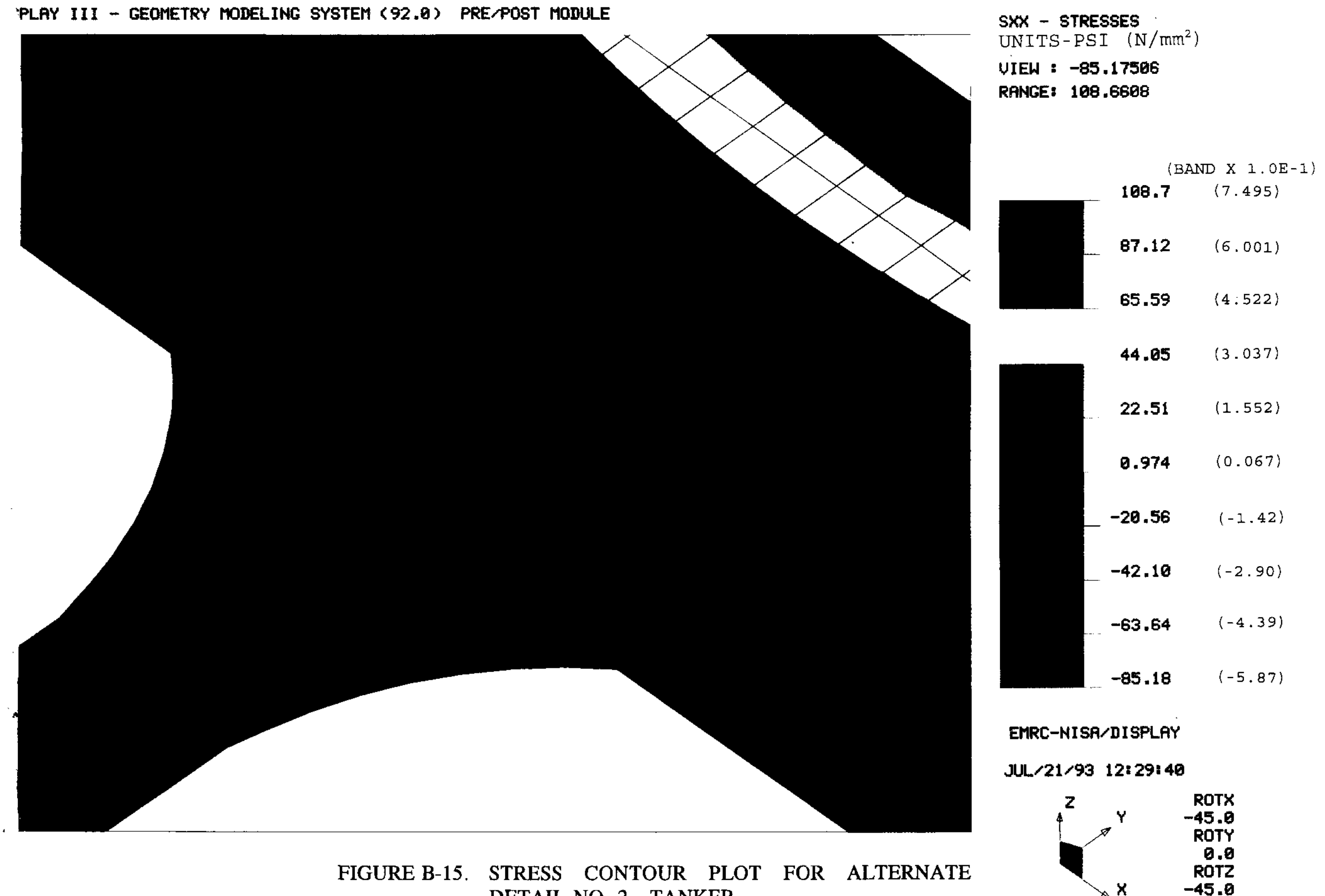

FIGURE B-15. STRESS CONTOUR PLOT FOR ALTERNATE DETAIL NO. 2 - TANKER

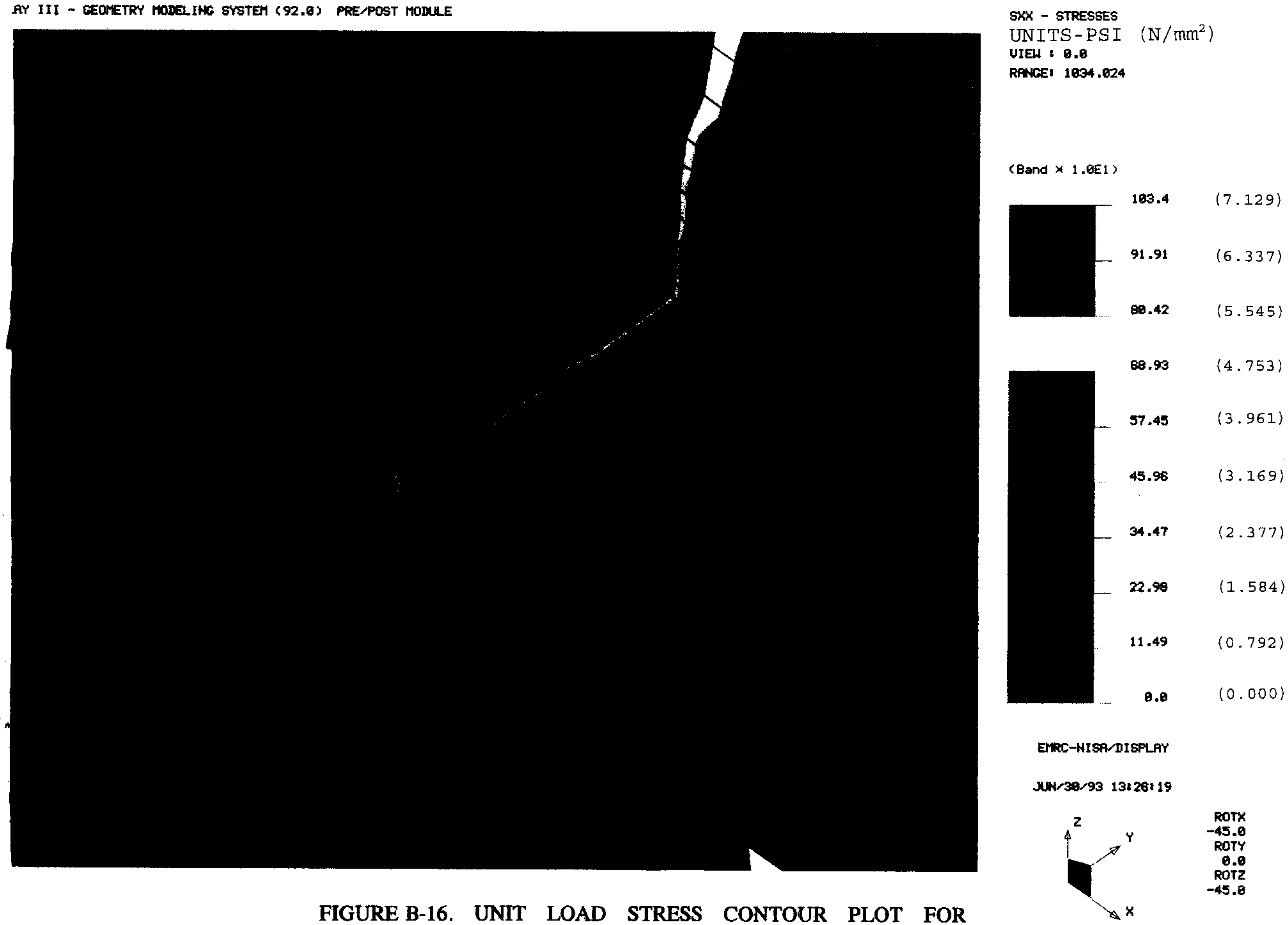

FIGURE B-16. UNIT LOAD STRESS CONTOUR PLOT FOR VERTICAL HULL PRIMARY STRESS - MODIFIED NAVAL COMBATANT DETAIL

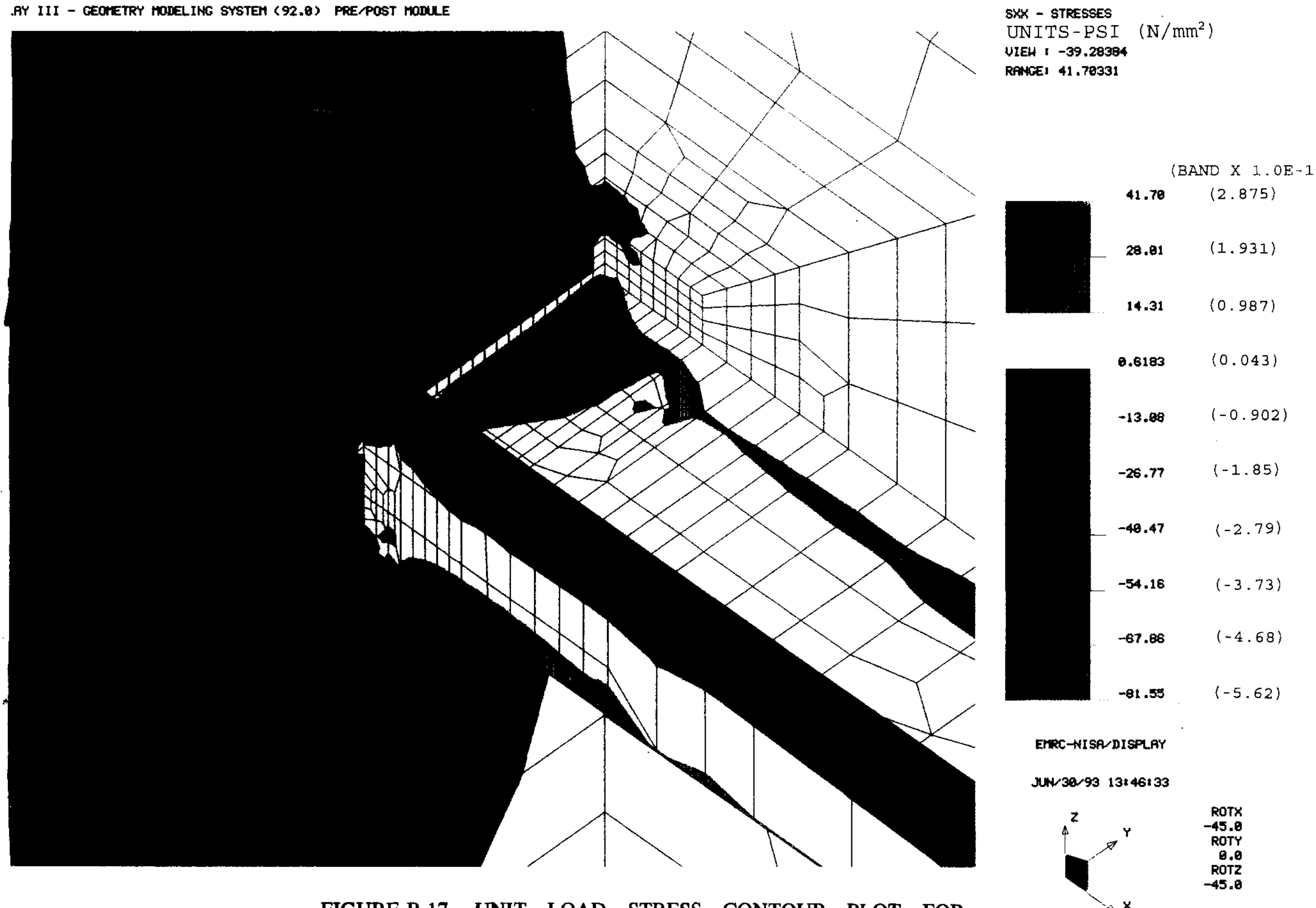

FIGURE B-17. UNIT LOAD STRESS CONTOUR PLOT FOR EXTERNAL HYDRODYNAMIC PRESSURE - MODIFIED NAVAL COMBATANT DETAIL

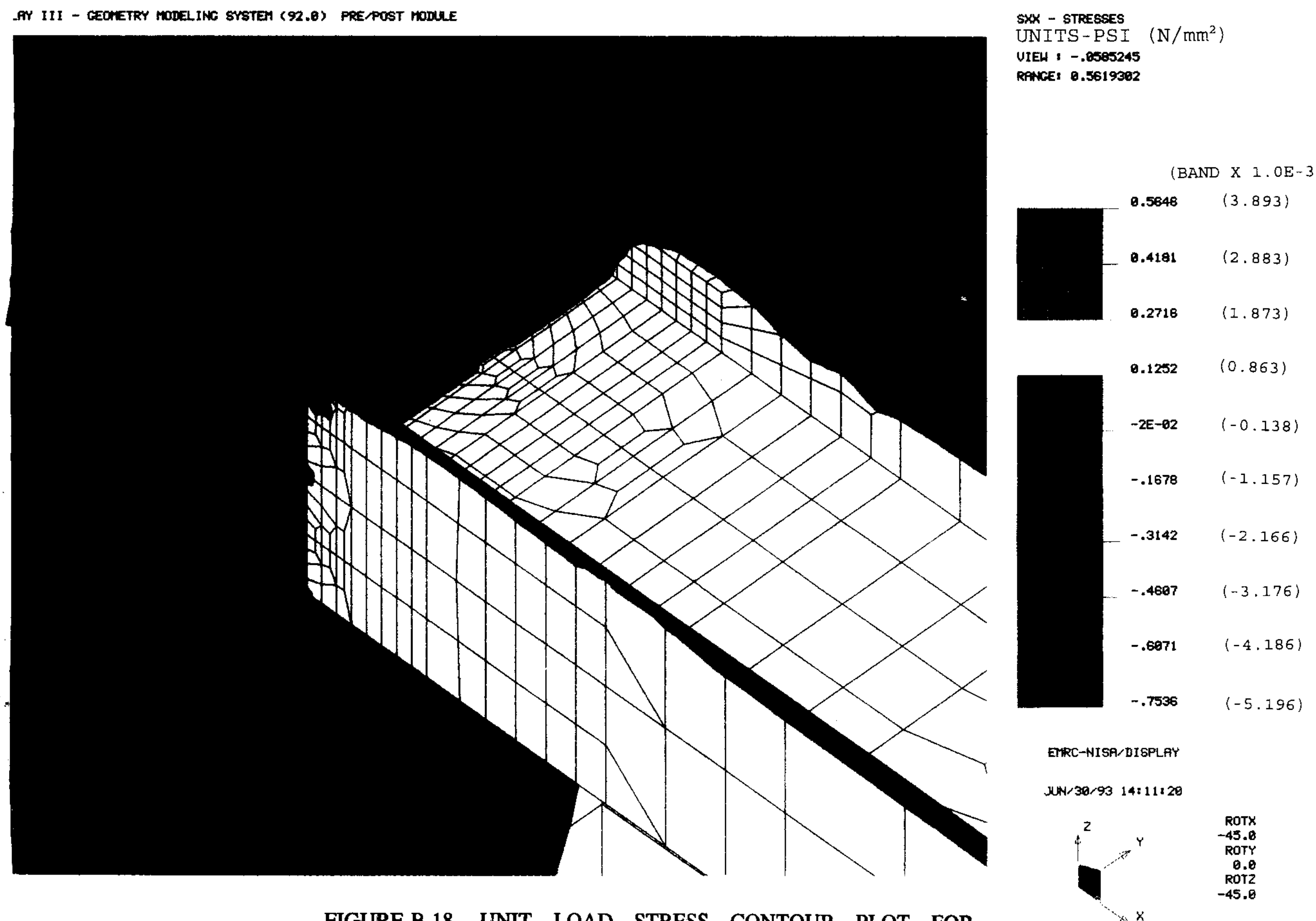

FIGURE B-18. UNIT LOAD STRESS CONTOUR PLOT FOR INTERNAL GIRDER MOMENT - MODIFIED NAVAL

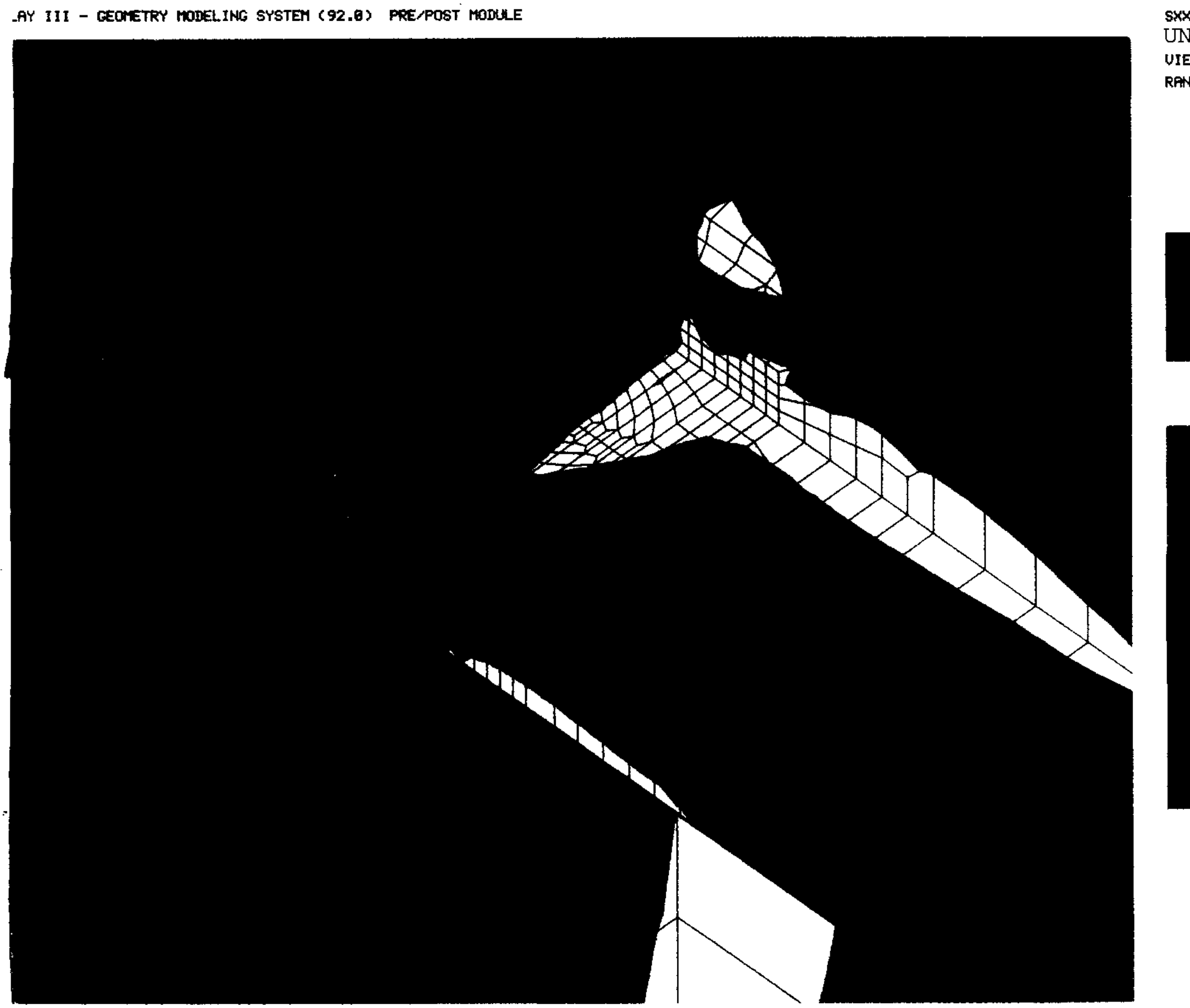

FIGURE B-19. UNIT LOAD STRESS CONTOUR PLOT FOR INTERNAL GIRDER SHEAR - MODIFIED NAVAL COMBATANT DETAIL

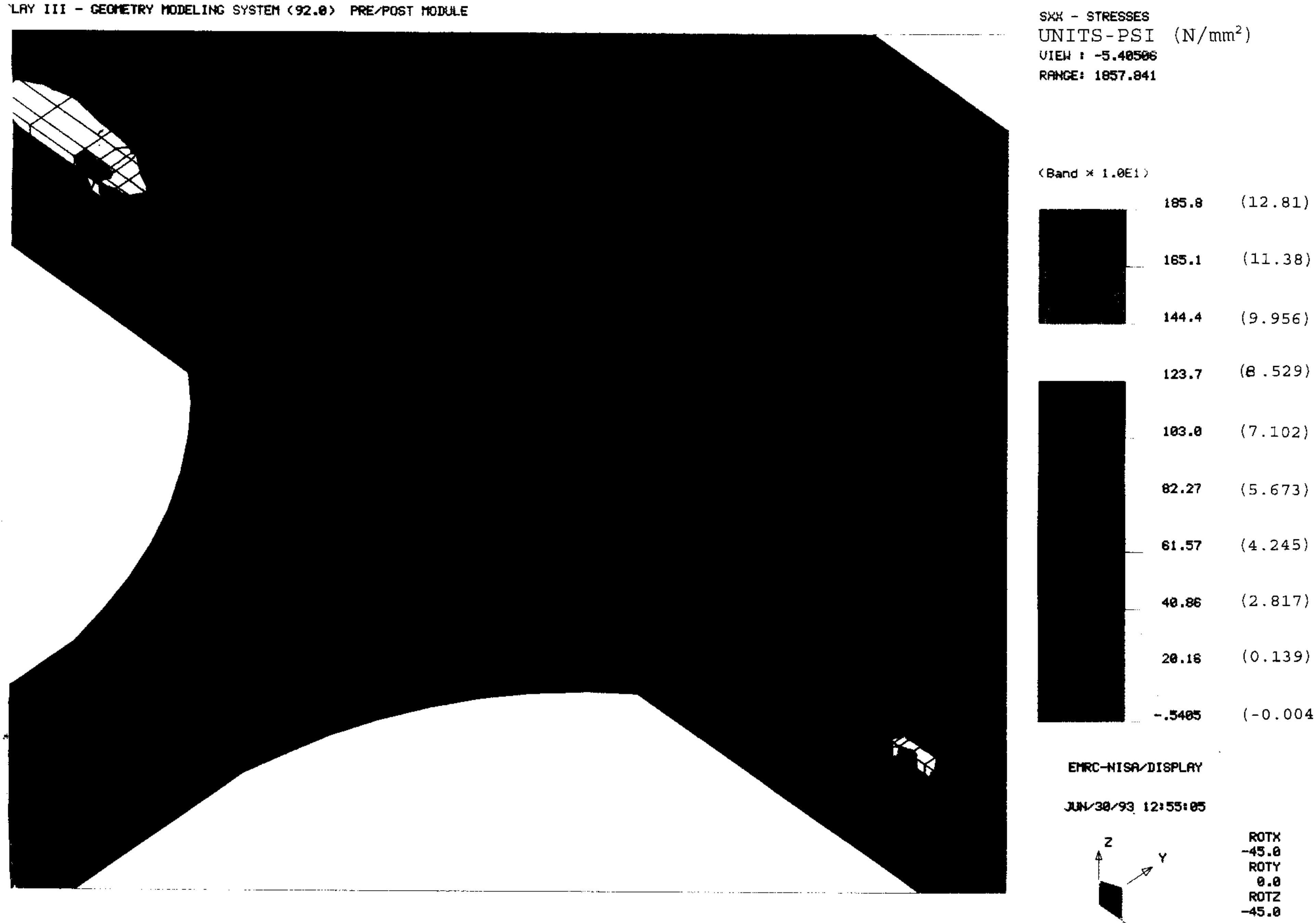

FIGURE B-20. UNIT LOAD STRESS CONTOUR PLOT FOR VERTICAL HULL PRIMARY STRESS - MODIFIED TANKER DETAIL

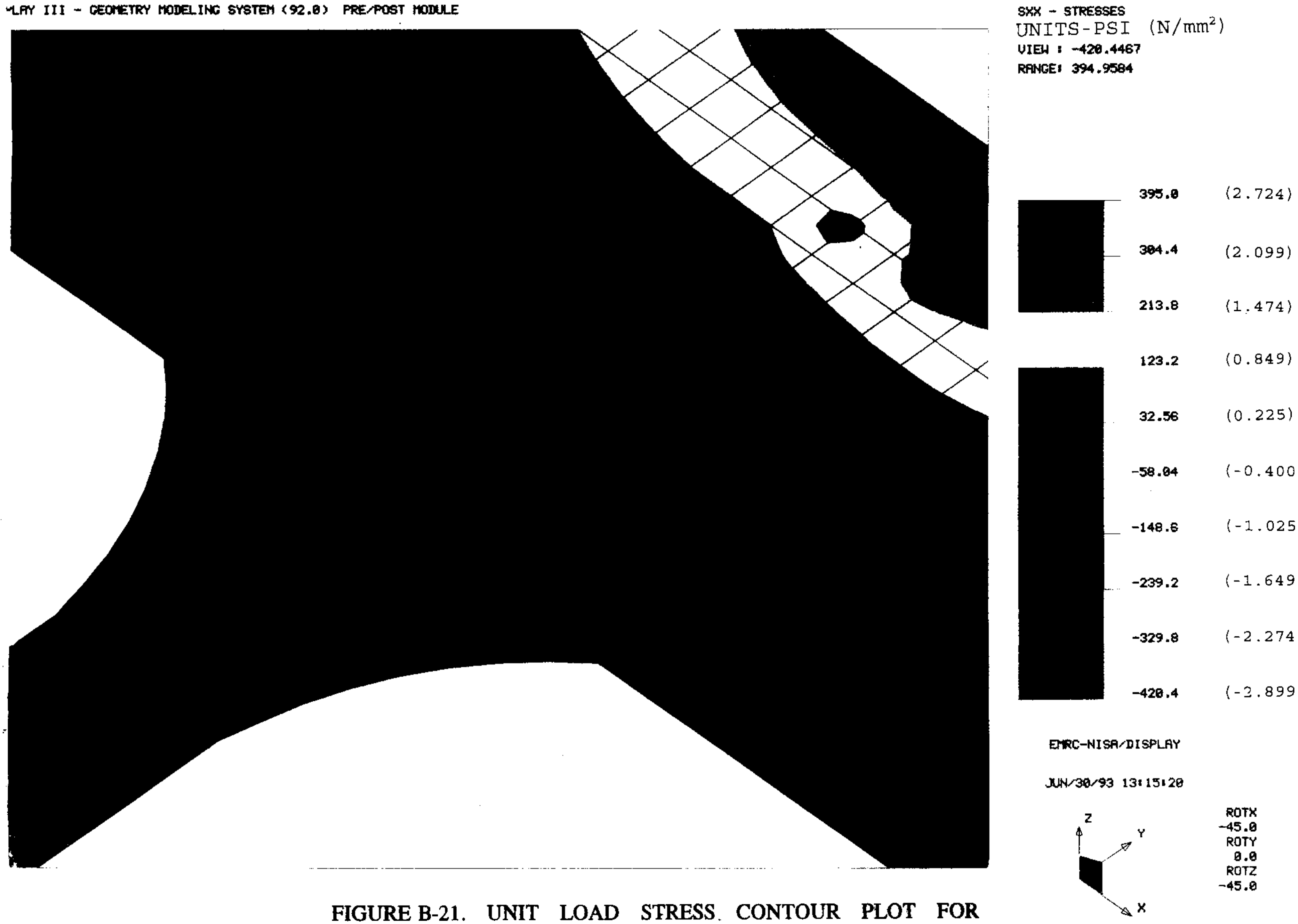

FIGURE B-21. UNIT LOAD STRESS CONTOUR PLOT FOR EXTERNAL/INTERNAL HYDRODYNAMIC PRESSURE - MODIFIED TANKER DETAIL

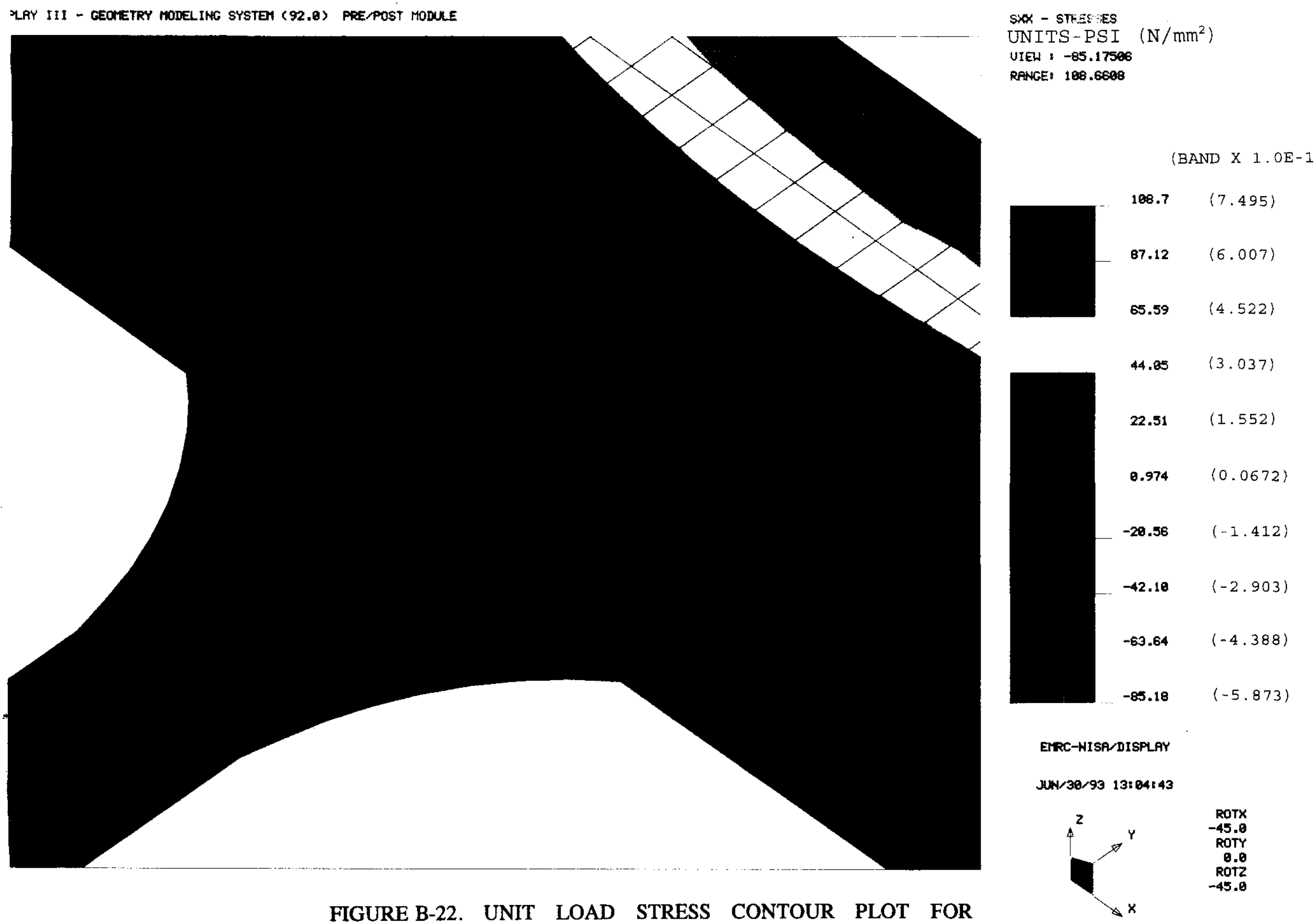

FIGURE B-22. UNIT LOAD STRESS CONTOUR PLOT FOR INTERNAL STIFFENER SHEAR - MODIFIED TANKER DETAIL

APPENDIX C

DETERMINATION OF WEIBULL DISTIBUTION TO FIT SL-7 SCRATCH GAGE DATA

(Note: Appendix C was reprinted from Reference (g).)

C.1 Determination of Weibull Parameters k and w

The principal need is to find the Weibull distribution that has the same mean peak-to-peak stress value and coefficient of variation as the SL-7 stress histogram in Figure C-1. (This histogram represents the maximum peak to minimum trough stress that occurred during more than 36,000 four-hour sampling periods in five data years of operation. It has been assumed that this distribution is representative of ship stress history during a life time of 10^8 cycles.)

The mean and standard deviation of the data in the loading histogram of Figure C-1 were found to be 4.397 and 3.772, respectively. Thus, the coefficient of variation is:

$$\delta = \frac{\sigma}{\mu} = \frac{3.772}{4.397} = 0.858$$

The expressions for the mean and standard deviation for the Weibull distribution are:

$$\mu_S = w\Gamma(1 + \frac{1}{k}) \qquad (C.1)$$

$$\sigma_S = w[\,\Gamma(1 + \frac{2}{k} - \Gamma^2(1 + \frac{1}{k})\,]^{1/2} \qquad (C.2)$$

It follows that the Weibull coefficient of variation is:

$$\delta_S = \frac{\sigma_S}{\mu_S} = \frac{[\,\Gamma(1 + \frac{2}{k}) - \Gamma^2(1 + \frac{1}{k})\,]^{1/2}}{\Gamma(1 + \frac{1}{k})} \qquad (C.3)$$

It should be noted that the coefficient of variation is a function of the Weibull shape parameter k. Equation C.3 is given in graphical form in Figure C-2 and in tabular form in Table C-1 for values of k in the range of 0.5 to 4.0.

The Weibull shape factor, k, which corresponds to the SL-7 coefficient of variation of 0.858 is found to be approximately 1.2 (from Figure C-2 or Table C-1). The Weibull parameter, w, can be determined by substituting the shape parameter, k = 1.2, and the mean value of the load histogram, μ = 4.397, into Equation. C.1:

$$w = \frac{\mu}{\Gamma(1 + \frac{1}{k})} = 4.674 \qquad (C.4)$$

The frequency diagram corresponding to the SL-7 data is shown in Figure C-1 along with the Weibull distribution determined above. The Weibull distribution shows excellent agreement with the actual data.

C.2 Estimation of $S_{10^{-8}}$ for Weibull Distribution

It should be noted that each stress range in the scratch gage data represents the maximum peak stress to the maximum trough stress which occurred during a four-hour sampling period and corresponds to one "occurence".

If it is assumed that the average wave period is 7.5 seconds. The number of load cycles experienced by the ship in one occurence is 1920. The number of occurences corresponding to one ship lifetime of 10^8 cycles is approximately 52000. The maximum stress range expected in a ship lifetime of 10^8 cycles, designated as $S_{10^{-8}}$, would correspond in this case to the stress range with the probability of exceeding 1/52000 occurrences.

$$Q_S(S_{10^8}) = \frac{1}{52000}$$

$$1 - F_S(S_{10^8}) = (52000)^{-1}$$

$$1 - \{1 - \exp[-(\frac{S_{10^8}}{w})^k]\} = (52000)^{-1}$$

$$S_{10^{-8}} = w[\ln(52000)]^{1/k} \qquad (C.5)$$

Substituting k = 1.2 and w = 4.674 (from Section C.1) into the above equation yields:

$$S_{10^{-8}} = 4.674[\ln(52000)]^{1/1.2} = 34.11\,ksi \ (235.2\,N/mm^2)$$

Thus, the maximum stress range to be expected during the life of the ship, based on the empirical data available and the assumed Weibull distribution, is approximately 34.1 ksi (235.2 N/mm^2).

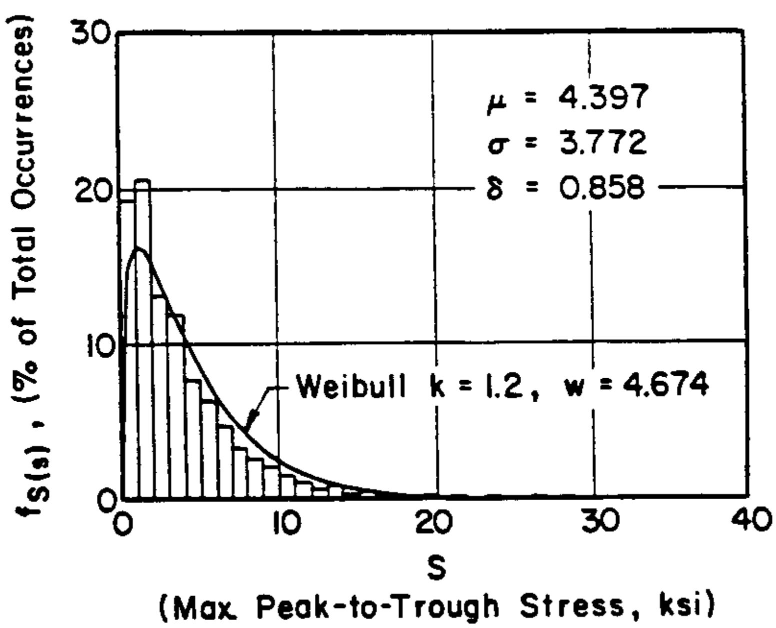

FIGURE C-1. SL-7 SCRATCH GAGE DATA WITH CORRESPONDING WEIBULL DISTRIBUTION

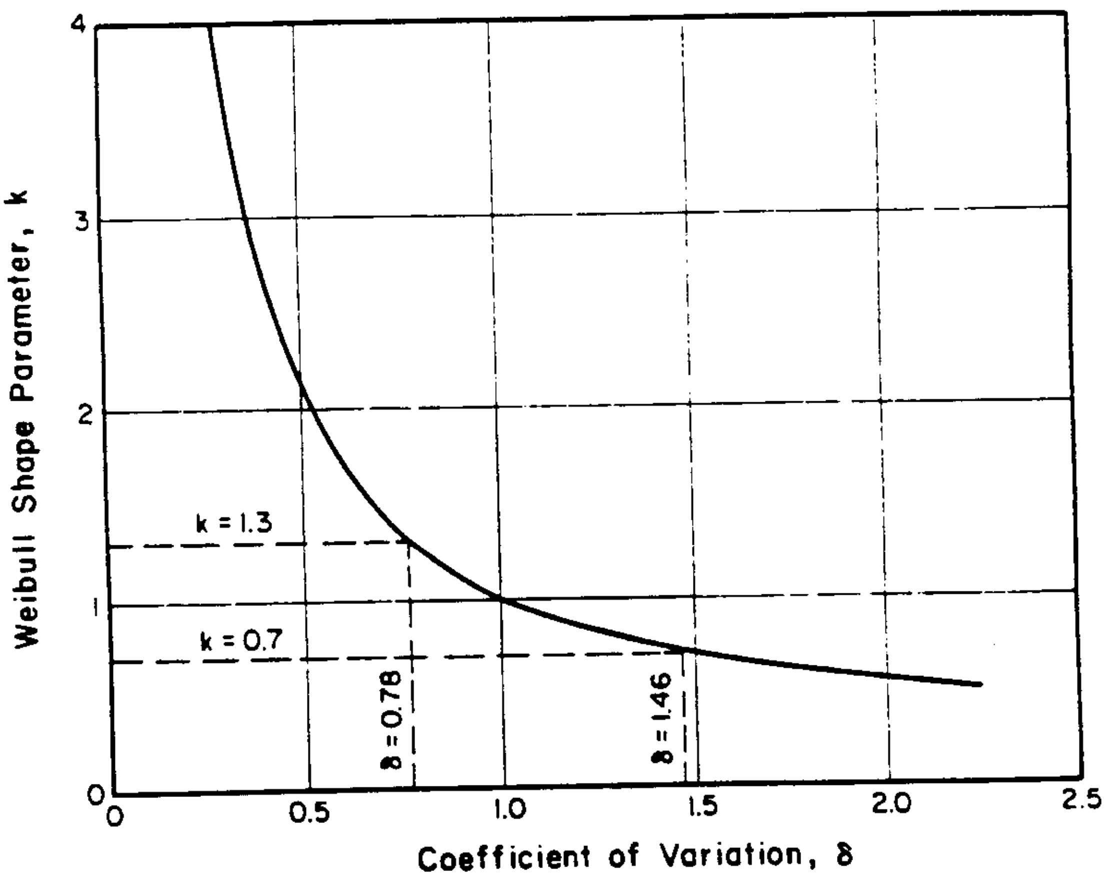

FIGURE C-2. COEFFICIENT OF VARIATION FOR WEIBULL SHAPE PARAMETER, k

TABLE C-1. TABLE OF WEIBULL SHAPE PARAMETER VALUES AND CORRESPONDING COEFFICIENTS OF VARIATION

Weibull Shape Parameter k	Coefficient of Variation δ
0.5	2.236
0.6	1.758
0.7	1.462
0.8	1.261
0.9	1.113
1.0	1.000
1.1	0.910
1.2	0.837
1.3	0.776
1.4	0.724
1.5	0.679
1.6	0.640
1.7	0.605
1.8	0.575
1.9	0.547
2.0	0.523
2.5	0.428
3.0	0.363
4.0	0.281

Project Technical Committee Members

The following persons were members of the committee that represented the Ship Structure Committee to the Contractor as resident subject matter experts. As such they performed technical review of the initial proposals to select the contractor, advised the contractor in cognizant matters pertaining to the contract of which the agencies were aware, and performed technical review of the work in progress and edited the final report.

Mr. Phil Rynn–Chairman	American Bureau of Shipping
LT Mike Roer	U.S. Coast Guard R&D Center
Mr. Natale Nappi	Naval Sea Systems Command
Mr. Chao Lin	Maritime Administration
Mr. Jadeep Sirkar	U.S. Coast Guard
LCDR Doug O'Reilly	National Defence Headquarters, Canada
Mr. Roger Kline	National Academy of Sciences, Technical Advisor, Committee on Marine Structures
Mr. Chris Cleary	U.S. Coast Guard
Mr. Marty Hecker	U.S. Coast Guard
Mr. William Siekierka	Naval Sea Systems Command, Contracting Officer's Technical Representative
Mr. Alex Stavovy Dr. Robert Sielski	National Academy of Science, Marine Board Liaison
CDR Mike Parmelee CDR Steve Sharpe	U.S. Coast Guard, Executive Director Ship Structure Committee

COMMITTEE ON MARINE STRUCTURES

Commission on Engineering and Technical Systems

National Academy of Sciences – National Research Council

The COMMITTEE ON MARINE STRUCTURES has technical cognizance over the interagency Ship Structure Committee's research program.

Peter M. Palermo Chairman, Alexandria, VA
Subrata K. Chakrabarti, Chicago Bridge and Iron, Plainfield, IL
John Landes, University of Tennessee, Knoxville, TN
Bruce G. Collipp, Marine Engineering Consultant, Houston, TX
Robert G. Kline, Marine Engineering Consultant, Winona, MN
Robert G. Loewy, NAE, Rensselaer Polytechnic Institute, Troy, NY
Robert Sielski, National Research Council, Washington, DC
Stephen E. Sharpe, Ship Structure Committee, Washington, DC

LOADS WORK GROUP

Subrata K. Chakrabarti Chairman, Chicago Bridge and Iron Company, Plainfield, IL
Howard M. Bunch, University of Michigan, Ann Arbor, MI
Peter A. Gale, John J. McMullen Associates, Arlington, VA
Hsien Yun Jan, Martech Incorporated, Neshanic Station, NJ
John Niedzwecki, Texas A&M University, College Station, TX
Solomon C. S. Yim, Oregon State University, Corvallis, OR
Maria Celia Ximenes, Chevron Shipping Co., San Francisco, CA

MATERIALS WORK GROUP

John Landes, Chairman, University of Tennessee, Knoxville, TN
William H Hartt, Florida Atlantic University, Boca Raton, FL
Horold S. Reemsnyder, Bethlehem Steel Corp., Bethlehem, PA
Barbara A. Shaw, Pennsylvania State University, University Park, PA
James M. Sawhill, Jr., Newport News Shipbuilding, Newport News, VA
Bruce R. Somers, Lehigh University, Bethlehem, PA
Jerry G. Williams, Conoco, Inc., Ponca City, OK

SHIP STRUCTURE COMMITTEE PUBLICATIONS

SSC-356	<u>Fatigue Performance Under Multiaxial Load</u> by Karl A. Stambaugh, Paul R. Van Mater, Jr., and William H. Munse 1990
SSC-357	<u>Carbon Equivalence and Weldability of Microalloyed Steels</u> by C. D. Lundin, T. P. S. Gill, C. Y. P. Qiao, Y. Wang, and K. K. Kang 1990
SSC-358	<u>Structural Behavior After Fatigue</u> by Brian N. Leis 1987
SSC-359	<u>Hydrodynamic Hull Damping (Phase I)</u> by V. Ankudinov 1987
SSC-360	<u>Use of Fiber Reinforced Plastic in Marine Structures</u> by Eric Greene 1990
SSC-361	<u>Hull Strapping of Ships</u> by Nedret S. Basar and Roderick B. Hulla 1990
SSC-362	<u>Shipboard Wave Height Sensor</u> by R. Atwater 1990
SSC-363	<u>Uncertainties in Stress Analysis on Marine Structures</u> by E. Nikolaidis and P. Kaplan 1991
SSC-364	<u>Inelastic Deformation of Plate Panels</u> by Eric Jennings, Kim Grubbs, Charles Zanis, and Louis Raymond 1991
SSC-365	<u>Marine Structural Integrity Programs (MSIP)</u> by Robert G. Bea 1992
SSC-366	<u>Threshold Corrosion Fatigue of Welded Shipbuilding Steels</u> by G. H. Reynolds and J. A. Todd 1992
SSC-367	<u>Fatigue Technology Assessment and Strategies for Fatigue Avoidance in Marine Structures</u> by C. C. Capanoglu 1993
SSC-368	<u>Probability Based Ship Design Procedures: A Demonstration</u> by A. Mansour, M. Lin, L. Hovem, A. Thayamballi 1993
SSC-369	<u>Reduction of S-N Curves for Ship Structural Details</u> by K. Stambaugh, D. Lesson, F. Lawrence, C-Y. Hou, and G. Banas 1993
SSC-370	<u>Underwater Repair Procedures for Ship Hulls (Fatigue and Ductility of Underwater Wet Welds)</u> by K. Grubbs and C. Zanis 1993
SSC-371	<u>Establishment of a Uniform Format for Data Reporting of Structural Material Properties for Reliability Analysis</u> by N. Pussegoda, L. Malik, and A. Dinovitzer 1993
SSC-372	<u>Maintenance of Marine Structures: A State of the Art Summary</u> by S. Hutchinson and R. Bea 1993
SSC-373	<u>Loads and Load Combinations</u> by A. Mansour and A. Thayamballi 1994
None	Ship Structure Committee Publications - A Special Bibliography